Australian Government
Bureau of Meteorology

The Centre for Australian Weather and Climate Research
A partnership between the Bureau of Meteorology and CSIRO

CSIRO

Defining heatwaves: heatwave defined as a heat-impact event servicing all community and business sectors in Australia

John Nairn and Robert Fawcett

CAWCR Technical Report No. 060

www.cawcr.gov.au

Defining heatwaves: heatwave defined as a heat-impact event servicing all community and business sectors in Australia

John Nairn and Robert Fawcett

The Centre for Australian Weather and Climate Research
- a partnership between CSIRO and the Bureau of Meteorology

CAWCR Technical Report No. 060

March 2013

Author:	Nairn, J. and Fawcett, R.
Title:	Defining heatwaves: heatwave defined as a heat-impact event servicing all community and business sectors in Australia
ISBN:	9781922173126 (Electronic Resource)
Series:	CAWCR technical report.
Notes:	Includes bibliographical references and index.
Subjects:	Heat waves (Meteorology)--Australia.
	Pyrometry.
	Dewey Number: 551.5250994

Contact details

Enquiries should be addressed to:

John Nairn
South Australian Regional Office
Bureau of Meteorology, GPO Box 421, Kent Town,
South Australia, 5071 AUSTRALIA
J.Nairn@bom.gov.au

Copyright and Disclaimer

Contents

List of figures

List of Tables

ABSTRACT

This report proposes a new objective definition for heatwaves and heatwave severity that may be applied to any location in Australia, or for that matter the world. Using this definition, it is now possible to compare severe and extreme heat events across time and space.

A heatwave intensity index has been created by combining measures of *excess heat*, the long-term temperature anomaly characterised by each location's unique climatology of heat, and *heat stress*, the short-term temperature anomaly measuring recent thermal acclimatisation. These two measures have been factored together to create the *excess heat factor* (*EHF*).

The Australian community understands that heatwaves are a common summertime experience and rarely anticipates significant human health risk. This is borne out by the cumulative distribution function of *EHF* which indicates that most heatwaves are of low intensity. It is only rarely that heatwaves become severe enough to impact vulnerable people and rarer still that they exhibit extreme intensities capable of causing widespread health problems. Generalised extreme value theory has been used to motivate a severity threshold for the *EHF*, a level at which the heatwave may be considered to be severe. Case studies of Australian and international severe and extreme heatwaves are examined with the aid of *EHF* intensity, demonstrating the utility of the index.

The methodology applied in the development of this heatwave index appeals to our common understanding of heatwave impact. Additionally, the objective statistical techniques employed here are easily extended to permit the development of a robust coldwave index, the logical extension to coldwaves being also proposed in this report.

EHF can be used to appropriately alert communities according to the intensity of impending heatwaves, whilst climates trends and projections of intensity, frequency, spatial extent and length can also be considered for Australian and international locations.

1. INTRODUCTION

Despite heatwaves being one of the most common natural hazards experienced across the Australian community, heatwaves remain imprecisely defined events with the varied impacts across different community sectors little understood. The increasing availability of high-quality climate and weather-forecast temperature datasets offers an opportunity to build a shared understanding of the hazard posed by sequences of high temperature days.

Heatwaves are obviously not unique to Australia, and not surprisingly international meteorological agencies similar to the Australian Bureau of Meteorology (henceforth, "the Bureau") have created heatwave services to close the gap between understanding and service demands. It is possible for the Bureau to develop and provide a heatwave service, since it has a statutory responsibility under the Meteorology Act 1955 to issue warnings for weather conditions likely to endanger life or property. The Bureau's capacity to develop and provide a heatwave service is however predicated on capacity building, (i) in developing a well-understood and scientifically defensible heatwave definition, (ii) in acquiring stable systems for the examination of the climate record, and (iii) the provision of reliable and robust forecast and warning services.

Other institutions, including Commonwealth, State and Territory authorities, are likely to respond appreciatively to the provision of heatwave services, as it would assist in the execution of their responsibilities for managing the impact of severe and extreme heatwaves under the prevention, preparedness, response and recovery emergency management framework.

Historically, heatwaves have been responsible for more deaths in Australia than any other natural hazard, including bushfires, storms, tropical cyclones and floods (Coates 1996). While heatwaves are not unusual for Australians, the trend towards more frequent and intense heatwaves (Alexander et al. 2007) is of significant concern. McMichael et al. (2003) has estimated that extreme temperatures currently contribute to the deaths of over 1000 people aged over 65 each year across Australia. The number of heat-related deaths in temperate Australian cities is expected to rise considerably by 2050 as the frequency and intensity of heatwaves is projected to increase under climate change from global warming. Underpinning this view is the building evidence supporting the notion of a warming planet (CSIRO and Bureau of Meteorology, 2007).

The impacts of severe heatwaves vary across many sectors of the Australian community, from the general public to government organisations and industries, health, utilities, commerce, agriculture and infrastructure. Impacts can be directly or indirectly accountable for:

- increased human morbidity and mortality, particularly among the elderly and infirm;
- stress for outdoor workers;
- increased bushfire risk;
- stress in animals;
- damage to crops and vegetation;
- increased energy demand, e.g. greater demand for air conditioning;
- stress on energy supply infrastructure;
- increased demand for water, e.g. human consumption, cooling in power stations, evaporative cooling in homes and offices;
- infrastructure stress: buildings, roads, rail and other infrastructure;
- shifts in tourism preferences due to higher temperatures; and
- increased risks for sporting and outdoor recreation activities.

A range of heat-health related warning services is currently provided across Australia utilising a diverse set of methodologies, definitions and thresholds. Products and services have been developed and maintained under local cooperative arrangements with jurisdictional authorities. For example, southeast Queensland implemented a service using "apparent temperature" following the

2004 severe heatwave. In 2008, Melbourne health authorities established a service using a one-day daily temperature, while in South Australia a service using three-day-average daily temperature was established. More recently, local authorities have engaged the Bureau in New South Wales and Western Australia to meet their service requirements. These various definitions are not particularly comparable.

Heatwaves are frequently defined as a period of unusually or exceptionally hot weather. Extreme events typically occur in mid-summer, although less intense heatwaves are also experienced during spring and early autumn. Heatwaves in Australia are driven by slow-moving synoptic-scale events that allow the continuous development of hot air masses to persist over large areas for a period of days and in rare events, weeks. Fortunately, modern numerical weather prediction (NWP) models are quite good at forecasting slow-moving systems and provide good guidance on the evolution of high temperature events on the one to seven-day time scale. There are also growing efforts to achieve multi-week predictions of monthly to seasonal conditions through the use of coupled ocean-atmosphere models (i.e., dynamical climate prediction or DCP). In both realms (NWP and DCP) it is important to note that advances in temperature forecast skill are expected to continue for some time, presenting vulnerable sectors with an opportunity to put in place responsible mitigation measures before the onset of heatwaves.

The heatwave literature has predominantly focussed on human health outcomes. Consequently sensible and latent heat are invariably combined together in order to account for effectiveness of thermo-regulation of biological systems. Frequently, regression equations (Braga et al. 2001; Curriero et al. 2002; Vandentorren et al. 2006; McMichael et al. 2003; Tong et al. 2010) or synoptic patterns (Kalkstein 2000) are used to relate and measure impacts on human health outcomes at city or regional scales. At this level of interplay between multiple variables, units and outcomes, it is difficult to visualise or compare heatwaves across time or compare the severity of local, national or international events.

Taking a step back from human impact, it is interesting to consider heatwaves as events where excessive sensible heat accumulates, resulting in a rising thermal load. Robinson (2001) adopted a *de facto* heatwave definition based on heat watch and warning criteria developed by the US National Weather Service. Robinson's approach incorporated frequency of exceedance of a fixed percentile of all observed heat index values (Steadman 1979a, 1979b, 1984). Whilst an advance in developing an objective heatwave definition, Steadman's heat index is difficult to employ in climate assessment and projections as past and projected records of humidity are difficult to create and quality control. Robinson's work established a baseline climate description of heatwaves for the United States of America, but was not considered able to provide a complete time series of events nor be suitable for epidemiological purposes. Characterising and carrying out comparative investigations across heatwave events is desired.

Robinson's method considered heatwaves as events where excessive biologically regulated heat accumulates. A sensible heat alternative identifies heatwaves as events where excessive sensible heat accumulates, resulting in a rising thermal load. Heatwaves identified purely by thermal load can be assessed in terms of peak and accumulated heat load, evolving in time and space, regardless of location across the globe. Human health considerations under this approach would be taken into account as a secondary step, as required, after establishing the threat and potential magnitude of an approaching (thermal) heatwave.

In Australia, heatwaves have traditionally been defined by the achievement of a minimum sequence of consecutive days where daily maximum temperatures reach a designated threshold[1]. However, daily maximum temperatures are only part of the story when considering impacts on human health, agriculture, infrastructure, the demand on utilities (water, electricity, etc.) and other environmental

[1] In Adelaide, for example, five consecutive days with maximum temperature at or above 35°C or three consecutive days at or above 40°C.

hazards such as fire. Previous research has highlighted the importance of incorporating minimum temperature through the utilisation of daily mean temperature (Pattenden et al. 2003; Nicholls et al. 2008). The extent to which heat is dissipated overnight following a very hot day dictates the accumulating thermal load impacting vulnerable people and systems. The accumulation of this heat which is not being dissipated results in "excess heat".

Heatwave intensity occupies a continuum on which low-intensity heatwaves have little impact whilst more intense events inflict severe consequences upon the community and business sectors. Rising intensity leads to extreme outcomes where widespread adverse impacts are experienced. It is anticipated that heatwave-impact thresholds of relevance to health outcomes are likely to differ from those for infrastructure, although there are probable inter-dependencies. Impacts will vary according to each location's experience or climatology of excess heat and each community's capacity to develop resilient strategies. By measuring heatwaves within a scale that captures intensity, it becomes possible to differentiate between heatwave events. This in turn permits a sensible analysis of resilient strategies that can be usefully shared between communities learning to combat the impact of severe and extreme heatwaves.

Systems susceptible to failure under thermal duress have natural or engineered design limitations. These limits are an adaptive response to commonly expected rates of heat accumulation found over both the long (local climate scale) and short-term (recent acclimatisation). When these limits are exceeded, systems begin to fail. The larger the thermal load attributable to both the long and short-term extremes, the deeper will be the impact and scale of failure. An index has been developed (Nairn et al. 2009, Appendix A), that combines the long and short term temperature anomalies which is sensitive to the scale of heatwave impact, its description and a discussion of its attributes being the primary purpose of this report. The statistical methodology employed in this measure addresses several issues critiqued in the detection of climate extremes (IPCC, 2012). The use of daily temperature benefits from the availability of datasets covering 70% of the global land area, whilst the employment of temperature anomalies mitigates time series homogeneity issues, particularly given that one of the two component indices is a thirty day temperature anomaly. These and other features provide a robust measure of local heatwaves which is applicable across a wide range of sectors, including human health.

This index is suitable for a nationally consistent heatwave service which is in line with emerging World Meteorological Organization guidelines on the development of national heatwave/heat health services. A heatwave service utilising this measure of intensity would provide information to enable the Australian community to self-assess thresholds of vulnerability to periods of excess heat, and to warn when severe or extreme heatwaves threaten.

Ideally, temperature datasets would be processed into an index format that assists decision makers in the assessment of heatwave severity. Past heatwave scenarios and their consequences would provide a context within which this information would aid increased knowledge and understanding of the challenges ahead. Under an accepted and shared understanding of heatwave hazard, best-practice hazard mitigation and response plans could progress to accepted national and international standards.

Finally, for a heatwave measure to become widely accepted, it must be:

- easily understood. People associate extreme values with their experience;
- measured with readily available data, where and when it is needed;
- mapped to provide timely and locally specific guidance;
- predictable with reasonable accuracy;
- useful as an indicator of impact; and
- supportive of the prevention, preparedness, response and recovery emergency management framework.

This report has been developed to meet these objectives, offering the potential for a national (if not international) definition of heatwaves.

In the following section (2) the meteorology associated with the evolution of Australian heatwaves is described. Section 3 provides the methodology for deriving a heatwave (and coldwave) intensity index, while Section 4 develops a methodology for determining local thresholds for severe and extreme events. Section 5 uses these definitions to examine the climatology of temperature extremes across Australia, while Section 6 examines Australian and international case studies.

A significant heatwave took place in January 2013, as this report was being finalised. That heatwave has not been included in the climatological assessments presented in the report.

2. HEATWAVE METEOROLOGY

Descending, drying air within an anticyclone results in dry and warming air under clear skies. These clear skies allow radiative heating of the underlying surface during the daytime, which over land diabatically exchanges heat into the overlying air. What would be a normal warming cycle ahead of the next cool air mass change can become stagnated when a slow-moving anticyclone prolongs the heating cycle, occasionally producing a heatwave.

McBride et al. (2009) notes the mechanisms for build-up of heat as:

- advection from lower latitudes;
- large-scale subsidence transporting higher potential temperature air from upper levels; or
- surface heating, development of the diurnal mixed layer, and replacement from below by the new mixed layer for the successive day;

concluding that the evidence supports surface heating as the dominant contributor.

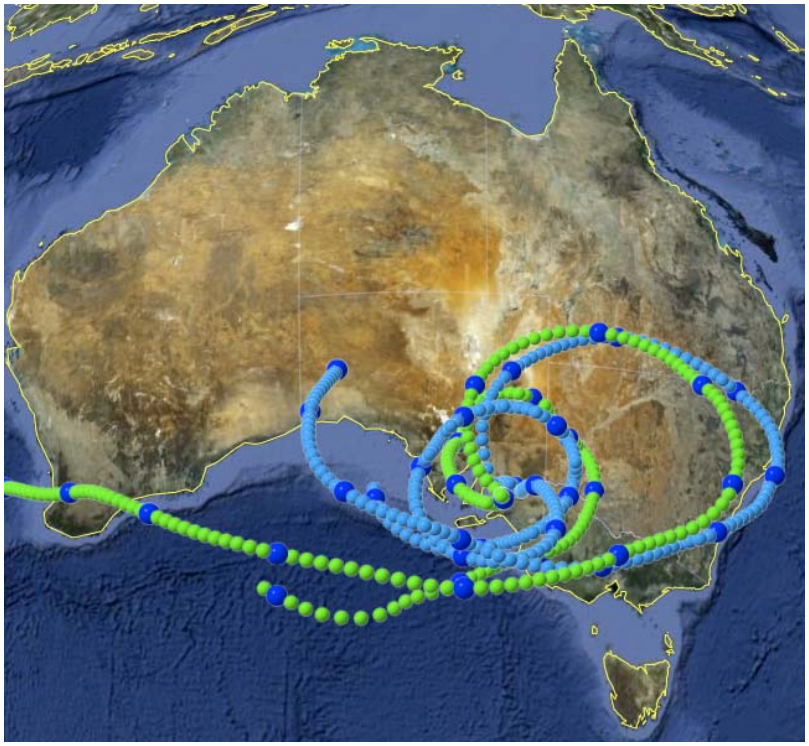

Figure 1: The March 2008 Adelaide heatwave. Five-day backward trajectories calculated using the HYSPLIT trajectory model based on ACCESS fields. The back-trajectories are from the city of Adelaide. Starting times are for 00UTC 10 March 2008 and 00UTC 14 March 2008. Trajectories are shown at hourly intervals for air ending over Adelaide at those times at the 850 hPa level (blue) and for the 700 hPa level (green). Data from McBride et al. 2009.

The sensible heat component of the land-surface radiation budget rises when the latent heat flux (evaporation) reduces due to drought. Nicholls and Larsen (2011) noted a 1-3 °C rise in Melbourne's maximum temperatures for situations typically associated with high temperatures following periods of drought.

Diurnal variation in boundary-layer depth features in the morphology of intense heatwaves. Daytime mixing will reach greater heights as surface sensible heat increases. In events where high surface temperature arises from dry soils, sensible heating into the shallow nocturnal boundary

layer continues, contributing to anomalously high overnight temperatures, a feature of extreme heatwaves noted in radiation balance studies for the 2003 European extreme heatwave by Black et al. (2004).

The trajectories in Figure 1 reveal a gyral circulation that allows day-time heated mixed layers to remain over the continent. Tropospheric heat storage is built up by subsequent daytime heating. The corresponding mean-sea-level pressure (MSLP) pattern in Figure 2 illustrates the extended poleward surface air trajectories that (on average) advected hot air over southeast Australia over five days during Adelaide's 15-day heatwave in 2008. Heatwaves are also characterized by a stationary or slow-moving Rossby wave pattern in the mid-troposphere. The mid-tropospheric (500 hPa) anticyclonically curved jet stream on the poleward side of the surface anticyclone shown in Figure 2 is a feature of the supporting long-wave ridge and an illustration of what McBride at al. (2009) called the "warm anticyclone'. The anticyclone tilts westward from the surface up to 700 or 500 hPa, depending upon the severity of the event. Unlike cooler-season stationary Rossby wave patterns, there is an absence of the typical split-jet structure which supports a classic "blocking pattern".

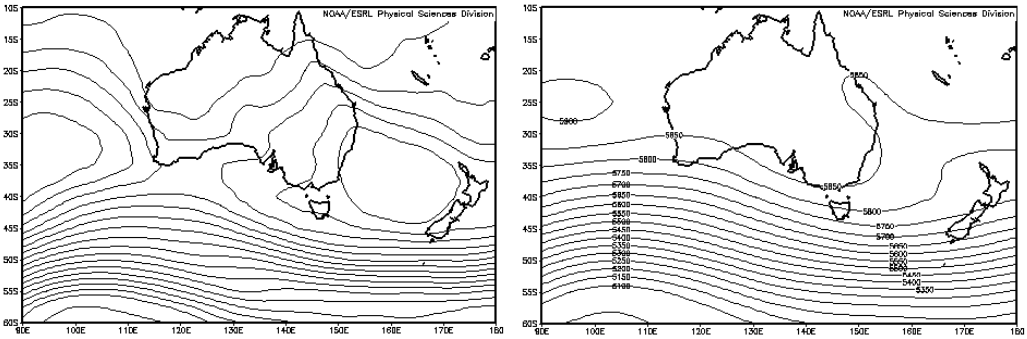

Figure 2: Five-day composite mean MSLP (hPa, left) and 500 hPa geopotential height (m, right) for 00UTC 10 to 14 March 2008. Data from the NCEP/NCAR reanalysis[2].

Severe Southern Australian heatwaves have been characterised by Pezza et al. (2012) with southeastern Australia and southwest Western Australia impacted by slow-moving anticyclones centred in the Tasman Sea and the western Great Australian Bight (Figure 3, a and b) respectively, noting heatwaves are driven by large scale synoptic events which derive their structure and longevity from planetary scale Rossby wave dynamics.

Predicting heatwave seasonality, onset and longevity is tied to the predictability of these Rossby waves and whether they may or may not become stationary. The rising incidence of northern hemisphere weather extremes has recently been tied to a slackening of mid-tropospheric temperature gradients which are conducive to standing Rossby waves. Arctic amplification (Francis and Vavrus, 2012) or enhanced Arctic warming is attributed largely to reduced sea ice which has significantly increased heat flux into the polar sea.

[2] This and subsequent analogous figures provided by the US NOAA/ESRL Physical Sciences Division, Boulder Colorado from its website at http://www.esrl.noaa.gov/psd/. For more information on the NCEP reanalyses, see Kalnay et al. 1996.

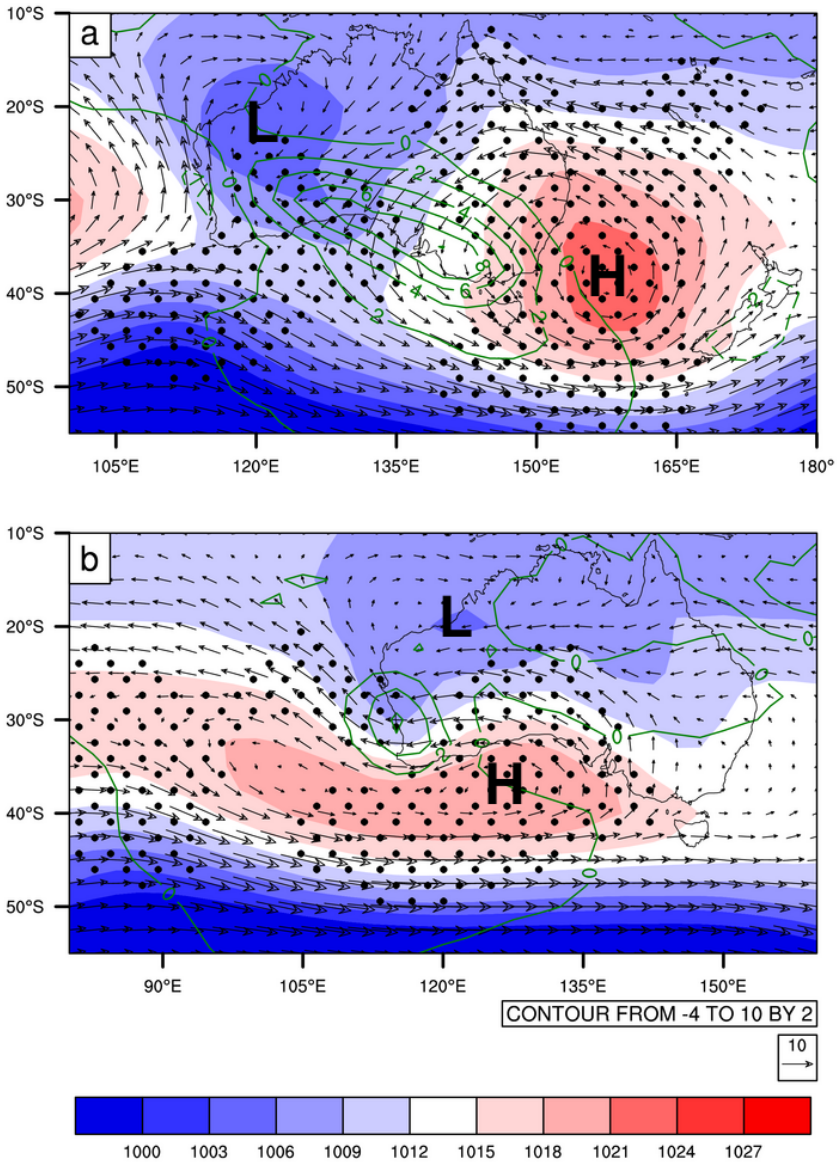

Figure 3: DJF composite of MSLP (shading) and surface temperature anomalies (contours) on the first day of heatwaves (three consecutive days criteria) in (a) Melbourne and (b) Perth overlaid with 950 hPa winds. Units are in hPa (colour scheme), K (contours) and wind magnitude in m s^{-1} given by vector size. Number of events is 13 for Melbourne and 19 for Perth. Statistically significant MSLP areas above the 95% confidence level are given by stippling (from Pezza et al. 2012).

In contrast to the northern hemisphere, the Antarctic continent is maintaining relatively stable surface fluxes. Southern hemisphere Rossby wave structure appears to be driven by anomalous mid to low latitude heat fluxes resulting in excitation of a stable wave train (Kosaka and Nakamura 2010). Ocean temperature structure shown in Figure 4 (Pezza et al. 2012) has a modality that sets up anomalous mid to low latitude meridional sea surface heat fluxes that have statistical significance for severe heatwaves. It is possible to associate the anomalously cool (warm) SST to long-wave ridge (trough) positions favourable for a stable, stationary Rossby wave train.

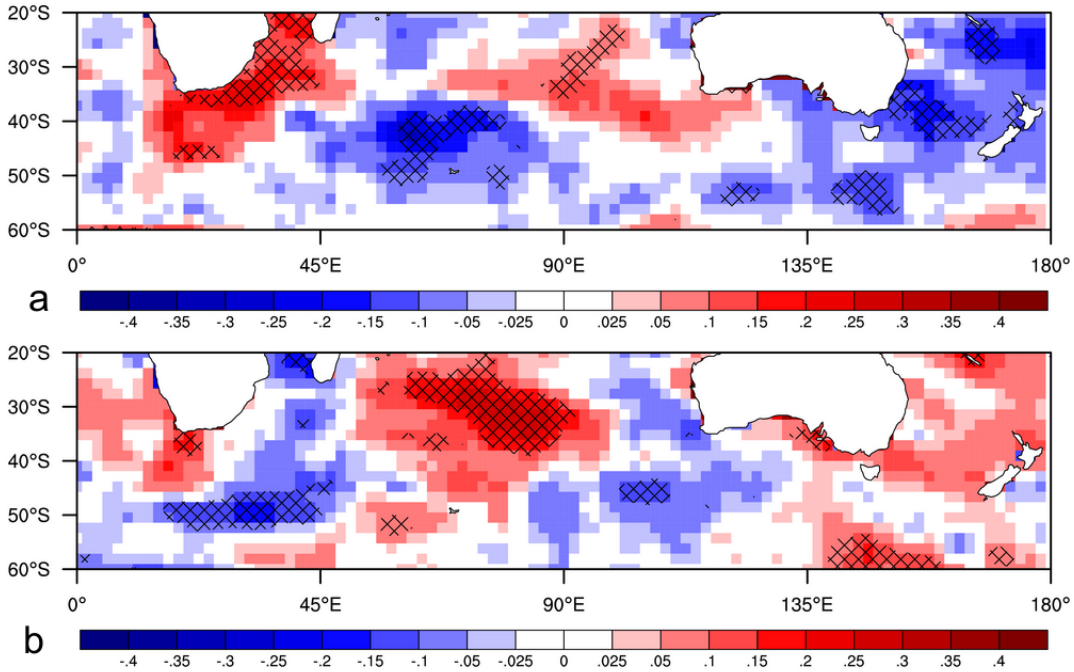

Figure 4: Average SST anomalies (°C) over the ocean for the seven days before a heatwave in Melbourne (a) and Perth (b). Hatched areas indicate regions of 90% statistical significance. Number of events is 13 in Melbourne and 19 in Perth, over the period 1979-2008 (from Pezza et al. 2012).

Understanding ocean SST influences on both rainfall (hence soil moisture) and Rossby wave evolution is an area for further heatwave research. The combination and permutation of heatwave intensification and longevity drivers will provide opportunities for the development of predictive tools across seasonal to weather system time scales.

3. HEATWAVE AND COLDWAVE CONCEPTS DEFINED

A heatwave is typically defined as a period of excessively hot weather. In Australia, a heatwave is thought of as being generally uncomfortably hot for the population and may adversely affect human health for those vulnerable to such conditions. However, threshold conditions for a heatwave vary across Australia and around the world, and consequently there is no universally accepted definition at the time of writing.

The development of a suitable definition is essential for real-time and historical climate monitoring of heatwaves across Australia and for the comparison and projection of heatwave trends around the world. The calculation of simple objective indices provides a means by which the community can gauge its historical sensitivity to excess heat intensity, spatial distribution, accumulated heat load and days of duration. Mitigation and response managers can benefit from access to objective time series and spatial tools that permit comparison of past and forecast events.

Heat impact is frequently identified as one of two forms of thermal stress. Most often it arises when the long-term thermal resilience of a system (e.g. biological, agricultural) is exceeded. The other form of heat impact occurs when the event is unusual in relation to recent heat exposure.

The following concepts are developed in order to provide a platform for developing a heatwave definition that is applicable to any location. Indices are adopted that match these concepts as detailed by Nairn et al. (2009), which is included as Appendix A.

3.1 Excess Heat

Excess Heat: *This is unusually high heat arising from a high daytime temperature that is not sufficiently discharged overnight due to unusually high overnight temperature. Maximum and subsequent minimum temperatures averaged over a three-day period are compared against a climate reference value to characterise this unusually high heat in an excess heat index. This is expressed as a long-term (climate-scale) temperature anomaly.*

In meteorological terms, the ability for systems to recover from high environmental heat load is dependent on the diurnal variation in temperature. A sufficient drop from the (usually afternoon) maximum temperature to the following (usually early morning) minimum temperature will allow the heat load to discharge. High minimum temperature however will result in an accumulated heat load, leading to excess heat. For this reason daily temperature (average of daytime maximum followed by overnight minimum) is used to calculate excess heat[3].

A related concept is "heat-health", which is introduced in this document because severe or extreme heat events are so frequently linked to health outcomes in the literature and services. Examples where this terminology is appropriately used for health services exist in the United Kingdom (Met Office 2012) and Victoria (Victorian Department of Health 2012). The heatwave definition introduced in this paper is not specific to health, although it does lend itself to heat-health outcomes. Biological systems thermo-regulate heat efficiently through evaporating moisture. Latent heat required for evaporation removes heat from moist surfaces. This process is inhibited where the partial pressure of water vapour (a measure of humidity) is high. Consequently many

[3] Maximum temperature in Australia is measured for the 24 hours from 9 am local time on the relevant day to 9 am the following day. Minimum temperature on the other hand is measured for the 24 hours to 9 am on the relevant day. We therefore construct the daily mean temperature for 20 January (for example) as the average of the maximum temperature for 20 January and the minimum temperature for 21 January. Both of these temperatures are derived from measurements pertaining to the period 9 am 20 January to 9 am 21 January (local time).

heat-health measures in the health sector incorporate humidity to account for the health impact of high-humidity heat events. Excess heat accounts for the sensible heat budget, where it provides a measure of heat load in excess of a climatologically determined threshold. The efficiency with which that excess sensible heat can be managed in biological systems is not explicitly captured.

A side benefit of incorporating maximum and minimum temperatures in this measure is their modulation in the presence of high humidity, resulting notably in high minima. High minima contribute to higher values of excess heat and heat stress, leading to higher values of the heatwave metric (Nairn et al. 2009).

Excess heat events in Australia are culturally associated with a period or "wave" of days. Choosing the minimum period for an excess heat event (or heatwave) is in part a response to this historical and cultural understanding of what constitutes a heatwave.

In Australia, documented health impacts arising from excess heat vary between one day in Melbourne (Nicholls et al. 2008) and three days in Adelaide (Nitschke et al. 2007). International understanding of heatwave health impacts varies, but predominantly is indicative that vulnerable populations are sensitive following three-day exposure (Braga et al. 2001; Curriero et al. 2002; Pattenden et al. 2003; Hajat et al. 2006; Le Terte et al. 2006).

Anecdotal vulnerabilities for sectors other than health suggest multi-day events are required before impacts are observed. On the basis of health and other sectors, a continuous period of three days was selected to define the occurrence of a heatwave (Nairn et al. 2009). Consequently one hot day does not by itself constitute a heat wave.

The long-term climate reference value for determining the existence of a significant excess heat event has been set as the 95th percentile of observed daily temperature (single-day, average of maximum and minimum temperature in a common 9 am to 9 am period) for all days spanning the period 1971 to 2000. Positive contiguous three-day-average daily temperature departures from this reference value indicate a significant excess heat event or heatwave. This motivates the form of our first excess heat index,

$$EHI_{sig} = \left(T_i + T_{i+1} + T_{i+2}\right)/3 - T_{95}\,, \tag{1}$$

where T_{95} is the 95th percentile of daily temperature (T_i) for the climate reference period 1971-2000, calculated using all days of the year. As previously mentioned, daily mean temperature (DMT) is defined as

$$T = (T_{\max} + T_{\min})/2, \tag{2}$$

across the 24-hour period, where the maximum temperature typically precedes the minimum temperature in the 9 am to 9 am (local time) observation period. The DMT T_i on day i is in °C. The units of EHI_{sig} are also °C. By construction, EHI_{sig} is in effect an anomaly of three-day DMT with respect to climatological 95th percentile of the DMT.

3.2 Heat Stress

Heat Stress: *This arises from a period where temperature is warmer, on average, than the recent past. Maximum and subsequent minimum temperatures averaged over a three-day period and the previous 30 days are compared to characterise this heat stress in a second index. This is expressed as a short-term (acclimatisation) temperature anomaly.*

Acclimatisation to higher temperatures is a feature of human physical adaptation which may take between two to six weeks, involving physiological adjustments of the cardiovascular, endocrine

and renal systems (Knochel and Reed 1994; Guyton and Hall 2000). In this work, 30 days (about 4 weeks) has been used as the period required for acclimatisation. This motivates our second excess heat index,

$$EHI_{accl} = \left(T_i + T_{i+1} + T_{i+2}\right)/3 - \left(T_{i-1} + \ldots + T_{i-30}\right)/30\,, \tag{3}$$

where T_i is the DMT on day i defined in the previous section. In effect, EHI_{accl} is an anomaly of three-day DMT with respect to the previous 30 days. The units of EHI_{accl} are °C.

This index can be applied to both biological and engineered systems. Heat regulation in biological systems requires an adaptive response by a range of interacting organs. Engineered systems are no less complex. Power systems may not have the capacity to keep up with sudden or unusual demand, or if capable, will require adaptive preparation procedures to make ready the required resources. If the impacting heatwave is unseasonable and unexpected, the requisite preparations are less likely to have been put in place, exposing the system to the risk of failure.

Heat Stress is quantified by the magnitude of the EHI_{accl} or the short-term temperature anomaly index, in contrast to the long-term temperature anomaly index of the previous section.

3.3 Excess Heat Factor

Excess Heat Factor (EHF): *The combined effect of Excess Heat and Heat Stress calculated as an index provides a comparative measure of intensity, load, duration and spatial distribution of a heatwave event. Heatwave conditions exist when the EHF is positive.*

Combining the measures of Excess Heat and Heat Stress provides a measure of heatwave which has a strong signal-to-noise ratio. Low-impact heatwaves register as low-amplitude *EHF* events. As the Excess Heat and Heat Stress temperature anomalies increase, their product increases as a quadratic response to increasing heat load. Multiplying these two indices (instead of adding them) has been favoured because a similar quadratic signal is detected in high impact data (see section 3.3). Quadratic responses to extreme heat events are noted for mortality, ambulance response and power consumption (Ziser et al. 2005). We define the excess heat factor as

$$EHF = EHI_{sig} \times \max\left(1, EHI_{accl}\right). \tag{4}$$

The units of *EHF* are °C^2.

These equation differs slightly from Nairn et al. (2009), in that the three-day DMT is sampled for the current and following two days (i.e., days i, i+1 and i+2), instead of the retrospective view (i.e., days i, i–1 and i–2). This slight change is motivated by the intention to apply these ideas in the context of a weather forecasting service looking forward in time, but the indices are of course easily calculated using historical data in a retrospective sense.

The definition of *EHF* as presented here has also undergone a subtle reformulation. In the original formulation, which had $EHF = EHI_{sig} \times |\, EHI_{accl} \,|$, the factor $|\, EHI_{accl} \,|$ sat in place of the factor $\max(1, EHI_{accl})$ now present in equation (4). The change to the new definition of the *EHF* was motivated by a consideration of what happens in heatwaves of long duration. For heatwaves which are short relative to the 30-day acclimatisation period, the two definitions are effectively equivalent in terms of their positive values, because EHI_{accl} stays positive for the duration of the event. [Negative values of *EHF* are obviously different in the two formulations, but are excluded from consideration because they denote the absence of a heatwave[4]; this aspect of the change is of little

[4] An alternative way of approaching this aspect of the definition, not adopted here, would be to define *EHF* as $\max(0, EHI_{sig} \times \max(1, EHI_{accl}))$. This variant of the definition resets all negative values to zero.

importance.] For long heatwaves, particularly as the event is winding down, EHI_{accl} may go negative before EHI_{sig}, an undesirable outcome in the original definition of *EHF* which the new definition corrects. [Specifically, we don't want *EHF* to be high when the three-day period is substantially milder than the previous 30 days.]

In summary, *EHF* is positive (meaning that a heatwave is in progress) when EHI_{sig} is positive (because the three-day period is hot in an absolute sense, being above the 95th percentile for DMT), but additionally *EHF* is large when the three-day period is substantially warmer than the preceding 30 days ($EHI_{accl} >> 1$°C).

The Excess Heat Factor is quantified by the magnitude of *EHF*, the combined index measure of long and short-term temperature anomalies. Unless otherwise stated, the three-day periods represented by values of EHI_{sig}, EHI_{accl} and *EHF* will be denoted by the first day of the three-day period.

In the case of a heatwave extending over more than one three-day period, we will define the *heat load* of the event as the sum of the consecutive positive *EHF* values. This definition has the benefit of simplicity, but it comes at the slight cost of down-weighting the DMT contributions from the first and last days of the multi-day ($n > 3$) period.

3.4 Heatwave – Severe and Extreme events

Heatwave: *A period of at least three days where the combined effect of excess heat and heat stress is unusual with respect to the local climate. Both maximum and minimum temperatures are used in this assessment.*

Tracking the intensity of heatwaves using *EHF* is simple. Increasing *EHF* is a quadratic response to rising thermal load. Low values of *EHF* occur more frequently in the climate record, and may be considered to be uncomfortable, but of little impact.

Severe Heatwave: *An event where EHF values exceed a threshold for severity that is specific to the climatology of each location.*

In distributional terms, most *EHF* values are negative, especially during the cooler months, but the upper end (the positive values) of the *EHF* distribution is fat-tailed which permits the identification of a transition threshold between more-frequent lower-intensity events and less-frequent higher-intensity events. This threshold will be referred to as the severe *EHF* threshold. Severe impacts are anticipated at heatwave intensities that are relatively rare, because systems adjust to local conditions and carry an adaptive capability developed through experience of the local heatwave intensity climatology, thereby enabling them to cope with heatwaves of low to moderate intensity. Vulnerable sectors of the community are mostly affected, particularly those exposed through poor health, age or social isolation.

Extreme Heatwave: *An event where EHF values are well in excess of the severity threshold, resulting in widespread adverse outcomes.*

Under extreme heatwave conditions, normally robust systems are compromised in a cascade of failing, interdependent systems. People are impacted who would normally be protected by reliable power, transport and health systems.

3.5 Excess Heat Indices

An example of EHI_{sig} and EHI_{accl} can be seen in Figure 5. The significance index is shown in red, the acclimatisation index in blue. In this scheme, a heatwave is considered to have been detected on

any occasion that $EHI_{sig} > 0$ (because the three-day DMT is above the 95th percentile for DMT). [By construction, this is equivalent to having $EHF > 0$.] The calculation uses observed daily maximum and minimum temperatures from the Adelaide (Kent Town) observation site (Bureau station number 023090).

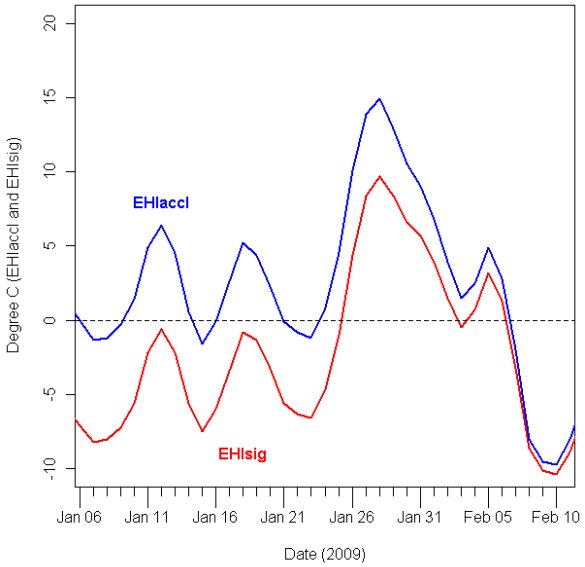

Figure 5: Acclimatisation (blue) and significance (red) Excess Heat Indices for Adelaide's 2009 extreme heatwave (06/01/2009 – 11/02/2009), calculated using site data.

Figure 6 shows the *EHF* for the same period shown in Figure 5. As indicated previously, the heatwave constitutes the set of three-day periods for which *EHF* (equivalently EHI_{sig}) is positive. In this case it extends from 25 January to 1 February 2009, with a smaller event beginning two days later. The impact of the *EHF* being a product of the two temperature anomaly contributions is quite evident in the figure, and points to the fact that the *EHF* is very responsive to increasingly excessive heat excursions.

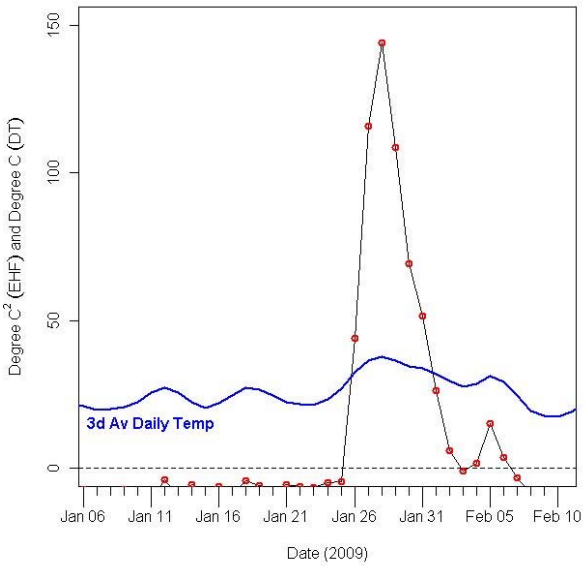

Figure 6: Excess Heat Factor (black line and red dots) and three-day-average DMT (blue line) for Adelaide's 2009 extreme heatwave (05/01/2009 – 11/02/2009), calculated using site data.

The calculation of these three indices requires continuous time series of daily maximum and minimum temperature. While these can be obtained from station-based data, for climate monitoring purposes, the Bureau's operational daily temperature analyses (Jones et al. 2009) have also been used. Those analyses were developed as part of the Australian Water Availability Project (AWAP), and in this report we use the low-resolution (0.25° or approximately 25 km) analyses. It is anticipated that future research will use the higher-resolution (0.05° or approximately 5 km) analyses in the development of an operational heatwave warning service.

Gridded forecast values of the three indices can be obtained for the next seven days using data from weather-forecast temperature grids, either from NWP models or generated in some other way by forecasters. Regardless of the weather-forecast data source, it must be integrated with climate data in order to calculate the acclimatisation excess heat index (EHI_{accl}), which may necessitate some degree of homogenisation. [This is because the Jones et al. (2009) analyses incorporate a statistical model of climatological temperature-elevation relationships across Australia which will likely differ from those implicit in any given NWP system, to say nothing of differences in the underlying digital elevation models.]

3.6 Coldwaves

The approach to excess heat indices is also applicable to coldwaves in a directly analogous fashion. Once again, a sensible heat approach is taken, recognising that only one component of the heat budget is being considered. This approach is aimed at isolating one ingredient of the total heat budget. Human exposure considerations will naturally consider other ingredients such as wind speed and humidity.

Coldwaves detected via excess cold indices also have sensible heat units of °C^2 which permits comparisons of events across time and space.

Examples are shown in following sections for Sydney, Australia and Newark, USA to compare extreme coldwave climatologies using these indices.

Excess cold indices and factor are proposed on the same principles as those used for excess heat. We define the two excess cold indices as

$$ECI_{sig} = \left(T_i + T_{i+1} + T_{i+2}\right)/3 - T_{05}, \tag{5}$$

where T_{05} is the 5th percentile of DMT (T_i) for the climate reference period 1971 to 2000, and

$$ECI_{accl} = \left(T_i + T_{i+1} + T_{i+2}\right)/3 - \left(T_{i-1} + \ldots + T_{i-30}\right)/30, \tag{6}$$

leading to the excess cold factor

$$ECF = -ECI_{sig} \times \min\left(-1, ECI_{accl}\right). \tag{7}$$

The ECI_{sig} index measures the degree of excess cold, while the ECI_{accl} measures cold stress. A negative ECI_{sig} means that the three-day period is cold by historical standards, having a three-day average daily temperature below the 5th percentile for daily temperature, while a negative ECI_{accl} means that the three-day period is cold in comparison to the recent past. *ECF* is negative (meaning that a coldwave is in progress) when ECI_{sig} is negative (because the three-day period is cold in an absolute sense, being below the 5th percentile for daily mean temperature), but additionally *ECF* is large when the three-day period is substantially cooler than the preceding 30 days ($ECI_{accl} << 1$ °C). Positive values of *ECF* mean a coldwave is not in progress[5].

[5] As with the heatwave definition, an alternative way of approaching this aspect of the definition, not adopted here, would be to define *ECF* as $\min(0, -ECI_{\text{sig}} \times \min(-1, ECI_{\text{accl}}))$. This variant of the definition resets all positive values to zero.

4. SEVERE AND EXTREME HEATWAVES

4.1 Severe Heatwave Threshold

An objective definition of severe heatwaves is motivated by the application of "probability of peaks over threshold" theory (Katz 2012), although ultimately a different technique yielding similar results will be proposed. As will be shown, heatwave events can be characterised as a heavy-tail distribution, well described by a generalised Pareto distribution. The cumulative distribution function (CDF) for the generalised Pareto distribution has the form

$$\Pr(X > x) = 1 - \left(1 - \frac{kx}{b}\right)^{1/k}, \tag{8}$$

where X is the random variable and k is a dimensionless shape parameter, while b is a positive scale parameter with dimensions equal to that of the random variable (here °C^2 because the random variable is positive *EHF*). When estimating k and b from a sample with mean $\hat{\mu}$ and standard deviation $\hat{\sigma}$, via the method of moments, we use

$$k = \frac{\hat{\mu}^2}{\left(2\hat{\sigma}^2\right)} - 1/2 \tag{9}$$

and

$$b = \hat{\mu}\left(k + 1\right). \tag{10}$$

The empirical CDF for Adelaide's heatwaves over the period 1958-2011 is shown in Figure 7, together with the generalised Pareto distribution computed using the method of moments. The modelled distribution in this case provides a good fit to the data. The *EHF* values are normalised against the maximum observed *EHF*, in this case 123 °C^2, resulting in scaled values which range from 0 to 1. Since a heatwave is simply characterised by having one or more *EHF* values (three-day events) greater than zero, it is necessary to construct an additional criterion to designate a severe heatwave. One approach would be to deduce this threshold from the modelled CDF as the ordinate at which the derivative of the normalised-*EHF* CDF is 1 (indicated by the red lines in Figure 7).

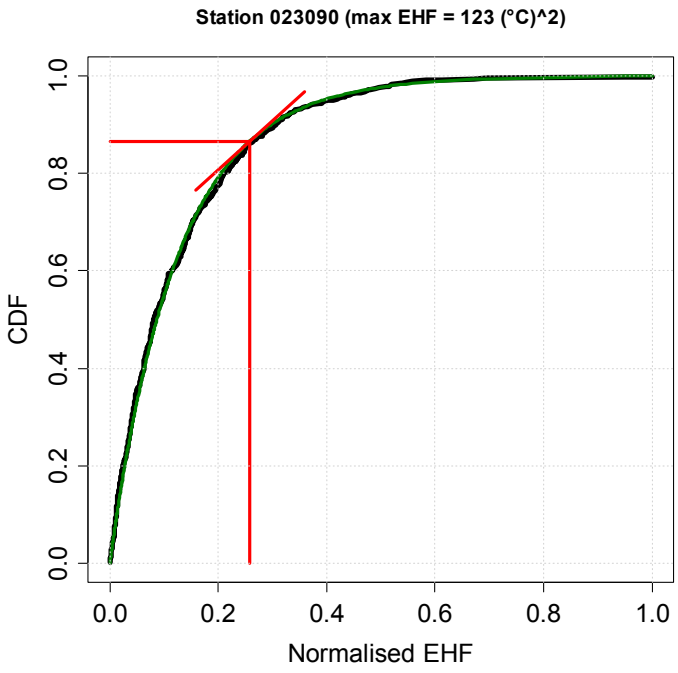

Figure 7: Adelaide cumulative distribution of positive *EHF* (black line and circles) normalised with respect to the maximum observed *EHF*, modelled generalised Pareto distribution (green line), and showing the turning-point method for determining the severe *EHF* threshold (red lines).

This has been described as the "turning-point" method[6], marking the shift between more common heatwaves of lower-intensity and rarer higher-intensity heatwaves. It is somewhat appealing to consider the usefulness of the Pareto Principle (Juran, 1974) when considering the proximity of this turning point value to the 80th percentile of the distribution function. Juran observed the "vital few and trivial many", a principle that 20 per cent of something are always responsible for 80 per cent of the results, which became known as Pareto's Principle or the 80/20 Rule. In this application, Pareto's power law relationship can be interpreted as "the last 20% of the cumulative distribution contains the top 80% of heatwave intensity space".

Whilst this method is appealing in its simplicity, it is not possible to assess whether an *EHF* sample population (i.e., *EHF* values for a defined period of 30 years or some longer period) contains a maximum *EHF* event that is truly representative of each site's climatology. In order to reduce the potential error that may arise from this sampling variability consideration, we will instead calculate the severe *EHF* threshold value as the 85th percentile of the distribution of positive *EHF* values at a given location (denoted EHF_{85}). This no longer depends on the modelled Pareto distribution, but rather is determined empirically from the observation record. A map of EHF_{85} calculated over the period 1958-2011, calculated using gridded DMT analyses (Jones et al. 2009) is shown in Figure 8.

[6] Obviously, the sense of the term "turning point" as used here is not the same as the standard "stationary value" sense in differential calculus.

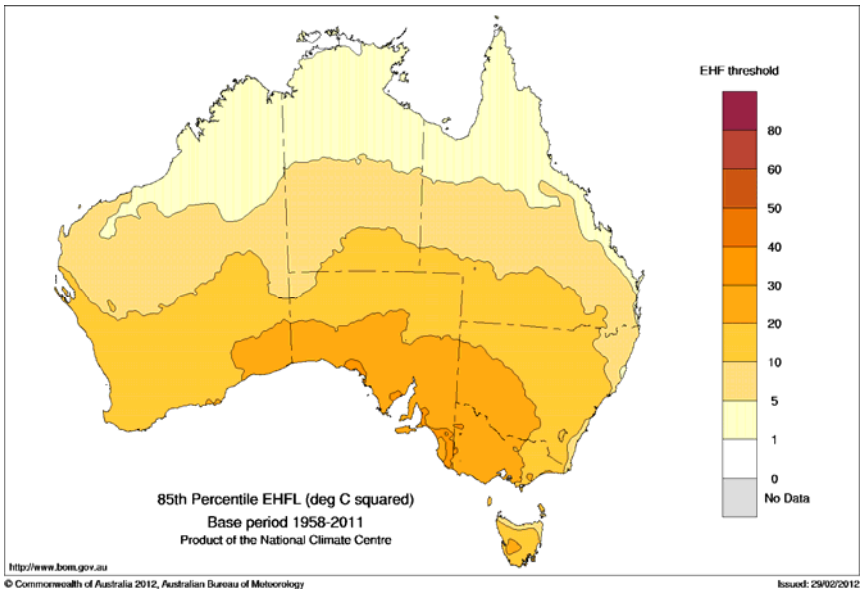

Figure 8: 85th percentile for positive *EHF* values (i.e., EHF_{85}), calculated over the period 1958-2011, using gridded DMT analyses.

Table 1: Severe *EHF* thresholds for Australian locations. Thresholds are calculated as the 85th percentile of the positive *EHF* values (i.e., EHF_{85}), obtained from time series interpolated from the gridded analyses.

Bureau station number	Place name	Threshold in $°C^2$
003003	Broome	2.4
009021	Perth	17.9
014015	Darwin	0.9
023090	Adelaide	30.7
029127	Mount Isa	5.5
031011	Cairns	2.5
040211	Archerfield (Brisbane)	5.4
062101	Mudgee	14.5
066062	Sydney	10.2
070339	Tuggeranong (Canberra)	14.2
072150	Wagga Wagga	19.5
079028	Longerenong	27.2
086071	Melbourne	24.2
094029	Hobart	15.7

The severe *EHF* thresholds shown in Table 1 have lower values for localities that normally have higher temperatures in the warm season (e.g. Darwin, Cairns and Broome). In these three places, the warm season is consistently hot and humid, resulting in very small heat anomalies. The benefit of a heatwave warning service, or more particularly a severe-heatwave warning service, for latitudes further north than the Tropic of Capricorn is not apparent, and is therefore not recommended.

In terms of interpolating gridded *EHF* calculations to specific locations, there are several alternative calculation paths available. One calculation path, the one we have generally followed, is to calculate everything required (e.g. DMTs, the climatological 95th percentile for DMT, three-day *EHI* and *EHF* values, the 85th percentile for positive *EHF*, the *EHF* severity threshold, etc.) at the grid level, and interpolate the results to locations as required. Alternative calculation paths can involve the interpolation of the DMT grids to form time series at interpolation locations, and compute some or indeed all of these derived quantities from the interpolated time series (e.g. Table

1). Because of rounding and truncation errors in the various interpolations, to say nothing of the inherent non-linearity of some of the calculations (e.g. the quantile calculations), slightly different results will be obtained depending on which calculation path is employed. In calculating the 85th percentile for positive *EHF* and the *EHF* severity threshold directly from the gridded calculations and from interpolated time series of DMT and three-daily *EHF*, we have found differences of up to 0.3 °C^2 in the *EHF* severity threshold and consequently up to 0.3 °C in the DMT severity threshold temperature (see next section), between the two calculation paths for the various interpolation locations listed in Table 1 and Table 2 (below).

4.2 Severe Heatwaves and Heat Health

Independent studies in Adelaide (Williams et al. 2012) and Melbourne (Nicholls et al. 2008) have determined DMT thresholds of 32 °C (over three days, Adelaide) and 30 °C (single day, Melbourne) for excess mortality in the 65 and older age group. These independently derived thresholds are shown to closely correspond to severe *EHF* thresholds.

A DMT indicative of the severe heatwave threshold can be estimated from equation (2) as

$$\hat{T}_{sev} \approx EHI_{sigsev} + T_{95}, \tag{11}$$

the equation being exact for three-day-averaged DMT (see equation (1)). EHF_{sigsev} is derived from the severe *EHF* threshold (EHF_{85}) by adjusting equation (4) as

$$EHI_{sigsev} = \frac{EHF_{sev}}{EHI_{acclsev}} \approx \sqrt{EHF_{85}}, \tag{12}$$

where $EHI_{sig} \cong EHI_{accl}$ is a first-order estimation during severe heatwaves. Whilst this convenient estimation is rarely correct (EHI_{accl} is frequently larger although within the same order as EHI_{sig}), the calculated severity threshold value for *EHF* and DMT is conservative, providing a slightly lower threshold value for a severe heatwave.

This method of estimating $\hat{T}_{sev}$ produces DMT thresholds of 31.5 °C (Adelaide) and 29.1 °C (Melbourne) (Table 2). These compare well to the slightly higher DMT thresholds of 32 °C for Adelaide and 30 °C for Melbourne established in the independent health studies.

Table 2: Severe DMT thresholds ($\hat{T}_{sev}$) for Australian locations.

Station number	Place name	DMT 95th percentile	Threshold T °C
003003	Broome	31.8	33.3
009021	Perth	27.9	32.2
014015	Darwin	30.7	31.6
023090	Adelaide	26.0	31.5
029127	Mount Isa	32.7	35.1
031011	Cairns	28.8	30.4
040211	Archerfield (Brisbane)	26.7	29.0
062101	Mudgee	24.9	28.7
066062	Sydney	24.6	27.8
070339	Tuggeranong (Canberra)	22.2	25.9
072150	Wagga Wagga	27.1	31.5
079028	Longerenong	25.7	30.9
086071	Melbourne	24.2	29.1
094029	Hobart	19.6	23.6

A separate study conducted by PricewaterhouseCoopers (2011) established severe *EHF* thresholds for seven Australian cities based on an examination of excess deaths over the period 1990 to 2009.

Excess mortality was used as it was difficult acquiring heat-related death data in the time available for this study. Within the limited span of daily mortality by capital city data available from the Australian Bureau of Statistics (1990 to 2009), excess deaths were calculated as the difference between actual deaths observed and assumed average daily deaths. The methodology for calculating average daily deaths accounted for population changes influencing the number of deaths observed, past trends in population mortality and changes in demographic mix, and the variation in number of deaths experienced in different seasons throughout the year. Pairing of actual deaths with *EHF* values was used to identify days that formed part of a heat event.

Results from this study are compared in Table 4 with data from Table 1 and Table 2. The relative values in derived severe *EHF* values are largely similar between these independent studies.

Table 3: Severe *EHF* and daily temperature thresholds for Australian locations derived by the statistical technique (columns 3 and 4) and the excess death technique (columns 5 and 6). Column 2 shows the 95th percentile for DMT.

Location	T_{95} (°C)	*EHF* threshold (°C^2), Table 1	T threshold (°C), Table 2	*EHF* threshold (°C^2), PwC	T threshold (°C), PwC
Brisbane	26.7	5.4	29.0	6.2	29.1
Sydney	24.6	10.2	27.8	10.8	27.9
Canberra	22.2	14.2	25.9	12.3	25.7
Hobart	19.6	15.7	23.6	17.0	23.7
Perth	27.9	17.9	32.2	15.4	31.8
Melbourne	24.2	24.2	29.1	27.5	29.4
Adelaide	26.0	30.7	31.5	31.4	31.6

These results support the use of this methodology for establishing a severe heatwave threshold that is sensitive to established heat-health impacts. The PwC health studies were confined to large population centres where it was possible to derive meaningful statistical indicators.

4.3 Extreme Heatwaves and Heat Health

The *EHF* provides a heatwave-intensity measure that exhibits a quadratic response under rising short-term and long-term daily temperature anomalies. A threshold for severe heatwave outcomes has been demonstrated under Australian conditions, where excess mortality and morbidity are detected. However, notable extreme heatwave events around the world have had high impact. We therefore seek to more fully establish the connection between high *EHF* values and mortality/morbidity data.

4.3.1 Australian 2009 Extreme Heatwave and Heat Health

In January and February 2009, nearly 500 excess deaths occurred across southeast Australia during a particularly intense heatwave. Figure 9 shows Adelaide's *EHF* time series, in conjunction with heat-related mortality (Mason et al. 2010). South Australian coronial investigations showed that 58 heat-related deaths occurred in a sequence, which can now be seen to be well correlated with the sequence of *EHF* values.

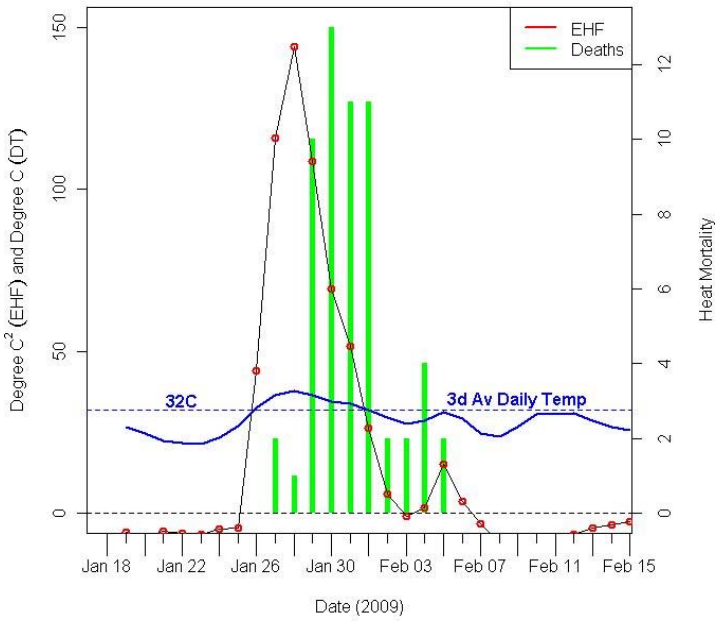

Figure 9: Heat-related mortality (green bars, right axis) and *EHF* (red squares, black line, left axis) for the 2009 severe heatwave in South Australia. The three-day-average DMT is superimposed, plotted against the first day of the three-day period (blue line), together with the 32 °C DMT threshold.

The coincidence of *EHF* and three-day-average DMT in the vicinity of their respective severity thresholds (31.5 °C^2 and 32 °C) is illustrated in this graph. The *EHF* as a lead indicator by two days is a much better predictor of the mortality than the three-day-average DMT for these mortality data. The first day in the four-day period of peak mortality is 29 January, which is the last day of the first three-day period (27-29 January) with *EHF* > 100 °C^2, consistent with the notion that heat stress impacts over several days.

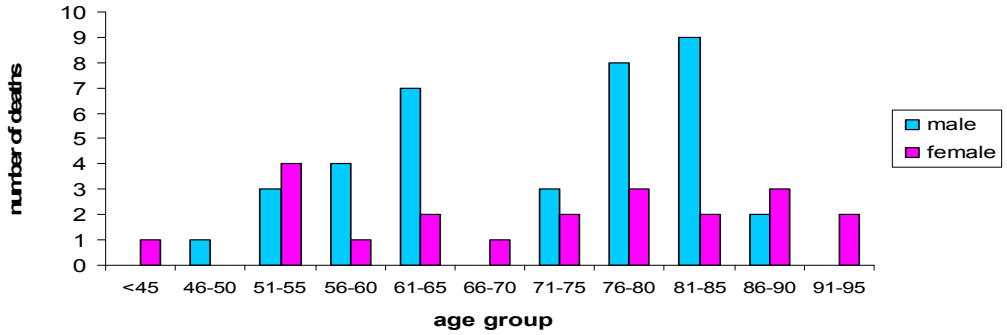

Figure 10: Heat-related-mortality age distribution for the 2009 severe heatwave in South Australia, (data from Mason et al. 2010).

A wide age demographic was impacted during the 2009 severe heatwave, as shown in **Figure 10**. Studies in heatwave mortality normally focus on those 65 years of age and older where increased presence of disease, reduced physical functionality and management of medication results in greater vulnerability. The presence of substantial mortality below 65 years of age on this occasion is an indicator of the greater human impact arising from a high-intensity (or extreme) heatwave.

In their study of French mortality from the 2003 heatwave, Toulemon and Barbieri (2006) considered that many of the victims were at least independent enough to live by themselves, suggesting that the majority would have likely lived many years without the heatwave. They estimated less than a third of the 15,000 deaths of August 2003 were attributable to "harvesting",

with the remaining being expected to live for another eight years in the absence of the heatwave. The harvesting effect implies the timing of mortality being displaced by only a few days or weeks, with the same numbers of deaths occurring over a sampling period greater than the event duration. This is in contrast to analyses of heatwave mortality across broader time scales (rather than by event) by Deschenes and Moretti (2009) and Hajat et al. (2005), who attribute mortality almost solely to harvesting. The greater human impact evident during extreme heatwaves offers evidence of mortality impact that exposes a group that is not vulnerable to mild to severe heatwaves. Interestingly, a nine-year (1996-2004) study by Huang et al. (2012) estimates the effect of extreme temperatures on years of lost life due to cardio-vascular disease. Their work reduced the influence of deaths in frail elderly people attributable to prior studies and found up to 264 years of lost life in Brisbane for heatwaves greater than or equal to four days at 95% confidence. Notably, this study period includes Brisbane's two top *EHF* events in its 120-year record (Section 6.1.7, Table 8), thereby biasing their study with extreme event outcomes. Harvesting and lost years of life are likely responses to severe and extreme heatwaves respectively.

Morbidity is an under-reported impact with significant ongoing human and economic consequences that are currently difficult to assess, requiring further research. The morbidity response in Figure 11 for Melbourne in early 2009 is similar to the mortality response shown in Figure 9 for Adelaide at the same time. *EHF* leads ambulance task loads by two days during the same severe heatwave in Melbourne. The lagged response to severe heatwaves is described in the literature, and it is not surprising to learn that mortuary admissions also lag, as most mortality are associated with social isolation (Vandentorren et al. 2003). 374 excess deaths across Victoria are ascribed to this event (Victorian Department of Health 2009).

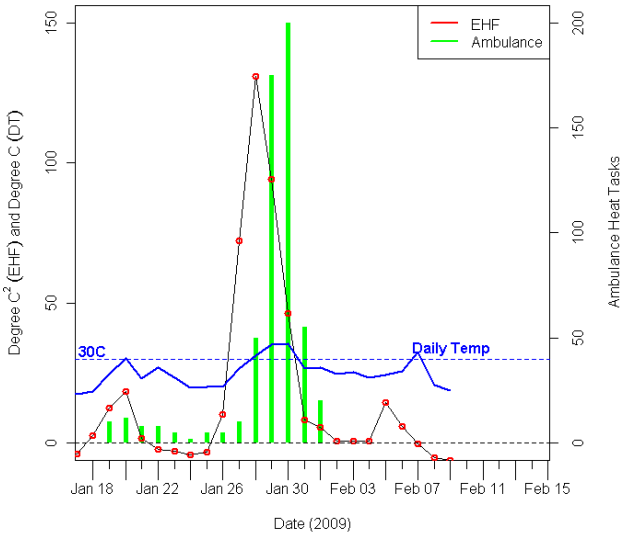

Figure 11: Melbourne *EHF* (red squares, black lines, left axis), ambulance heat-related tasks (green bars, right axis), DMT (solid blue line) for the 2009 heatwave and Victorian Department of Health warning threshold of 30°C (dashed blue line).

A spatial interpretation for part of this excess heat event can be seen in Figure 12. The maps show the spatial spreading of the peak *EHF* amplitude from the Eyre Peninsula on 26 January across the southeast of South Australia into western Victoria on 27 January, followed by further intensification in the western vicinity of Melbourne in Victoria on 28 January 2009, where the peak *EHF* values for this event were observed. These maps provide an opportunity to evaluate the breadth of heatwave impact, particularly when viewed in conjunction with site-specific time series of *EHF*.

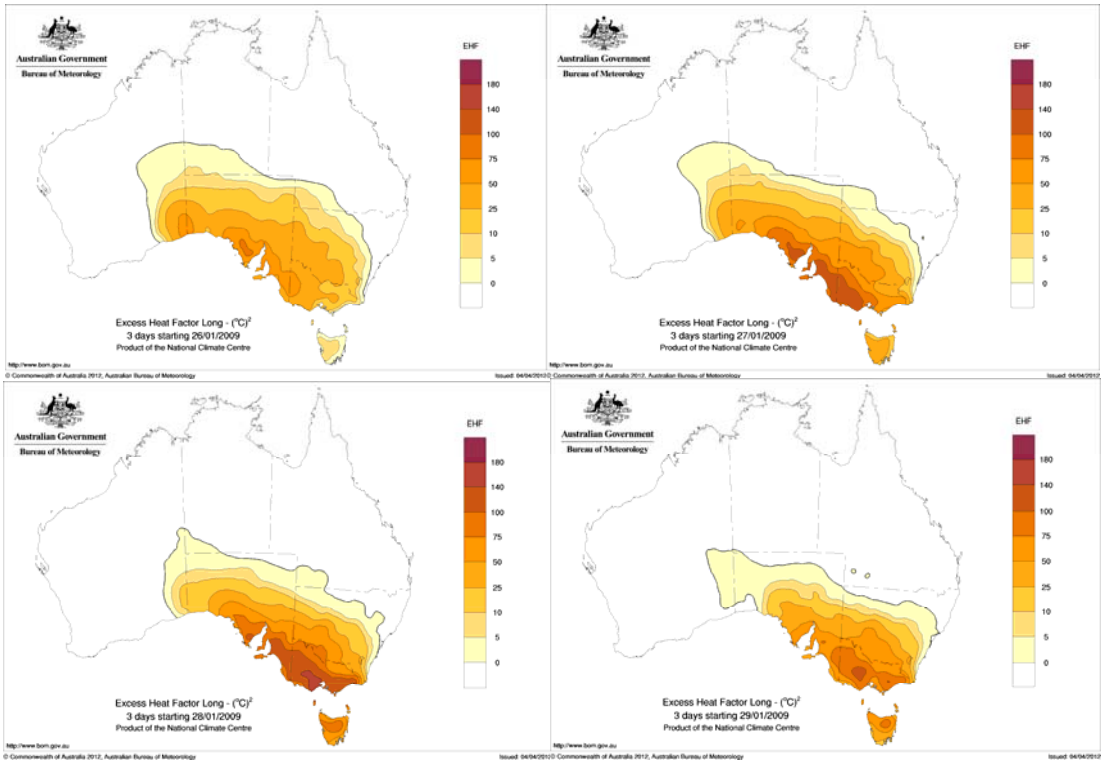

Figure 12: *EHF* for 26-29 January 2009, calculated using gridded DMT analyses.

4.3.2 Extreme Heatwave Comparisons and Heat Health

Extreme heatwave events have also been examined for Paris, Moscow and Chicago (Nairn 2011, Appendix B). The time series for each of these events is comparable in magnitude to the Australian 2009 extreme heatwave event. The peak intensity of each heatwave is two to four times larger than the severe *EHF* threshold value. The Paris extreme heatwaves peaked near 60 °C^2, approximately three times the severe *EHF* threshold of 18 °C^2, whilst Chicago and Adelaide peaked at over four times their severity thresholds (Table 4).

Table 4: Comparing severe heatwave threshold, intensity, heat load, event length and average intensity as measured by *EHF* (°C^2). The Paris 2003 and Moscow 2010 extreme heatwaves were themselves preceded by significant heatwaves, values in brackets. Estimated mortality is also shown.

	Paris 1976	Paris 2003	Chicago 1995	Adelaide 2009	Moscow 2010
Est. mortality (people)	6,000	15,000	700	500	10,900[7]
Severe *EHF* threshold (°C^2)	18	18	13	32	20
Peak *EHF* (°C^2)	63	(25) 62	57	144	(21) 46
Heat load (°C^2)	647	(80) 574	174	566	(81) 818
Event length (days)	17	(14) 17	7	12	(8) 49
Average heat load (°C^2)	38	(6) 34	25	47	(17) 17

Moscow peaked at 46 °C^2, just over twice the severity threshold, although it is interesting to note this occurred during an exceptionally long event. [Indeed, a consideration of this event motivated

[7] Estimated excess deaths in Moscow (Barriopedro et al. 2011). The report includes an estimate of 55,800 excess deaths across Russia during this heatwave, although they are not exclusively heat-health related and include drownings, fires, etc.

the minor reformulation of the *EHF* definition, described above.] An alternative impact analysis considers the heat load for each event, where event heat load may be considered in conjunction with event length. In the European heatwaves of 1976, 2003 and 2010, the heatwave intensity rose two to three times above the severe *EHF* threshold. Whilst Moscow experienced lower intensity, it was a much longer event (49 *EHF* days!) with a larger accumulated heat load.

Chicago and Adelaide both reached heatwave intensities over four times the severe *EHF* threshold. The southeast Australian indicators for heat load (566 $°C^2$) and average intensity (47 $°C^2$) are very high, suggesting that the population is resilient to heatwave, and was protected to some degree by current infrastructure and practices. The higher mortality toll in Chicago (700), compared to Adelaide (500) at lower peak *EHF* (57 $°C^2$), heat load (174 $°C^2$) and average intensity (25 $°C^2$) suggest the vulnerable population was less resilient.

5. HEATWAVE CLIMATOLOGIES

Spatial analysis of *EHF* can now provide a new understanding into the distribution of Australian heatwaves in space and time. We use gridded daily maximum and minimum temperature analyses from late-1957 to 2011 (Jones et al. 2009). These analyses extend back to 1911, although many studies (e.g. Trewin and Vermont 2010) have not used pre-1956 data, as there are considerably fewer pre-1957 digitised Australian daily temperature data than post-1956 data at the present time. [Future digitisation of extant paper records may improve this situation in time.] Even though recent work (Trewin 2012) has homogenised some of the earlier data, the lower site density in the Trewin (2012) dataset considerably reduces spatial detail in the analyses. Analyses of *EHF* using site data can obviously be extended much further back where this data exist, and the Trewin (2012) dataset is an obvious candidate for such an analysis. At some sites, these data extend back to the mid-19th century.

The more recent spatial record is presented first to establish the geographic context for heatwaves, followed by station records to establish heatwave variability over a longer timeline.

5.1 Australian Climatology

Figure 13 shows a north-south gradient in mean positive *EHF* (i.e., the mean of the positive *EHF* values, the much more frequent non-positive values being excluded from the calculation) which is highest around the southern coasts of the continent and extremely low in the north. Investigation of the *EHF* distribution demonstrates its signal amplitude diminishing with lower latitudes. At low latitudes, warm season temperatures are high but with little daily variability, resulting in low *EHF* values. Excess heat events are naturally rare in latitudes where high temperatures are sustained (because large EHI_{accl} values don't occur). Consequently severe heatwaves are even less likely.

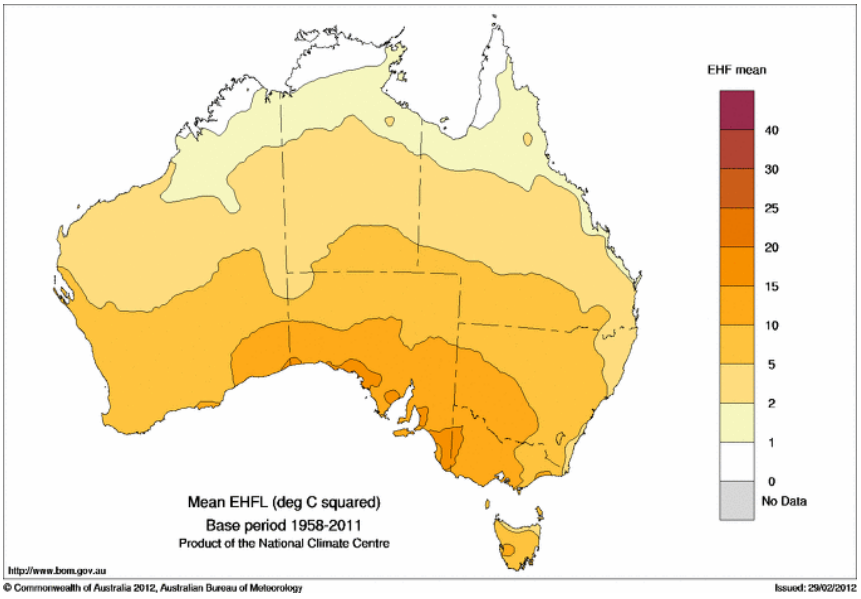

Figure 13: Mean positive *EHF* (in °C^2) across Australia for period 1958 to 2011, calculated using gridded DMT analyses.

The maximum *EHF* for the 1958-2011 period shown in Figure 14 has a similar spatial pattern to that shown in Figure 13. There is, however, significant evidence of the influence of particular events. The intensities of the 1960 (central Australia) and 2009 (south and southeast Australia) heatwaves are evident (e.g. compare Figure 13 with Figure 12). The evidence of these particular

heatwaves raises a question over what would be a reasonable sample period for determining a representative mean *EHF* for Australia.

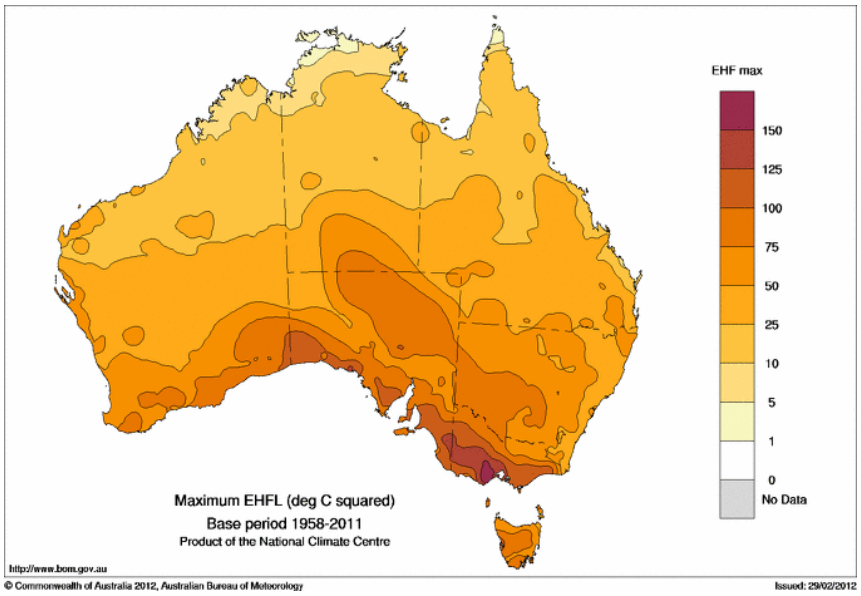

Figure 14: Maximum *EHF* across Australia for the period 1958 to 2011.

This is tested using Adelaide site data in Table 5 where the standard error has been calculated for a range of epochs.

Table 5: Adelaide mean *EHF*, number of *EHF* events, *EHF* standard deviation, Standard Error (units of °C^2), average Standard Error and *EHF* Standard Error at 95% confidence for a range of epochs.

Period (yrs)	Epoch	Mean *EHF*	*EHF* events	Std Dev	Standard Error	Average SE	95% CI
20	1891-1910	22.47	220	22.2	4.96	4.08	7.041
20	1911-1930	15.82	166	17.40	3.89		
20	1931-1950	19.47	152	19.36	4.33		
20	1951-1970	13.51	167	13.76	3.08		
20	1971-1990	15.98	185	16.76	3.75		
20	1991-2010	18.45	248	20.02	4.48		
40	1891-1930	19.61	386	20.52	3.25	2.96	4.985
40	1931-1970	16.35	319	16.90	2.67		
40	1971-2010	17.39	433	18.71	2.96		
60	1891-1950	19.57	538	20.18	2.61	2.44	4.077
60	1951-2010	16.31	600	17.55	2.27		
120	1891-2010	17.85	1138	18.90	1.73	1.73	2.868

At 95% confidence, the mean *EHF* (17.9 (°C)^2) is accurate to within ±7.04, ±4.99, ±4.08 or ±2.87 (°C)^2 for 20, 40, 60 and 120 year epochs respectively. This shows that Adelaide's long-term (120-year) *EHF* sample mean accuracy varies by about 16% at a high confidence level. The 60-year and 40-year records vary in accuracy by 22 to 28%, and at 20 years by 39%. The AWAP charts have been constructed from a 54-year record corresponding to about 25% error variation in the sample mean (95% confidence interval) found for Adelaide's site record.

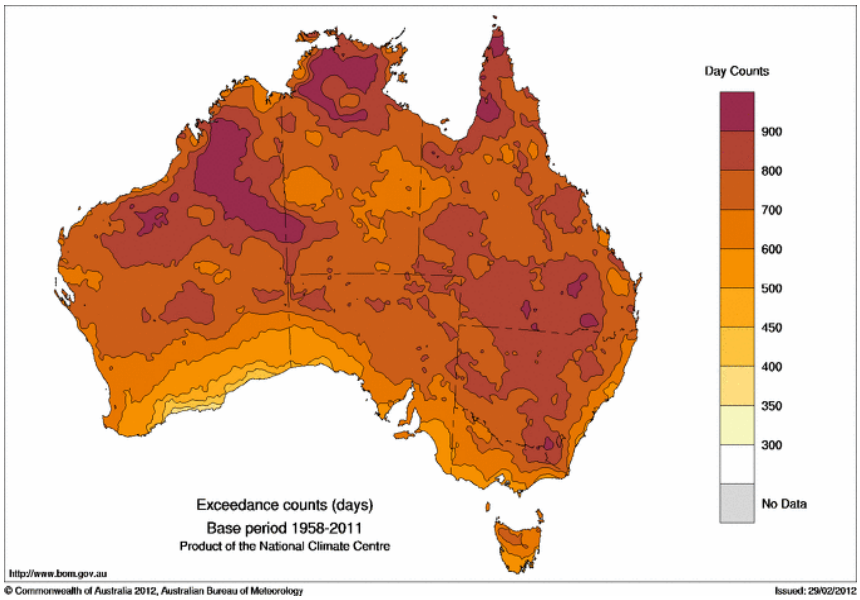

Figure 15: Number of positive *EHF* periods in the period 1958-2011.

Figure 15 provides an indication of the number of *EHF* events for the period sampled. It shows the number of three-day periods with positive *EHF* at each grid point. No exclusion is made in the counting for overlapping three-day periods. So, for example, a four-day period counts as two three-day periods. Higher numbers of positive-*EHF* periods are seen in the north of the country, but with lower amplitude (Figure 13), indicating a hot but stable climate. Lower numbers of events with higher *EHF* in the south of the country indicate stronger (more impactful), less frequent, episodic events.

The two approaches to determining the severe *EHF* threshold proposed above are shown in Figure 16 (using the turning-point method) and Figure 17 (EHF_{85}). These maps have been derived utilising the techniques discussed in Section 3.1. There is very little difference between these charts, indicating stability in the methodology and calculations.

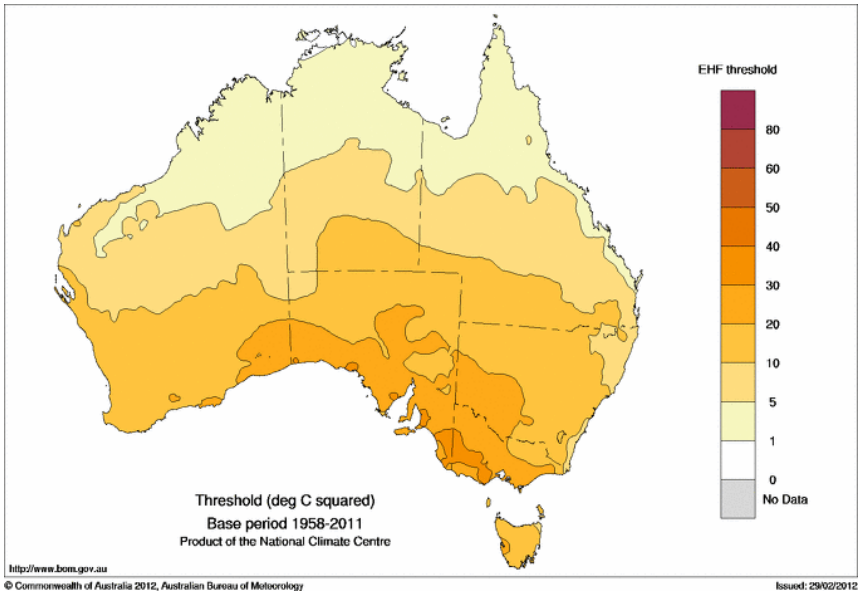

Figure 16: Severe *EHF* threshold derived via the "turning-point" method.

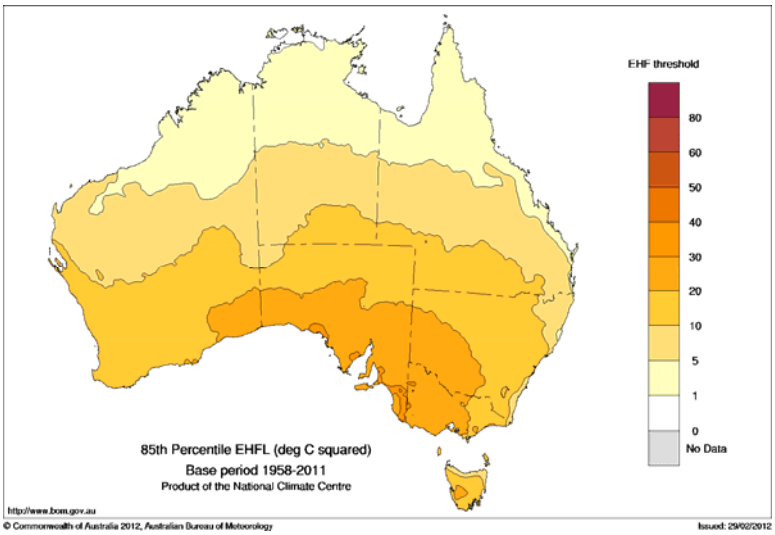

Figure 17: Severe *EHF* threshold determined from the 85th percentile of the positive *EHF* distribution (base period 1958-2011).

Finally, the proposed severe *EHF* threshold (using the "turning-point method") has been tested against the 1958-2011 period to determine a gross warning rate. Figure 18 shows a maximum of three events per year predominantly occurring in central Western Australia, the Top End of the Northern Territory and inland areas of Queensland and New South Wales. Regions of Australia north of the Tropic of Capricorn should be dismissed, as the intensity of *EHF* is very low, denoting hot and humid wet-season conditions with very little heat variability. Some parts of central Western Australia are difficult to assess, due to low observational density impacting the accuracy of the gridded analyses. Errors in this region are hopefully minimised, due to the anomaly methodology employed in the calculation of *EHF*. Where these data are reasonably stable, the actual incidence of severe heatwave conditions will exhibit interannual and event variability which has not been analysed here, but will be the subject of future investigations. However, it is reasonable to expect that some years will not experience severe heatwaves, whilst others will either have multiple events or event lengths exceeding three *EHF* days (five-day events).

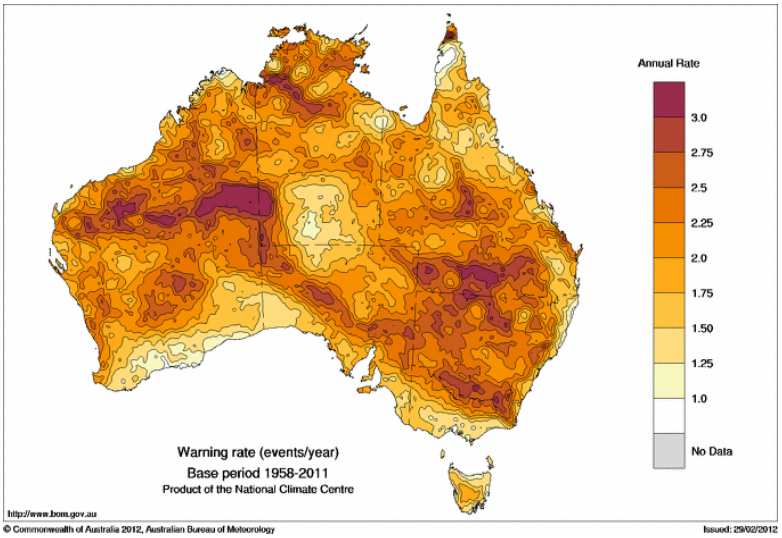

Figure 18: Severe *EHF* warning rate, calculated as the number of three-day periods per year exceeding the threshold set by the "turning-point" method. Periods may overlap in the calculation.

5.2 Global Climatology

Global trends in heatwaves and warm spells have been examined for the 60-year period 1951-2011, via a multi-index multi-aspect framework (Perkins et al. 2012). Indices for three-day spells of maximum temperature, minimum temperature and *EHF* were separately examined over annualised and five-month summer periods. The multi-aspect framework considered the total number of events, the length of the longest event, the total number of days satisfying each index criteria and the hottest day (amplitude) of the hottest event.

The study established an increasing trend for heatwave frequency, intensity and duration across the globe. The rising trend in globally averaged length of heatwaves and peak amplitude are shown in Figure 19. The close correlation over time is evident emphasising their qualitative similarity.

The global spatial trend in Figure 20 demonstrates regional variability. It is important to note that the *EHF* "HWF warm spell" signal in Figure 20g dilutes this warm season index over the annualised period. [In Perkins et al. 2012, HWF is the total number of days satisfying a heatwave index criterion.] A comparison of Figure 20d, 20e and 20f demonstrates the strong contribution minimum temperature heat anomaly periods contribute to global trends outside (frequency) and inside the heatwave (five-month summer period) season.

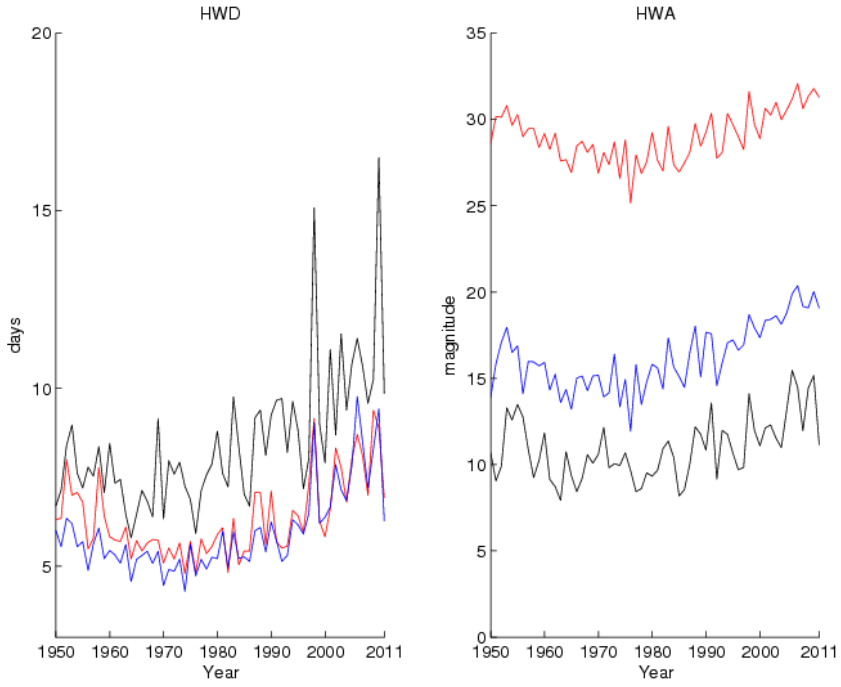

Figure 19: Annual globally averaged warm spell time series of HWD (heatwave event length, left panel) and HWA (peak magnitude of hottest event, right panel) for TX90pct (red), TN90pct (blue) and *EHF* (black). HWD units are average days/year, and HWA units are °C for TX90pct and TN90pct, and *EHF* (°C^2; excess heat) units for *EHF*. See Table 1 for corresponding trends. Figures from Perkins et al. 2012.

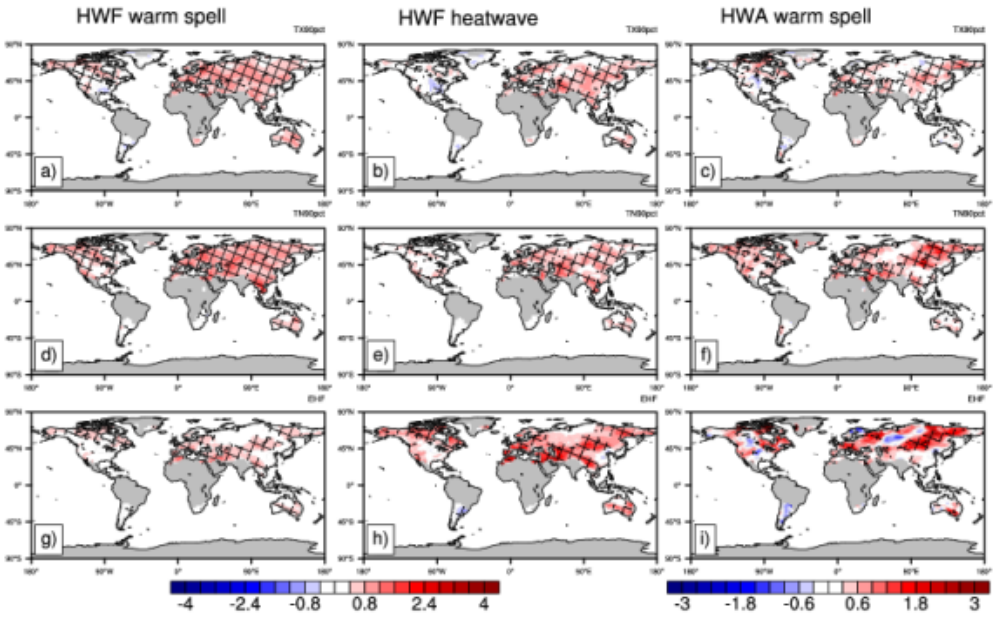

Figure 20: Warm spell (left column) and heatwave (middle column) trends in the number of days participating in an event (HWF), in which conditions persist for at least three consecutive days; and warm spell (right column) trends in the peak of the hottest event (HWA). Indices include TX90pct (a, b, c), TN90pct (d, e, f) and *EHF* (g, h, i). Trends are for the period 1950-2011, computed by the non-parametric Kendall slope estimator (Sen, 1968). Units are percentage of days per season/decade for the left and middle columns. Units for the right column are °C/decade for TX90pct and TN90pct, and $°C^2$/decade for *EHF*. Hatching represents where trends are significant at the 5% level, and grey indicates areas where there are insufficient observations for this study. Figures from Perkins et al. 2012.

5.3 Site-specific Climatology

5.3.1 Australian Sites

Australian station temperature data in some instances extend back to the mid-1800s. An analysis of the climate record for a number of stations is presented requiring the reader to consider each station's length of record. The longest record analysed is for Melbourne (1855), with subsequent records shorter in length: Hobart (1882), Adelaide (1887), Brisbane (composite sites, 1887), Perth (1897) and Alice Springs (1941).

Over the 130 years shown in Table 6, the incidence of top-ranked heatwave events is evident at the very start and end of the record, particularly notable for Melbourne and Adelaide, noting that the use of the now-standard Stevenson screen for the housing of daily maximum and minimum temperature thermometers cannot be assumed for pre-1910 data, and so temperature data from the mid-1850s are not likely to be completely homogenous with recent data. The late 19th and early 20th centuries are notable for the breadth of heatwaves incident across eastern and southeast Australia. Perth is a notable exception where the most significant heatwave occurred in 1933, with a steady decline in significance thereafter. The reduced significance of heatwaves across east and southeast Australia in the 1960s and 1970s is counterbalanced by a relative increase in significant heatwaves in the west.

Table 6: Top-ranking *EHF* intensity listed by Year for Melbourne, Adelaide, Hobart, Brisbane and Alice Springs, for period 1855-2010. Note that only the highest *EHF* for each year is included in the ranking. An asterisk denotes temperature/*EHF* record commenced recently.

Year	Melbourne		Adelaide		Brisbane		Hobart		Perth		Alice Springs	
	Rank	*EHF*	Rank	*EHF*	Rank	*EHF*	Rank	*EHF*	Rank	*EHF*	Rank	*EHF*
1875	1	140										
1887				*		*	4	84				
1897			4	87			1	142		*		
1899	6	69	2	112	9	21	9	67				
1900			3	93								
1908	4	86	12	68								
1933									1	73		
1940			10	80	3	29	12	57				
1941											4	34*
1959	3	100										
1960											1	69
1965									2	67		
1968					5	25			3	67		
1972					4	27					5	32
1982			8	84			3	86				
1991									4	57		
1994					8	22	2	113				
1996									8	49	2	45
2000					2	35					3	34
2004					1	40						
2009	2	131	1	144								

5.3.2 New South Wales/Australian Capital Territory Sites

An analysis is also presented for a denser array of sites within New South Wales and the Australian Capital Territory, where some stations are much more recent. From west to east, these stations commence with Canberra (commencing in 1939), Mudgee (1962), Katoomba (1957), Richmond (1940) and Sydney's Observatory Hill (1859). The analysis period presented in Table 7 ends in 2009.

Table 7: Ranked *EHF* by date and station for Canberra, Mudgee, Katoomba, Richmond and Sydney's Observatory Hill. Significant heatwave events have been highlighted: 1960 (pink), 1968 (blue), 1979 (green) and 2009 (purple).

Canberra		Mudgee		Katoomba		Richmond		Sydney	
EHF	**Date**	***EHF***	**Date**	***EHF***	**Date**	***EHF***	**Date**	***EHF***	**Date**
55.4	07/01/1979	38.1	31/01/1968	70.5	09/01/1979	49.4	08/01/1979	73.9	26/01/1960
52.1	08/01/1979	35.4	30/01/1968	65.8	08/01/1979	43.4	07/01/1979	58.1	25/01/1960
51.7	31/01/1968	29.3	20/02/1965	61.9	07/01/1979	40.2	04/02/1973	46.9	27/01/1960
50.8	30/01/1968	27.7	08/01/1979	58.4	06/02/2009	39.5	09/01/1979	45.2	11/01/1896
47.4	06/02/2009	25.9	23/01/1982	53.0	25/11/1997	36.7	19/12/1994	41.4	22/12/1972
42.8	09/01/1979	23.9	17/01/1987	48.9	27/11/1997	34.1	06/02/2009	38.5	23/12/1972
42.2	06/01/1979	23.1	21/02/1965	48.6	06/01/1979	34.1	21/01/1992	37.3	15/02/1926
39.1	19/12/1994	22.9	07/01/1979	48.2	13/01/2005	32.2	05/02/2009	35.0	21/12/1972
36.1	05/02/2009	22.4	20/12/1994	47.8	26/11/1997	31.3	22/12/1972	35.0	04/02/1973
34.7	23/01/2001	22.0	19/02/1965	46.4	26/01/1960	31.3	21/12/1972	34.7	22/01/2009
32.3	13/02/2004	21.7	26/01/1981	43.7	27/01/1960	30.8	26/01/1960	33.5	12/01/1870
32.1	12/02/2004	21.2	09/01/1979	42.0	21/01/1992	29.9	06/01/1979	33.1	08/01/1983
31.1	02/01/2004	20.8	02/01/1990	41.1	10/01/1979	28.2	11/02/1979	30.9	12/01/1896
31.0	15/12/1945	20.8	08/02/1983	39.9	08/02/1983	27.2	23/01/2001	29.1	12/10/2004
30.0	24/01/2001	20.7	25/01/1981	39.7	26/12/1963	26.6	20/12/1972	28.7	08/01/1929
30.0	12/01/1988	20.2	16/12/1982	39.0	20/11/2009	25.5	31/01/1968	26.6	06/01/1994
29.6	23/01/1982	19.9	22/01/1982	38.8	21/11/2006	25.2	02/01/1994	26.5	20/11/2009
29.5	13/01/1988	19.4	24/01/1981	35.5	07/02/2009	25.0	03/02/1973	26.3	07/01/1929
29.3	01/01/2004	19.4	27/01/1981	35.3	27/12/1963	24.8	01/01/1955	26.0	23/01/2009
28.7	04/01/1942	19.1	06/01/1979	35.2	28/02/1958	24.8	08/01/1983	25.8	30/01/1977
28.6	10/01/2010	19.0	01/02/1968	34.2	29/01/1961	23.6	30/01/1968	25.2	27/01/1915
28.2	22/01/2001			32.9	14/01/2005			24.6	09/01/1983
28.2	26/01/1947			32.9	27/02/1958				

Heatwave coherence is evident on the regional scale. The 1979 heatwave is the highest *EHF* event in the record for Canberra, Katoomba and Richmond. The 1960 event is the highest ranked *EHF* event for Sydney, with evidence that it is also present and significant at Richmond and Katoomba. Mudgee's highest ranked event is also evident in Canberra and Richmond. The 2009 event which was extreme in southeast Australia is also evident in New South Wales; however it is not evident at Mudgee. The 1960 heatwave is reviewed in the following section.

6. CASE STUDIES

6.1 Australian Heatwaves

There are numerous heatwaves that could be investigated using this new approach. The following are only a sample but serve to illustrate the utility of the Excess Heat Factor in diagnosing the evolution and climatology of heatwaves with this measure.

6.1.1 January 1908

The 1908 extreme heatwave is estimated to have resulted in 246 deaths, including three in Broken Hill, 21 in Melbourne, 83 in country Victoria and 105 in South Australia, (QUT, 2010). "Heat waves and suicides" featured in *The Argus* (Melbourne) on 20 January 1908, noting that eleven suicides had occurred in proportion to the heat during January. "Heat wave in other States" in *The Advertiser* (Adelaide) on 22 January 1908 provided insight into the impact of coincident heatwaves in Melbourne, Horsham, New South Wales and Perth. Over-exertion and frailty featured, with an example of a Melbourne hospital treating 58 people suffering from sunstroke over a six-day period. *The Advertiser*'s reports were limited to noting the death of an elderly couple at Kadina with little to indicate the relative scale of mortality in South Australia. The impact of the local event may not have been evident to the paper's editor, nor would it have been easily followed by the authorities of the day. Heatwave fatalities are handled quietly and efficiently by the medical sector and are invariably under-estimated during an event.

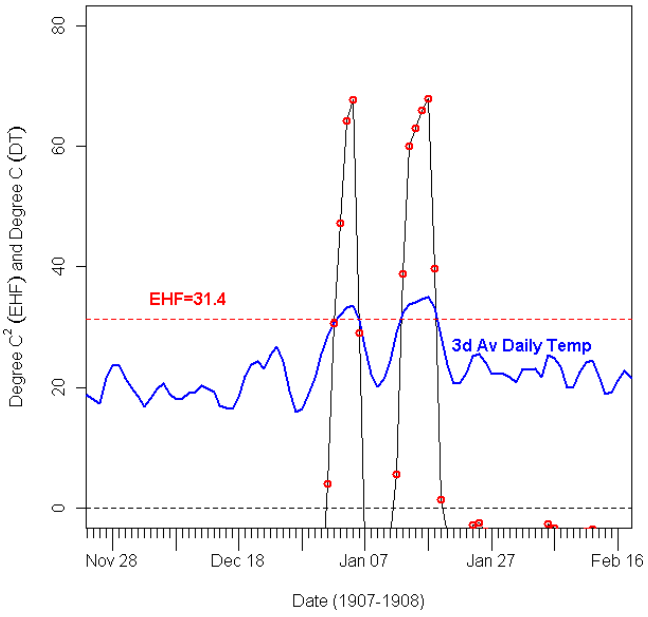

Figure 21: *EHF* (black line, red circles) and three-day-averaged DMT (blue line) for Adelaide, South Australia, in the summer of 1907-1908. The severity threshold *EHF* = 31.4 °C^2 is also shown (dashed red line).

For both Adelaide and Melbourne, this meteorological event is the most comparable with the 2009 extreme heatwave. January 1908 had lower peak temperatures but set records in both locations for consecutive days above 40 °C (National Climate Centre 2009). The time series in Figure 21 shows two severe heatwaves affected Adelaide during January, with sustained peak amplitudes approximately twice the severe *EHF* threshold.

By contrast, the Melbourne time series in Figure 22 shows four distinct heatwaves (i.e., four discrete periods with *EHF* > 0), although only two were of significance. Both events are in phase with the Adelaide heatwaves, although the first just registers as a severe event, whilst the second event is more extreme with a sustained peak at three times the severity threshold.

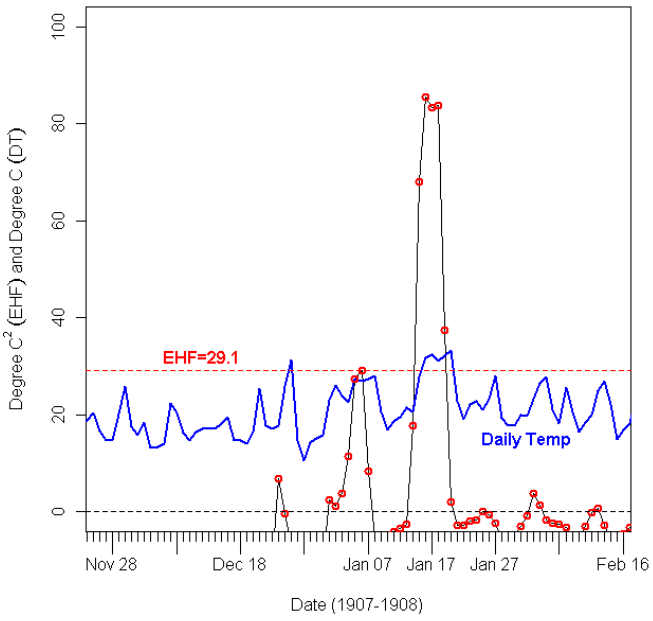

Figure 22: *EHF* (black line, red circles) and DMT (blue line) for Melbourne, Victoria, in the summer of 1907-1908. The severity threshold *EHF* = 29.1 °C^2 is also shown (dashed red line).

Figure 21 and Figure 22 suggest this heatwave had an extreme footprint across southeast Australia. This interpretation is supported by below-average antecedent rainfall (red shades) indicated for southeast Australia in Figure 23. The calculation in the figure uses the Bureau's operational monthly rainfall analyses (Jones et al. 2009).

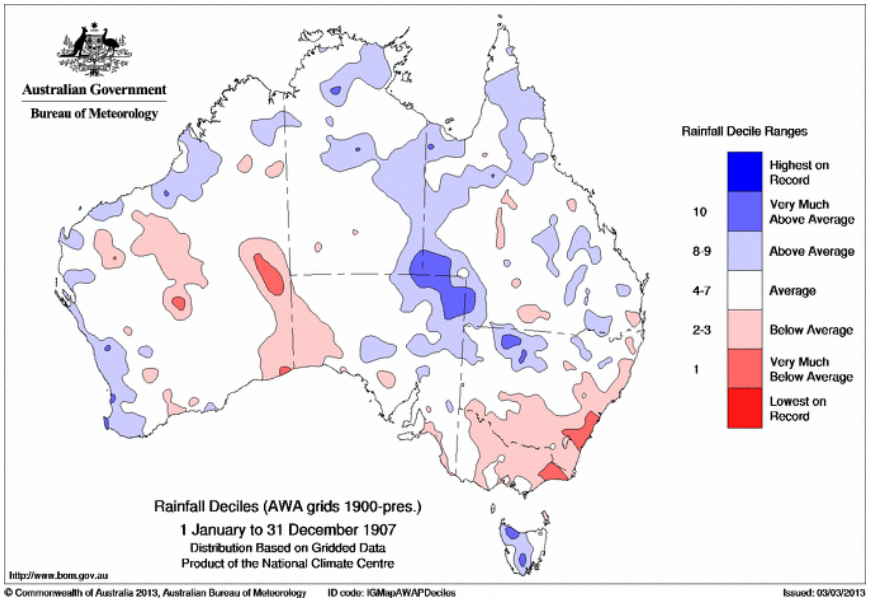

Figure 23: Australian rainfall deciles for 1907.

Further supporting evidence is presented in Figure 24 where both upper-layer and lower-layer soil moisture is very low across Victoria and eastern New South Wales.

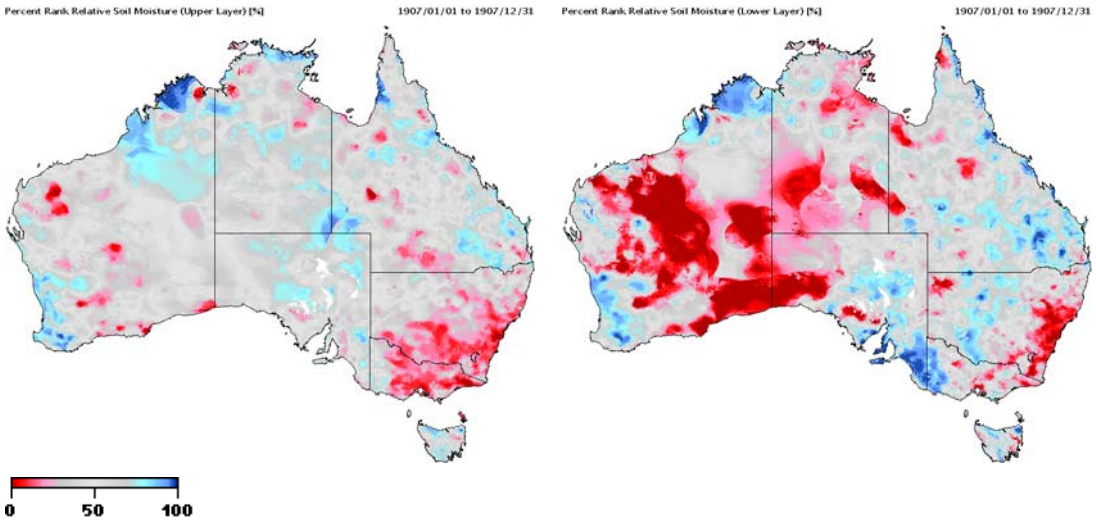

Figure 24: Per cent rank relative soil moisture, upper-layer (left) and lower-layer (right, %) for 1907.[8]

Extrapolating the potential for heatwave activity into Western Australia is a doubtful exercise given the likely poor availability of rainfall data across this region at this time. The reduced rainfall across inland and south east Western Australia evident in Figure 23 and the reduced soil moisture in Figure 24 are likely to be misleading.

6.1.2 January 1939

Black Friday is a notorious event in Australian history, particularly for Victoria where 71 people died, several towns were destroyed and almost 2,000,000 ha of land burnt (Lewis et al. 2006). The strong winds that drove the destructive fires developed in the wake of an extreme heatwave which accounted for 438 deaths across country New South Wales, Victoria and South Australia. These fatalities include 300 from country New South Wales, 5 in Sydney, 19 in the Northwest Slopes of New South Wales, 70 in the Riverina, 35 in Central and western New South Wales and six in Melbourne (QUT, 2010).

It is worth noting the similarity between the cessation of extreme heatwaves in 1939 (Figure 25) and 2009, and the onset of destructive winds that drove the Black Friday (1939) and Black Saturday (2009) bushfires. In each case a strong Southern Ocean front translated across the affected region. The cool Southern Ocean air mass collided with the unusually hot continental air mass producing an extremely strong thermal gradient. The unusually strong and persistent winds that drove these devastating fires were a direct result of the strong baroclinic process created by the heat stored over the continent and coincident Southern Ocean front.

[8] Australian Water Availability Project, http://www.eoc.csiro.au/awap/, accessed October 2012.

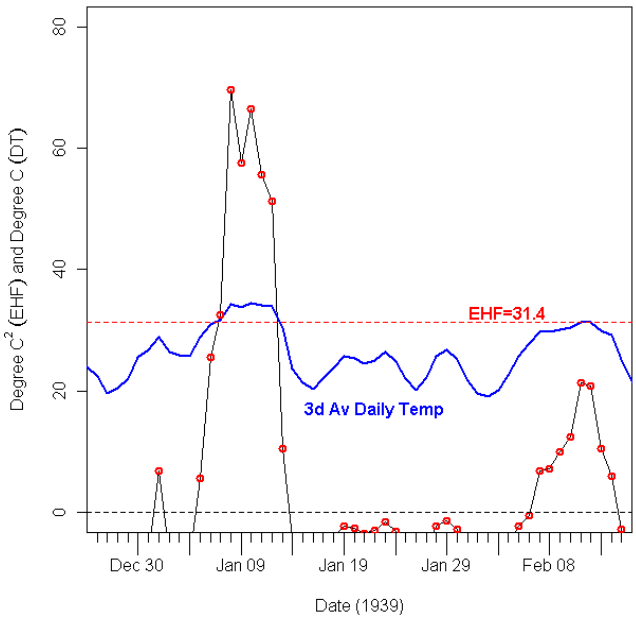

Figure 25: *EHF* (black line, red circles) and three-day-averaged DMT (blue line) for Adelaide, South Australia in the summer of 1938-1939. The severity threshold *EHF* = 31.4 °C^2 is also shown (dashed red line).

Adelaide experienced a week of severe heatwave conditions (Figure 25), with peak *EHF* amplitude about twice the severity threshold. Another heatwave occurred in February but was not severe. Melbourne's *EHF* time series is a little odd given that minimum temperatures were lower that might normally be expected with very high maximum temperatures. This may be accounted for by coastal wind changes that provided intermittent relief whilst further inland the extreme heatwave continued, unrelieved.

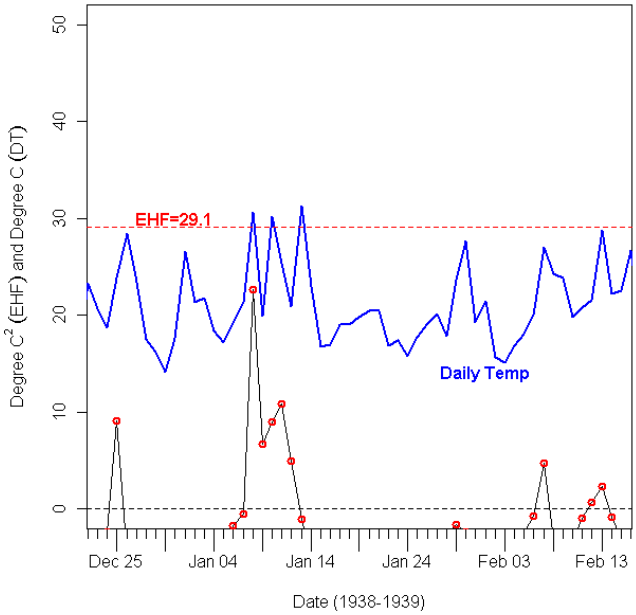

Figure 26: *EHF* (black line, red circles) and DMT (blue line) for Melbourne, Victoria in the summer of 1938-1939. The severity threshold *EHF* = 29.1 °C^2 is also shown (dashed red line).

Antecedent rainfall deficiencies (note that 1938 was markedly drier than 1907) across Victoria) and commensurate soil dryness in Figure 27 and Figure 28 provide strong support for the development of heatwaves across most of the continent. These conditions were also conducive to extreme forest drought conditions amplifying the risk of fire, particularly with the approach of Southern Ocean fronts bring strong temperature gradients and commensurate wind strength.

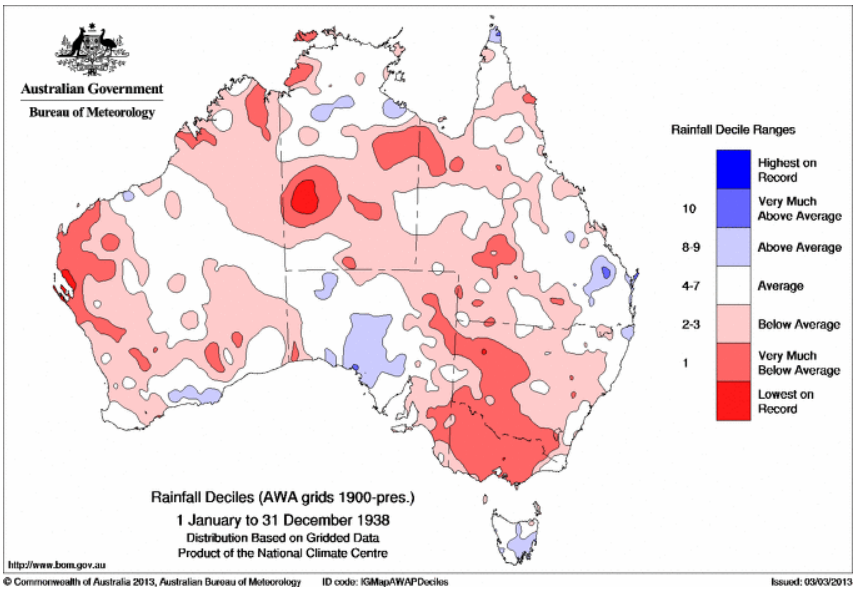

Figure 27: Australian rainfall deciles for 1938.

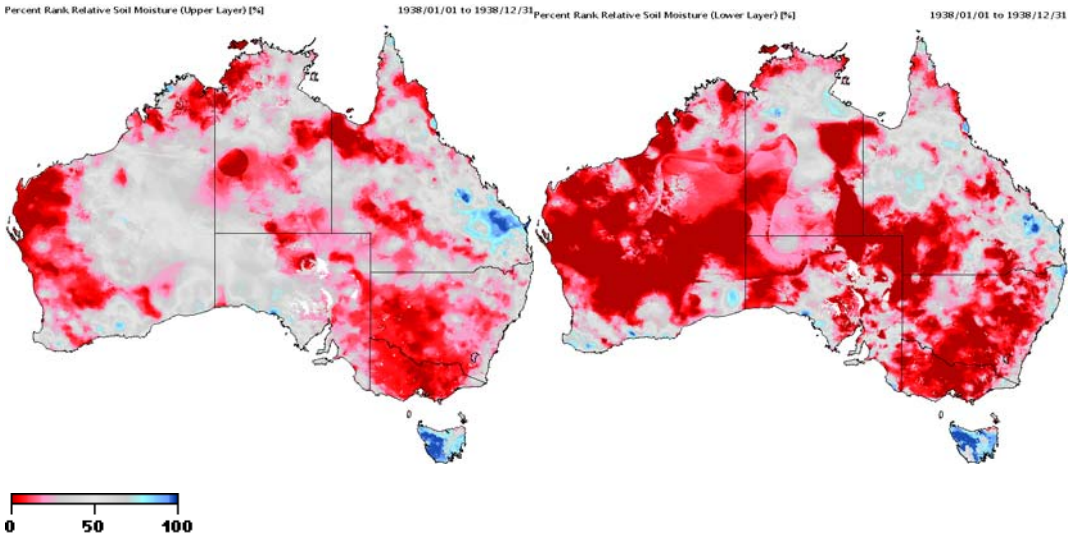

Figure 28: Per cent rank relative soil moisture, upper-layer (left) and lower-layer (right, %) for 1938.

6.1.3 New Year 1960

The newspaper headline "Heatwave Toll Now Seven" (*Sydney Morning Herald*, 5 January 1960) provides an insight to the significance of this heatwave across the interior of Australia with fatalities noted in Broken Hill, Lake Frome and Alice Springs. The Alice Springs *EHF* time series in Figure 29 shows a sudden onset of a severe heatwave that lasted for nearly a week.

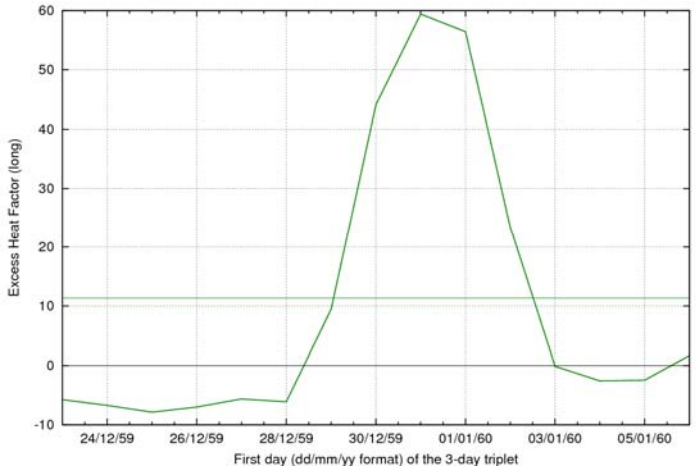

Figure 29: *EHF* at Alice Springs (Post Office) for the period 23/12/1959 to 6/01/1960. The horizontal line represents the 85th percentile for positive *EHF* values (i.e., EHF_{85}). Data based on gridded daily temperature analyses.

The accumulated heat load shown in Figure 30 shows a severe, possibly extreme heatwave that is confined to the interior of the continent, notable for its impact upon rural rather than urban communities. The estimated death toll of 98 people (QUT, 2010) in the 1959/60 summer is very likely attributable to two heatwaves shown in this and the next case study.

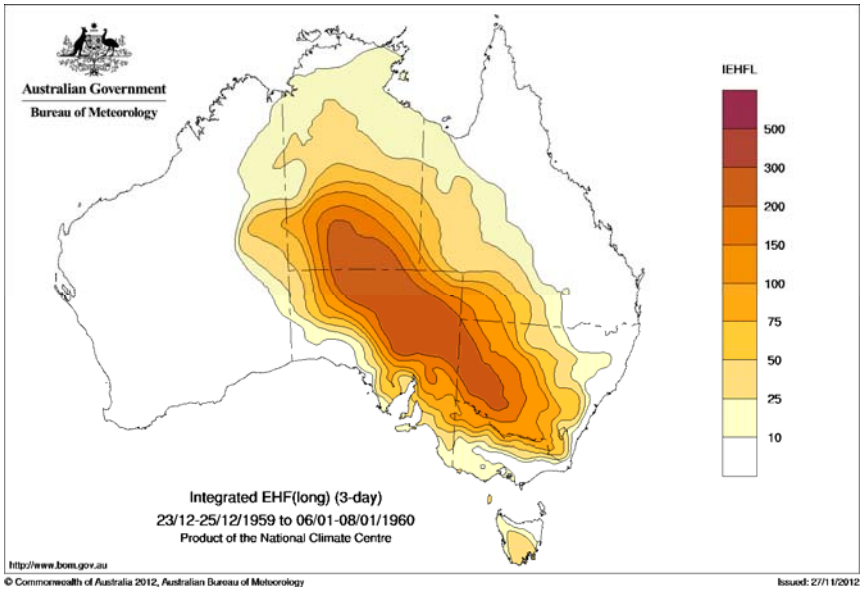

Figure 30: Integrated positive *EHF* for the severe heatwave of January 1960. The event had significant impact from Alice Springs to Broken Hill, across the interior of Australia.

Synoptic charts for MSLP and 500 hPa (Figure 31) demonstrate the heatwave characteristics discussed in Section 3. A large slow surface anticyclone is on this occasion dominates the Tasman Sea extending a ridge up the east coast, with a large shallow heat low dominating the continent.

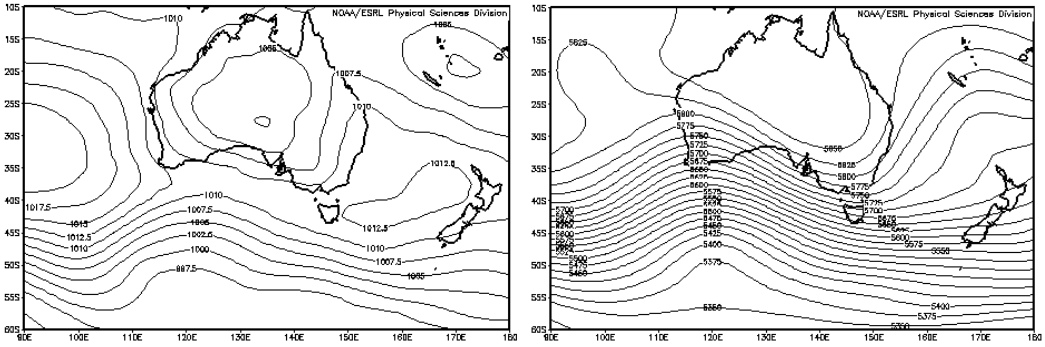

Figure 31: Five-day composite mean MSLP (hPa, left) and 500 hPa Geopotential Height (m, right) for 00UTC 29 December 1959 to 2 January 1960. NCEP/NCAR reanalysis.

Low antecedent rainfall and soil moisture (Figure 32 and Figure 33) create ideal conditions for temperatures that can remain high into the night.

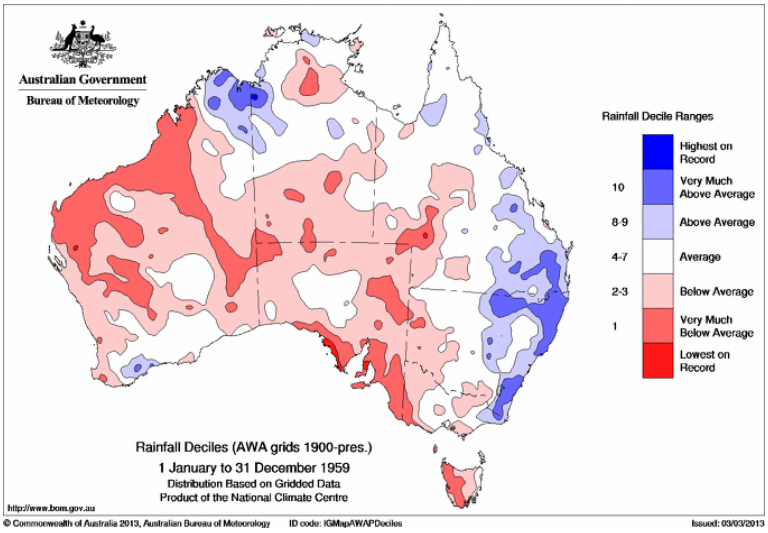

Figure 32: Australian rainfall deciles for 1959.

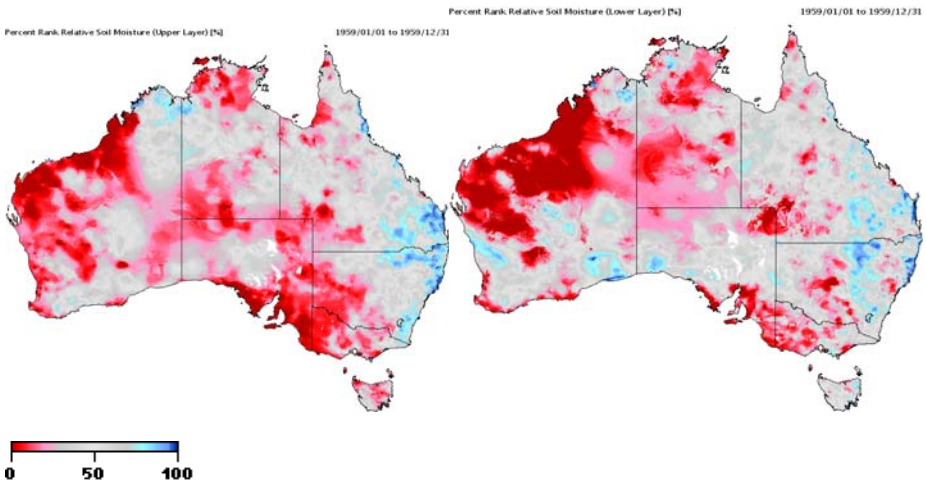

Figure 33: Per cent rank relative soil moisture, upper-layer (left) and lower-layer (right, %) for 1959.

6.1.4 Late January 1960

As shown in Table 6, Sydney's highest ranked heatwave by *EHF* amplitude occurred in late January 1960.

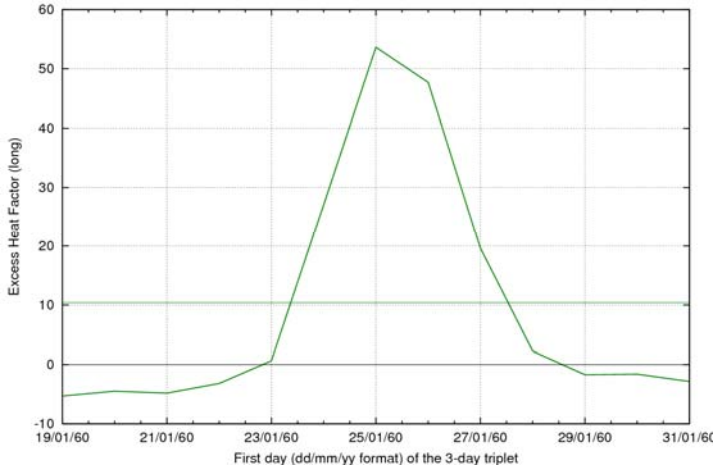

Figure 34: *EHF* at Sydney (Observatory Hill) for the period 19/01/1960 to 31/01/1960. The horizontal line represents the 85th percentile for positive *EHF* values. Data based on gridded daily temperature analyses.

The 1960 *EHF* time series in Figure 34 for Observatory Hill shows a six-day *EHF* event, thereby signifying a heatwave lasting eight days as the *EHF* is a three-day-period index. The event peak is four to five times the magnitude of Sydney's severe *EHF* threshold of 10.2 °C^2 (Table 1), which establishes this event as an extreme heatwave. The heat load shown in Figure 35 reveals the spread of the heatwave across New South Wales into southern Queensland and northern South Australia.

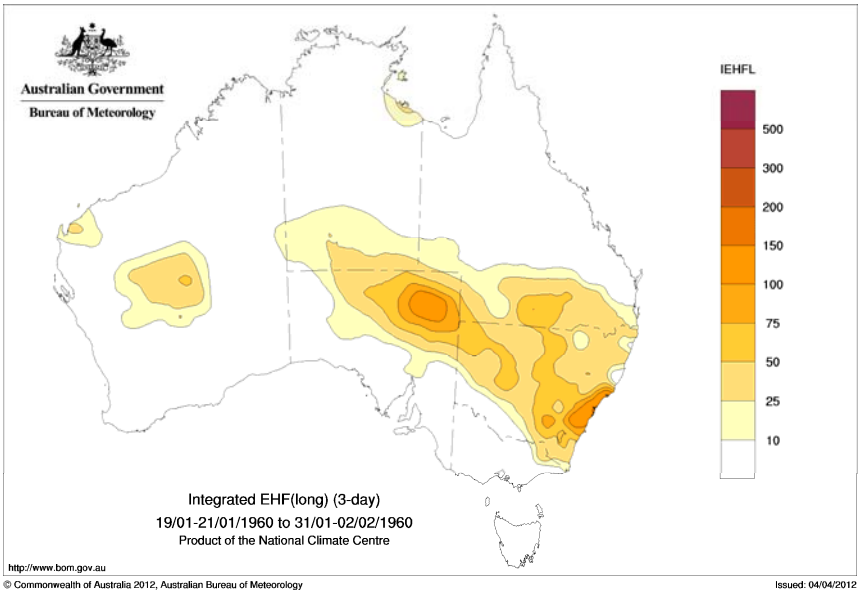

Figure 35: Integrated positive *EHF* for the severe heatwave of 1960. The event peaked around Sydney, NSW, and in northeast SA.

Antecedent rainfall and soil moisture shown in Section 6.1.3 is very low across most of the continent. In contrast the local conditions for the eastern seaboard had very-much-above to highest-on-record rainfall deciles, and very moist soil layers. The heatwave in Sydney on this occasion

relied upon advection of high temperatures from the drier interior in a stable north westerly gradient flow, as shown in Figure 36.

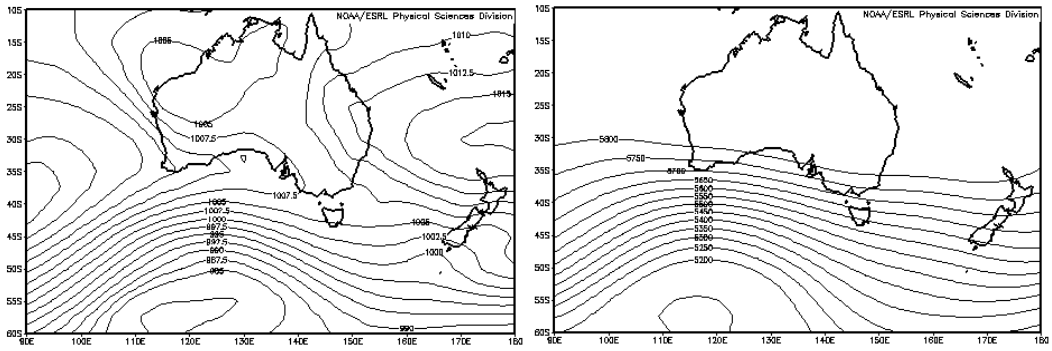

Figure 36: Five-day composite mean MSLP (hPa, left) and 500 hPa Geopotential Height (m, right) for 00UTC 23 January 1960 to 27 January 1960. NCEP/NCAR reanalysis.

6.1.5 Summer 1972/1973

The time series for Alice Springs in Figure 37 shows two to three heatwaves over a period of several weeks. The first heatwave is an extreme event, reaching a peak amplitude approximately three times Alice Spring's severity threshold of approximately 12 °C[2] (see Figure 8), consistent with levels where extreme outcomes may be anticipated.

The heat of this first heatwave was remarkably widespread across the country, and led to the three days 20 to 22 December 1972 being the three hottest days in Australia's instrumental record (1911-2012) in terms of Australian-averaged daily maximum temperature (based on the gridded daily maximum temperature analyses of Jones et al. 2009)[9].

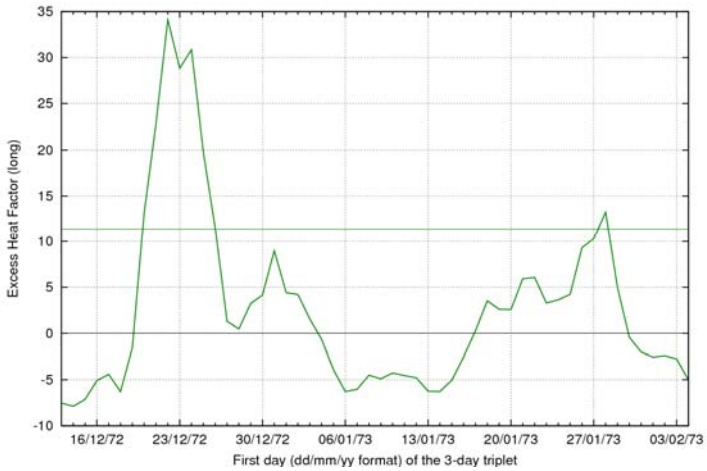

Figure 37: *EHF* at Alice Springs (Airport site) for the period 13/12/1972 to 04/02/1973. The horizontal line represents the 85th percentile for positive *EHF* values. Data based on gridded daily temperature analyses.

The surface heat low centred over the northwest of the continent disguises the dominant long wave ridge, evident in the ridge extending from the Indian Ocean into the anticyclone centred in the

[9] The 1972 record for the hottest day (in area-averaged terms) was ultimately broken during the January 2013 heatwave.

Coral Sea. The depth and dominance of this system is evident in the 500 hPa anticyclone positioned over Western Australia, and the nearly flat, anticyclone mid tropospheric jet lying to the south (Figure 38).

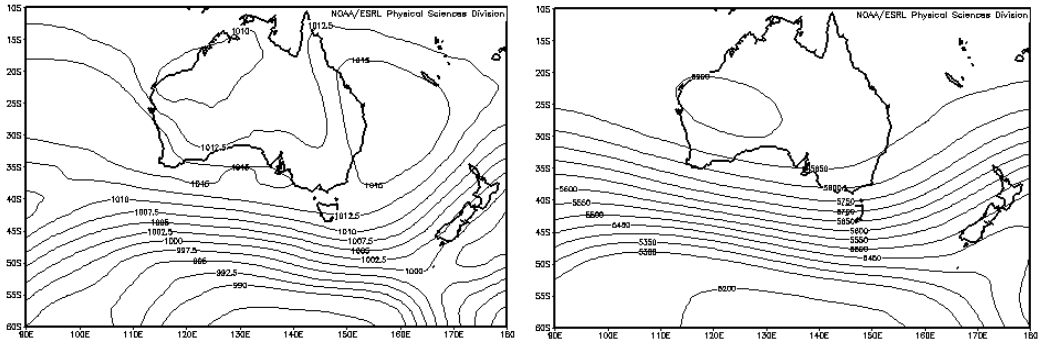

Figure 38: Five-day composite mean MSLP (hPa, left) and 500 hPa Geopotential Height (m, right) for 00UTC 18 December 1959 to 22 December 1972. NCEP/NCAR reanalysis.

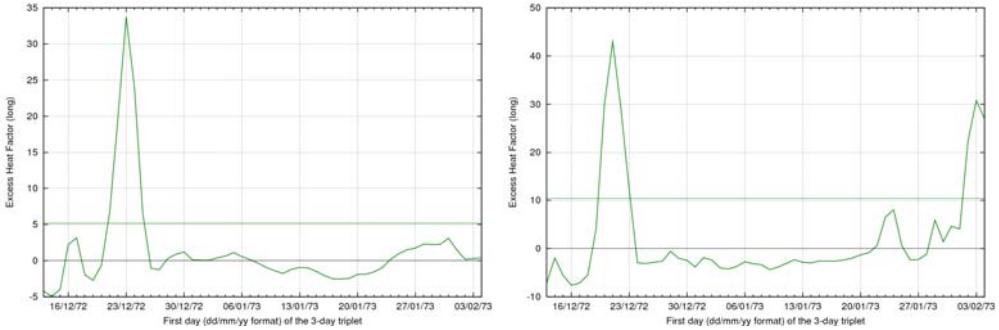

Figure 39: *EHF* at Brisbane (city site, left) and Sydney (Observatory Hill site, right) for the period 13/12/1972 to 04/02/1973. The horizontal line in each case represents the 85th percentile for positive *EHF* values. Data based on gridded daily temperature analyses.

Remarkably, extreme heatwaves are coincident on the eastern seaboard, as shown in the time series plots for Brisbane and Sydney (Figure 39).

The heat load for this December to February period shown in Figure 40 is unusual in the proportion of the continent registering high accumulations. The QUT (2010) report attributing 99 deaths to this event may therefore be under-reporting the scale of impact.

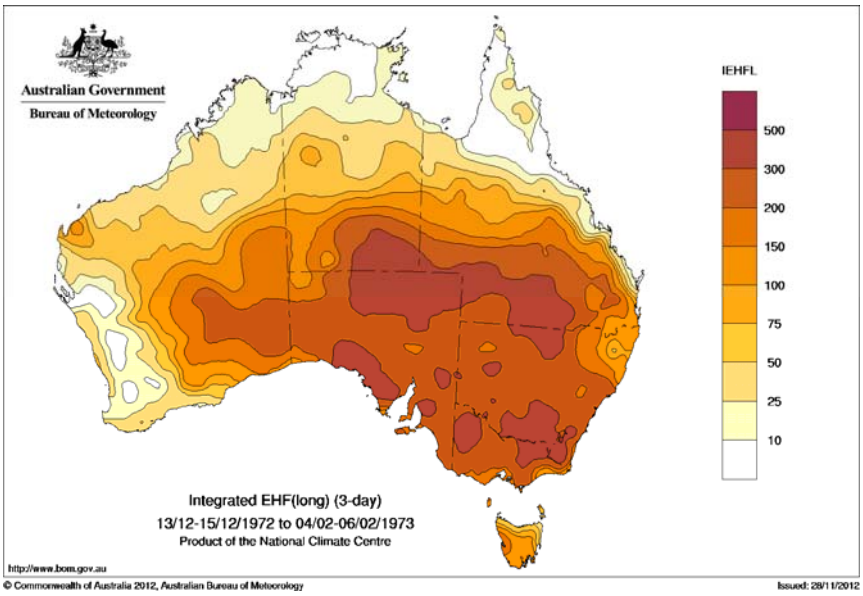

Figure 40: Integrated positive *EHF* for the severe heatwave of summer 1972/1973.

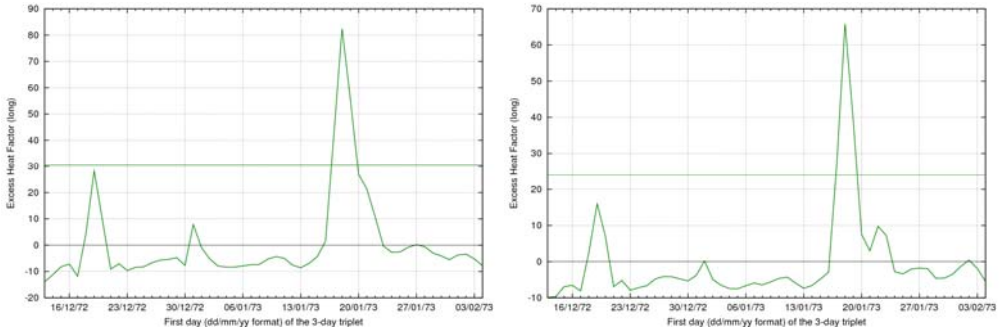

Figure 41: *EHF* at Adelaide (Kent Town site, left) and Melbourne (Regional Office site, right) for the period 13/12/1972 to 04/02/1973. The horizontal line in each case represents the 85th percentile for positive *EHF* values. Data based on gridded daily temperature analyses.

By mid-January extreme heatwave conditions had redeveloped over southeast Australia with Adelaide and Melbourne coincidentally experiencing severe to potentially extreme heatwave conditions (Figure 41).

The antecedent rainfall in 1972 (Figure 42) was very much below average across a large area of the continent with reduced lower and upper soil moisture (Figure 43) contributing to high temperatures.

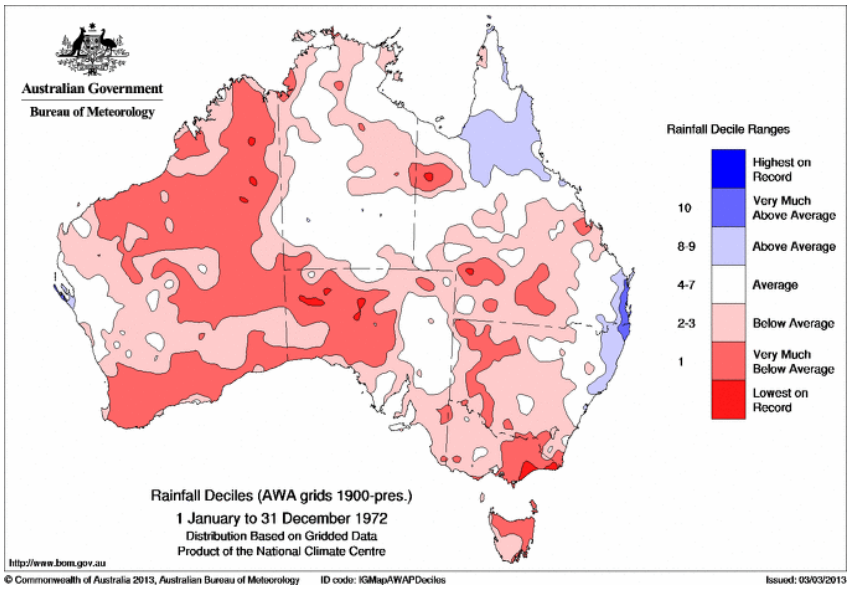

Figure 42: Australian rainfall deciles for 1972.

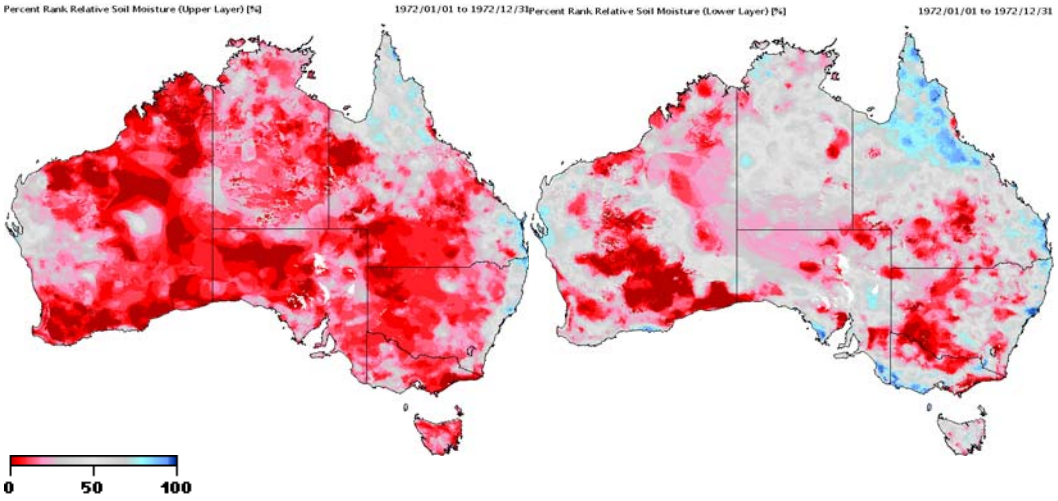

Figure 43: Per cent rank relative soil moisture, upper-layer (left) and lower-layer (right, %) for 1972.

6.1.6 February 2004

The *EHF* time series in Figure 44 shows a two-week heatwave which reached a peak intensity of 25 °C^2 which is four times Brisbane's severity threshold of 6 °C^2. Tong et al. (2010) attributes 75 non-external (other than injury or suicide) and 41 cardiovascular excess deaths to this extreme heatwave. The climatological range of *EHF* is lower at Brisbane's latitude, arising from high warm season temperatures with little variability.

It is significant to note that this is Brisbane's top-ranked event (Table 8). The table data are derived from station data, whilst the time series data in Figure 44 is extracted from gridded data. On occasion the gridded interpolation in the AWAP climate data may reduce the amplitude of the signal. In this instance the observed station-data peak *EHF* amplitude of 39.5 °C^2 is about six times the severity threshold.

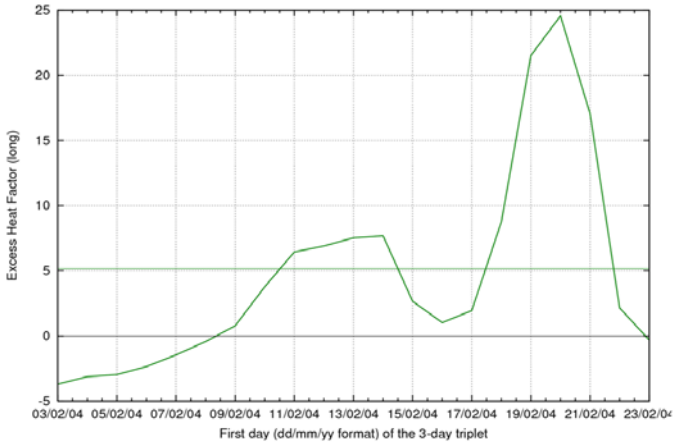

Figure 44: *EHF* time series for Brisbane (city site) in February 2004. The horizontal line represents the 85th percentile for positive *EHF* values. Data covering the period 3 to 23 February 2004 derived from gridded daily temperature analyses.

Table 8*:* Brisbane's top ranked *EHF* events by individual peak day in event

Rank	*EHF* (°C^2)	Date
1	39.5	20/2/2004
	33.1	21/2/2004
	21.3	19/2/2004
2	35.3	20/1/2000
	26.2	19/1/2000
	23.0	21/1/2000
3	28.8	25/1/1940
	27.5	26/1/1940
	26.7	24/1/1940
	26.4	27/1/1940
	23.5	28/1/1940
	21.7	29/1/1940
4	26.6	24/12/1972
	21.5	23/12/1972
5	24.9	19/11/1968

The synoptic charts in Figure 45 show a dominant ridge extending from the Indian Ocean to the Coral Sea, with a heat trough lying across the continent from northern Australia to the eastern seaboard. The mid-tropospheric anticyclone over central Australia establishes the depth of the mixed layer and the strength of the long wave ridge contributing to the slow-moving Rossby wave.

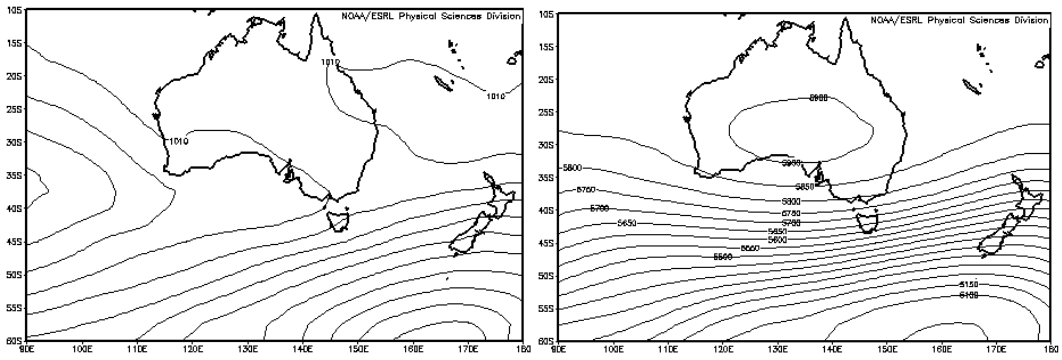

Figure 45: Five-day composite mean MSLP (hPa, left) and 500 hPa Geopotential Height (m, right) for 00UTC 17 February 2004 to 21 February 2004. NCEP/NCAR reanalysis.

Brisbane's top-ranked (Table 8) 2004 extreme heatwave event is particularly interesting in spatial terms (Figure 46), where large areas of South Australia and New South Wales experienced accumulated positive *EHF* values comparable to the 2009 extreme heatwave (National Climate Centre 2009) as shown in Figure 50. The difference on this occasion is that southeast Australian coastal regions remained cooler due to periodic incursions of southern ocean sea breezes, under the influence of southwest to southeast gradient wind regimes depicted in Figure 45.

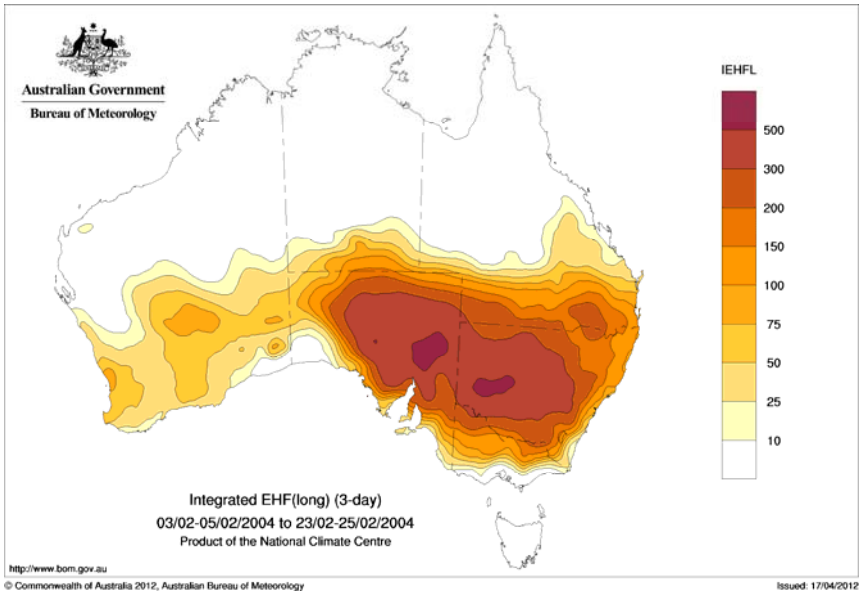

Figure 46: Integrated positive *EHF* for the severe heatwave of February 2004.

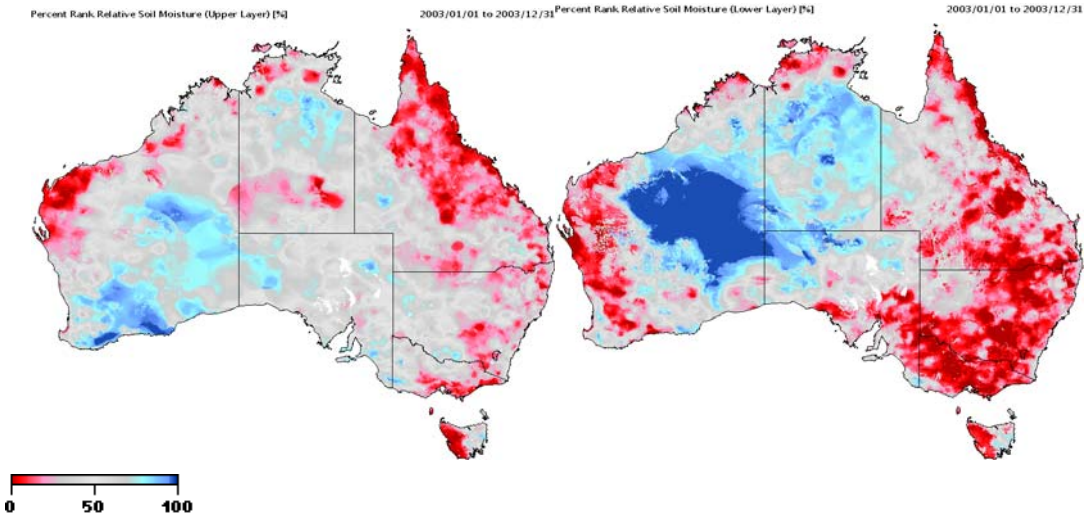

Figure 47: Per cent rank relative soil moisture, upper-layer (left) and lower-layers (right, %) for 2003.

Brisbane's high day and night temperatures were driven by low soil moisture content in upper and lower layers (Figure 47) arising from low antecedent rainfall (Figure 48) across eastern Australia.

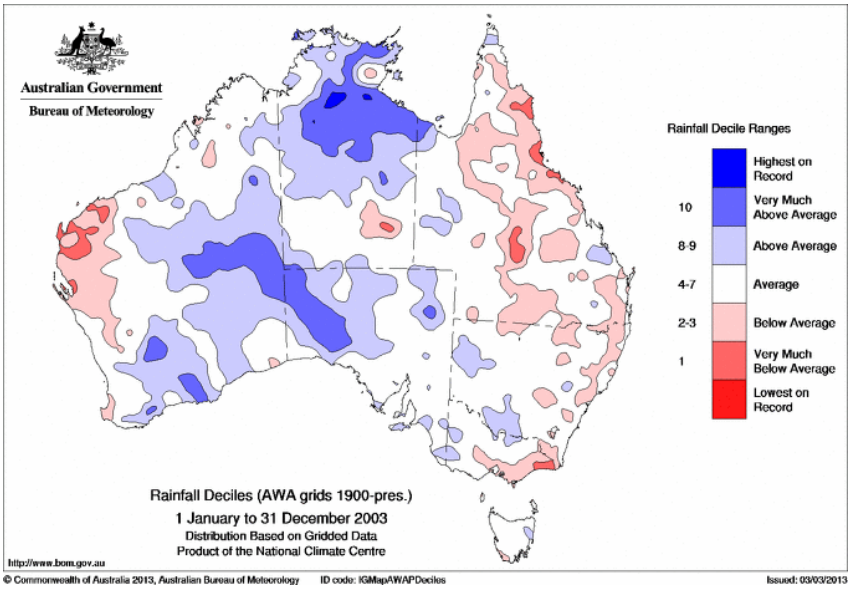

Figure 48: Australian rainfall deciles for 2003.

6.1.7 Mid-January to Early February 2009

Two heatwaves are evident in Canberra's *EHF* time series in 2009 over a three week period (Figure 49). The first is relatively minor, with the peak approaching the severity threshold of 14.2 °C^2. The second heatwave was extreme, temporarily reaching nearly twice the severity threshold, followed a few days later by a sustained period at nearly three times the severity threshold. Widespread high heat load is evident in much of southern Australia as seen in Figure 50, with the extreme heatwave impacting South Australia, Victoria, New South Wales and Tasmania.

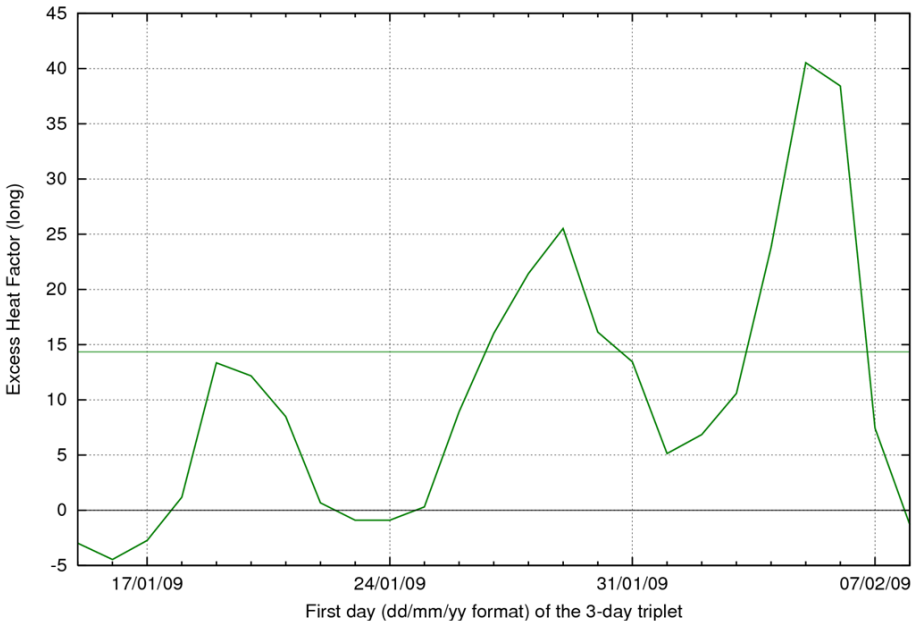

Figure 49: *EHF* at Canberra (Parliament House site) for the period 15/01/2009 to 08/02/2009. The horizontal line represents the 85th percentile for positive *EHF* values. Data based on gridded daily temperature analyses.

The extreme heatwave that impacted southeast Australia in January and February 2009 resulted in somewhere between 400 and 500 excess deaths, with Victoria reporting 374 excess deaths (Victorian Department of Health 2009) and the South Australian Coroner recording 58 heated-affected deaths (Langlois et al. 2013). This wave of mortality immediately preceded the Black Saturday Bushfire where 173 people in Victoria died.

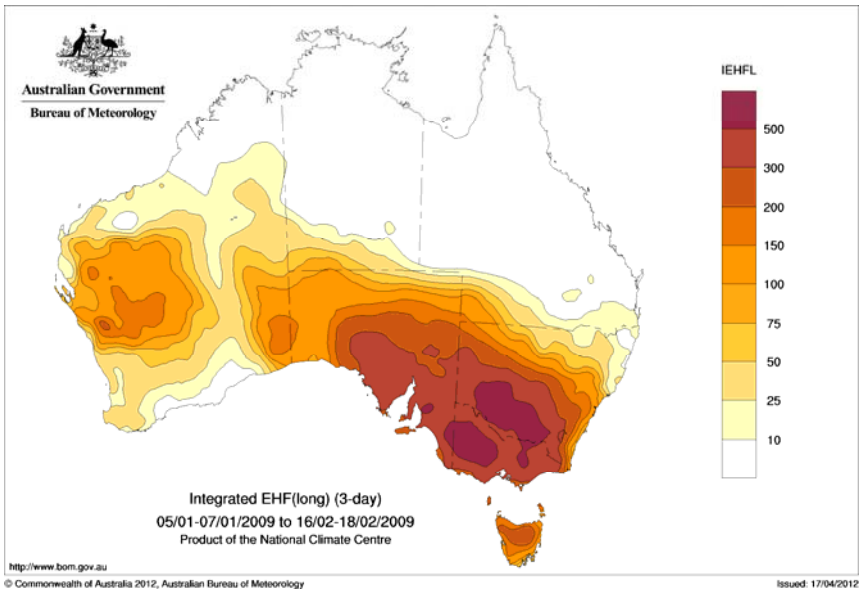

Figure 50: Integrated positive *EHF* for the extreme heatwave of January and February 2009.

The heatwave time series in Figure 51 shows that Adelaide experienced a sustained intensity at about four times the severe *EHF* threshold of 32 °C^2.

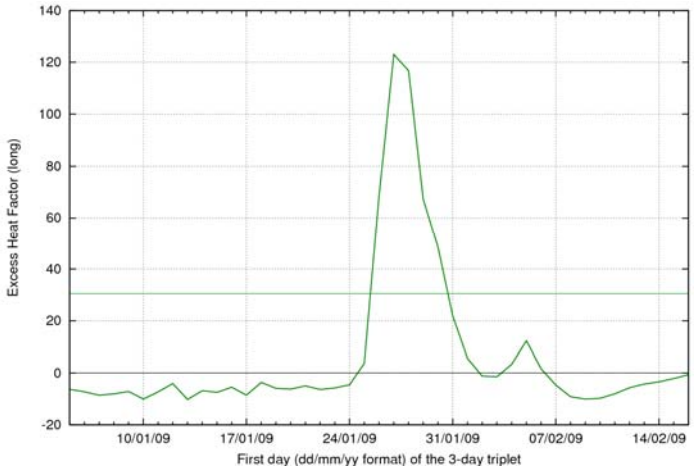

Figure 51: *EHF* time series for Adelaide (Kent Town site) in 2009. The horizontal line represents the 85th percentile for positive *EHF* values. Peak values are around four times the proposed severity threshold. Data covering the period 05/01/2009 to 16/02/2009 based on gridded daily temperature analyses.

The synoptic charts in Figure 52 show a dominant surface ridge extending from the Indian Ocean into the Tasman Sea, with a large heat low and trough covering the western half of the continent. The depth and dominance of the long wave ridge is illustrated by the large closed mid-tropospheric anticyclone positioned over southeast Australia which signifies the stationary Rossby wave.

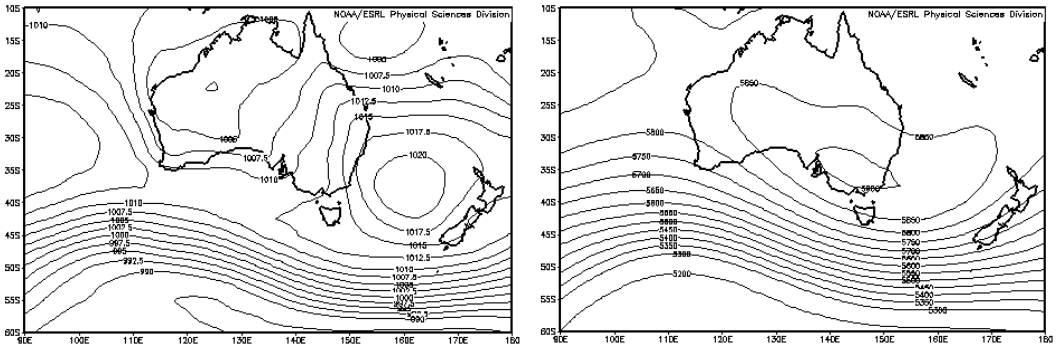

Figure 52: Five-day composite mean MSLP (hPa, left) and 500 hPa Geopotential Height (m, right) for 00UTC 26 January to 30 January 2009. NCEP/NCAR reanalysis.

The dry antecedent conditions (Figure 53) and resulting low soil moisture content (Figure 54) across southern Australia were strong contributors to the intensity of day and night extreme temperatures during this extreme heatwave.

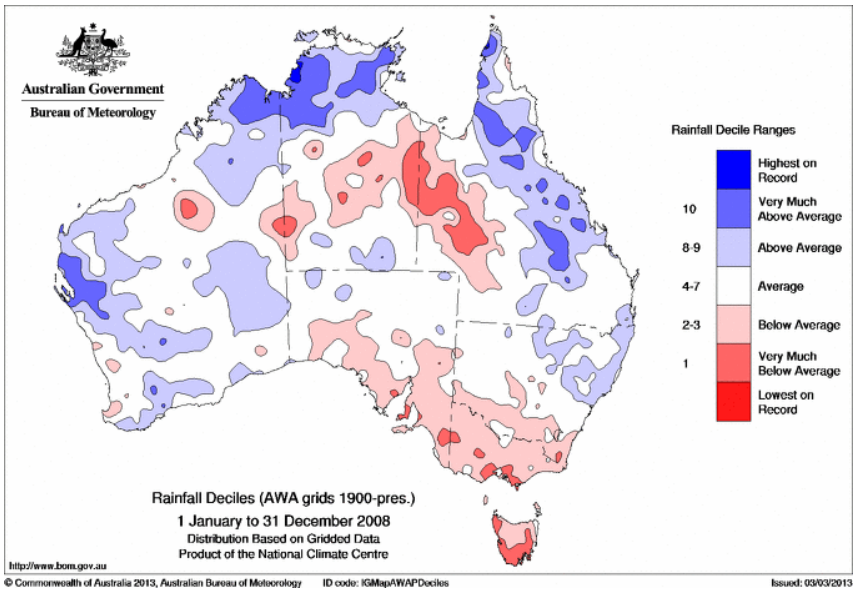

Figure 53: Australian rainfall deciles for 2008.

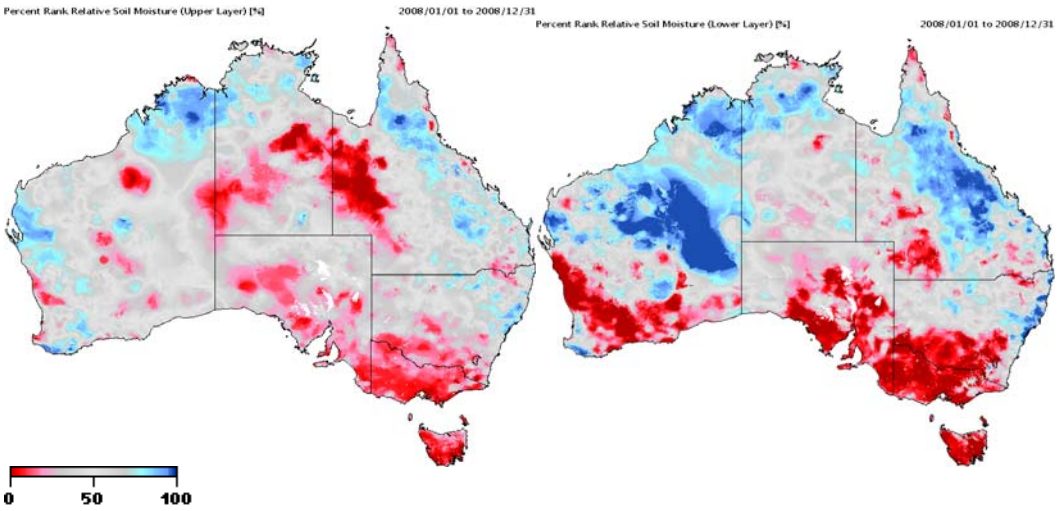

Figure 54: Per cent rank relative soil moisture, upper-layer (left) and lower-layers (right, %) for 2008.

6.2 International Heatwaves

Investigations have been carried out for Paris (data commencing in 1945), Moscow (1937[10]), Newark (1948), Chicago (1947) and St Louis (1945). As discussed in Appendix B, for Paris, Moscow and Chicago there is considerable sensitivity for recent extreme heatwaves (Paris figures are now corrected for a scale error present in the figures included in the paper at Appendix B). Impacts for these extreme heatwaves were tabulated (Table 4) and discussed in Section 4.3.2.

Drawing upon the technique discussed in Section 3.1, Figure 55 shows how Newark's severe *EHF* threshold of 12 °C^2 has been determined.

[10] Data gaps during 1938-49, 1958, and 1972.

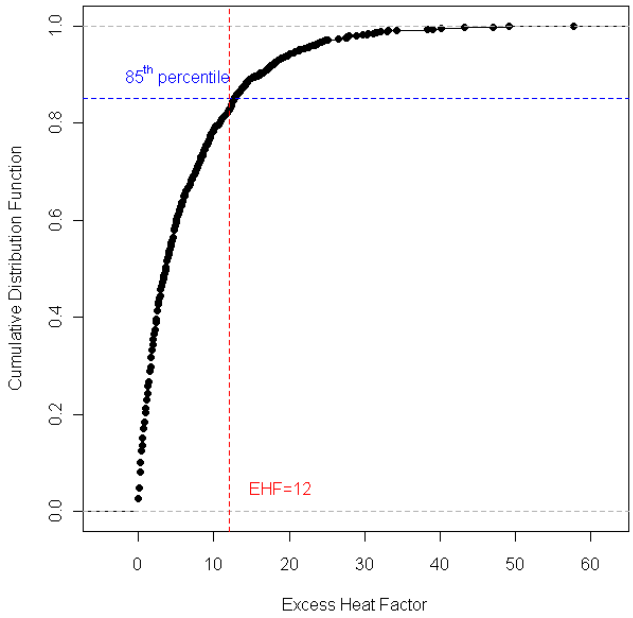

Figure 55: Cumulative distribution function for positive *EHF* at Newark, New Jersey USA. The severe *EHF* threshold is 12 °C^2, calculated as the 85th percentile of positive *EHF*.

The 1993 *EHF* time series in Figure 56 shows Newark's top ranked extreme heatwave. The peak amplitude for this event is about five times the severe *EHF* threshold.

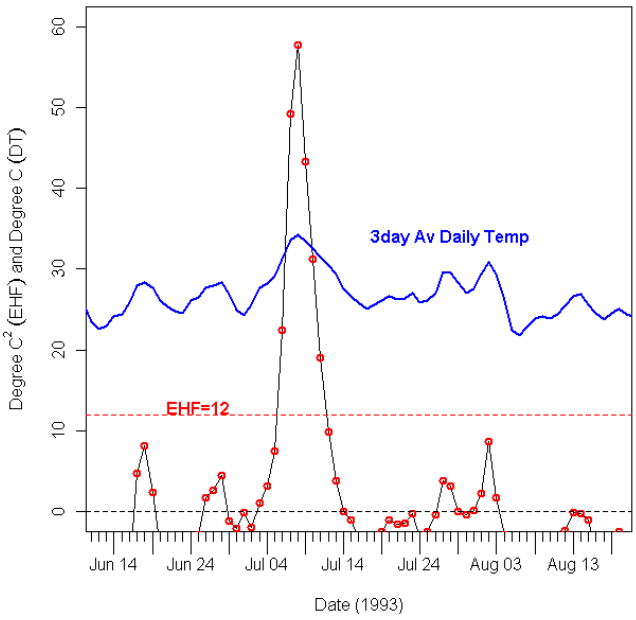

Figure 56: Newark *EHF* (black line, red circles) and three-day-averaged DMT (blue line) for an extreme north American heatwave in 1993. The severity threshold *EHF* = 12 °C^2 is shown as a dashed red line.

Paris, Moscow, Chicago and St Louis have each had their severe *EHF* threshold calculated as shown for Newark. The Paris extreme heatwaves in 1976 (Figure 57) and 2003 (Figure 58) are both shown as they are the top ranked peak intensity events for the period examined. Both events are notable for mortality across France with 6,000 and15,000 deaths in 1976 and 2003 respectively (Appendix B).

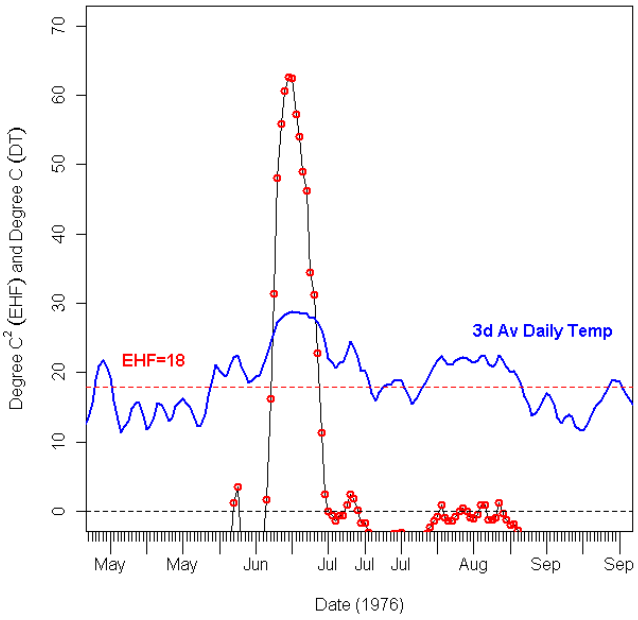

Figure 57: Paris *EHF* (black line, red circles) and three-day-averaged DMT (blue line) for the 1976 extreme European heatwave.

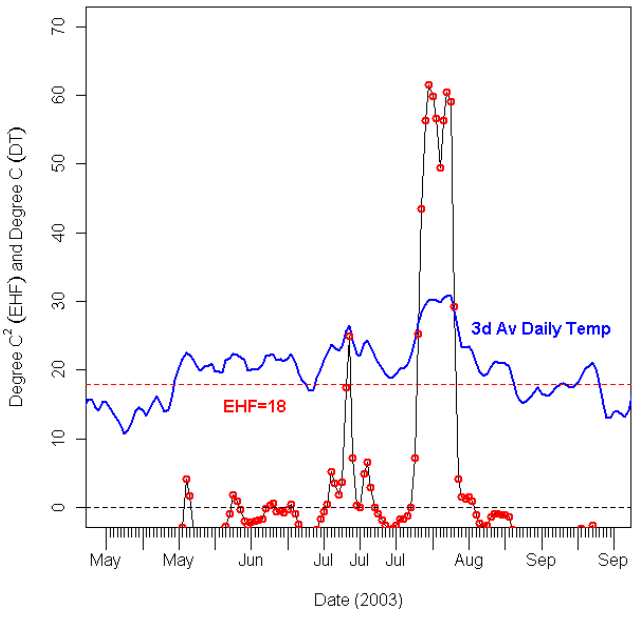

Figure 58: Paris *EHF* (black line, red circles) and three-day-averaged DMT (blue line) for the 2003 extreme European heatwave.

The Moscow 2010 extreme heatwave (Figure 59) is notable for the heatwave lasting 51 days.

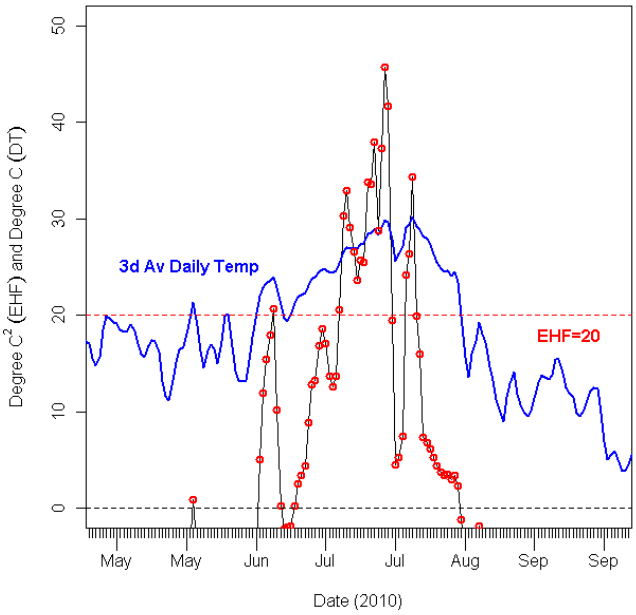

Figure 59: Moscow *EHF* (black line, red circles) and three-day-averaged DMT (blue line) for the 2010 extreme European heatwave.

The coincident heatwave in Chicago (Figure 60) and St Louis (Figure 61) in 1995 has been noted for the comparative lack of deaths in St Louis (Palecki et al. 2001). The difference in *EHF* peak amplitude of these events appears to be a significant contributing factor.

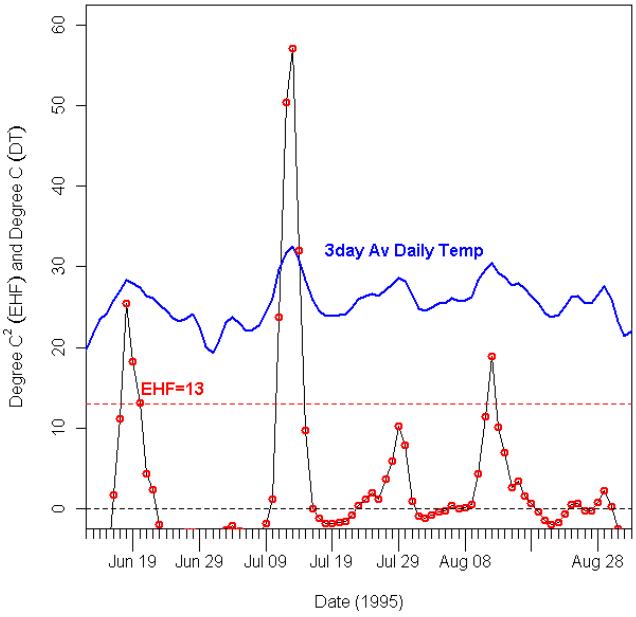

Figure 60: Chicago *EHF* (black line, red circles) and three-day-averaged DMT (blue line) for the 1995 extreme North American heatwave.

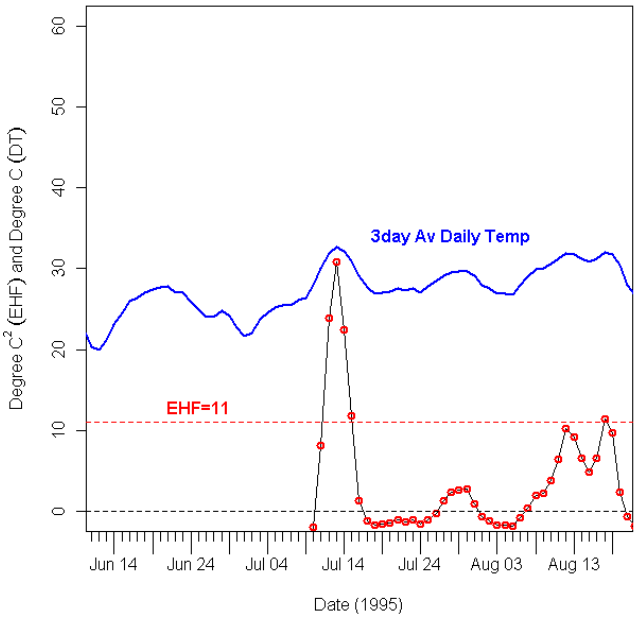

Figure 61: St Louis *EHF* (black line, red circles) and three-day-averaged DMT (blue line) for the 1995 extreme North American heatwave.

6.3 Australian Coldwaves

6.3.1 Eastern Australia

The short-term and long-term temperature anomalies that are combined to create *ECF* are conceptually analogous to those used to create *EHF*, varying substantively in the long-term temperature anomaly tests which are respectively the 30-year, 5th and 95th percentile of DMT. Some interesting heatwave and coldwave climatology features can be diagnosed by plotting the short and long term anomalies, as shown in Figure 62 for Sydney (New South Wales). Heatwaves on the eastern seaboard of the Australian continent are characterised by the warm-season tail of red points in the top-right quadrant. Coldwaves are found in the cool-season tail of blue points in the bottom-left quadrant. Notably heatwaves also occur in the cool-season, representing the largest acclimatisation signal in Sydney's record. This suggests they occur in September, with an abrupt rise against the normally milder temperatures. A strong acclimatisation signal at the end of summer in April is highly unlikely to provide an acclimatisation challenge at the end of the warm-season. Coldwaves on the other hand only occur in the cool-season and exhibit a shorter range of both long and short term temperature anomalies. The constrained cool-season anomalies and wider ranging warm-season anomalies accurately reflect the climate of this site, located in the sub-tropics on the eastern seaboard of the Australian continent.

Sydney heatwaves with both significance and acclimatisation anomalies greater than 5 °C are extreme events, producing *EHF* values greater than 25 °C^2, more than twice the severity threshold of 10.8 °C^2 (*EHI* significance values are not shown).

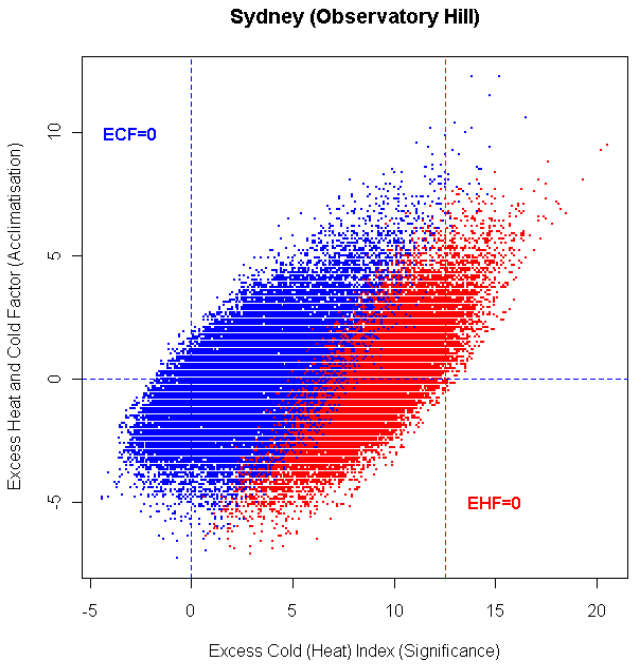

Figure 62: Significance (horizontal axis) and Acclimatisation (vertical axis) Excess Cold (Heat) Indices over the period 1860 to 2010 for Sydney (Observatory Hill). Warm season months (October-March) in red, cool season (April-September) in blue. Points in the top-right quadrant, having positive *EHI*s of both types, have positive *EHF*. Points in the bottom-left quadrant, having negative *ECI*s of both types have negative *ECF*.

The climate record for *ECF* at the Observatory Hill site in Sydney across the period 1858 to 2009 is ranked in Table 9, showing most strong *ECF* events are at the start of the observational record. This trend is consistent with either the establishment and persistence of an urban heat island, a warming climate or the combined effect of both warming effects. The lowest *ECF* event recorded in the 21st century is −7.2 °C^2 in 2010.

Table 9: Top 10 Excess Cold Factor (°C^2) events for Sydney (Observatory Hill), NSW.

Rank	*ECF* (°C^2)	Date
1	-21.7	01/07/1862
2	-21.2	02/07/1862
3	-19.5	07/07/1861
4	-16.1	06/07/1861
5	-16.0	11/07/1890
6	-15.9	09/08/1872
7	-15.7	26/07/1986
8	-15.7	24/06/1903
9	-15.6	10/07/1890
10	-15.3	30/06/1862

The severe *ECF* threshold is calculated using the 15th percentile (ECF_{15}) of the distribution of negative *ECF* values, analogous to the *EHF* calculation in Section 3.1. Observatory Hill (Sydney) has a value of –4 °C^2 as shown in Figure 63.

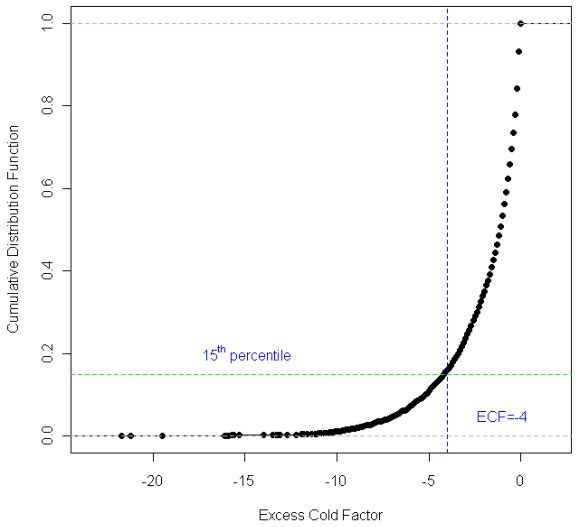

Figure 63: Cumulative distribution function for negative *ECF* values for 1859-2010 at Sydney (Observatory Hill). The severe *ECF* threshold is −4 °C^2.

Sydney's top ranked event in 1862 is shown as the *ECF* time series in Figure 64. Four cold waves are evident; the late July and August the events are minor while the June and August events are severe, possibly extreme as peak intensity is five and two times the magnitude of the severity threshold, respectively.

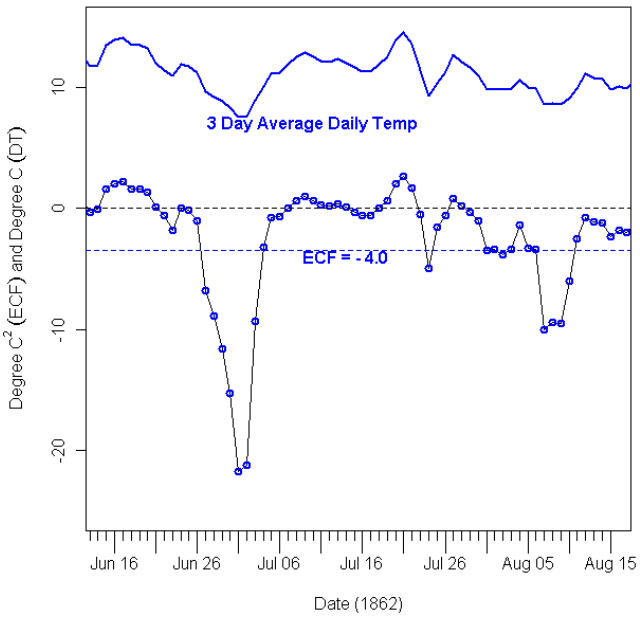

Figure 64: *ECF* time series (black line, blue circles) and three-day-averaged DMT (blue line) for Sydney (Observatory Hill, NSW) in 1862. The severity threshold *ECF* = –4 °C^2 is shown as a dashed blue line.

The impact of the late June to early July severe coldwave in 1862 is difficult to assess. The anomalies captured within this event are not very large, with the peak three-day average DMT of 7 °C representing single-digit maximum and minimum temperatures. It is highly likely that sustained frosts would have impacted agriculture. The extent of the cold across southeast Australia is captured by the following newspaper columns;

- "The frosts during the last few days have been much more severe than usual. Yesterday morning was very cold, and the ice in many places was fully an inch thick. A large number of water pipes were reported to have been burst by the frost. The day, however, was clear and fine with a gentle bracing breeze." (*Launceston Examiner*, Saturday 28 June 1862);
- 'We have had some intensely cold and frosty weather here lately. In fact, such a severe season is without a precedent in the memory of the "oldest inhabitant"' (article titled "Wellington", *The South Australian Advertiser*, Friday 4 July 1862); and
- "Queanbeyan has lately experienced the severest frosts known in the district for many years. Water, and even milk, one of the last fluids to yield to the congealing effects of the cold, have been frozen in vessels within doors. In some cases out of doors the ice has been strong enough to bear the weight of a man" (*Queanbeyan Age and General Advertiser*, NSW, Saturday 5 July 1862).

How *ECF* changes over time offers an additional climate monitoring tool. The time series of *ECF* in Figure 65 spans the full observational record from 1858 to 2010 at Observatory Hill. There is a noticeable set of severe *ECF* events with values below –13 °C^2 that (almost entirely) disappear at the turn of the 20th century. The Sydney observation site was relocated in 1917, from a location which had lower maximum and higher minimum temperatures (ACORN-SAT station catalogue, 2012).

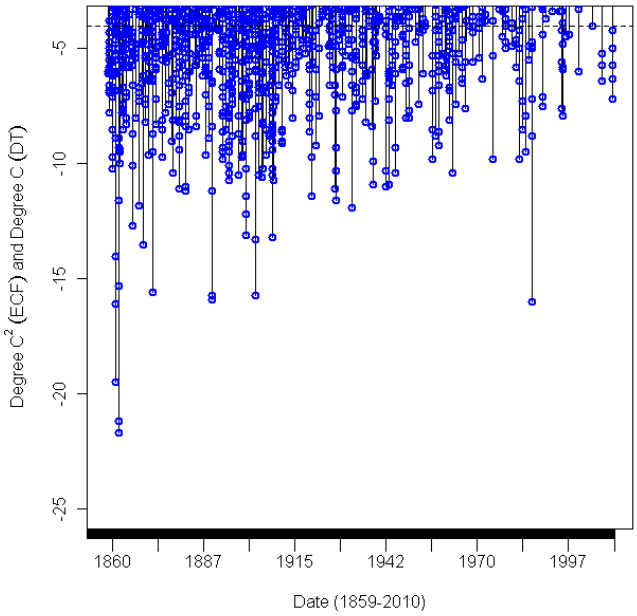

Figure 65: Time series for Sydney (Observatory Hill, NSW) showing all *ECF* below –4 °C^2 in the period 1859 to 2010.

The relocation of the Sydney site to Observatory Hill is accommodated with a reanalysis from 1918 onwards. The top 10 ranked events in this shorter record are shown in Table 10. These coldwave events are also focussed toward the start of this period, apart from the strong outlier event in 1986 (Table 10).

Table 10: Top-ranked *ECF* events for Sydney (Observatory Hill), NSW for the period 1918-2010. *ECF* in °C^2.

Rank	*ECF* (°C^2)	Date
1	–16.0	26/07/1986
2	–11.9	21/06/1932
3	–11.6	10/06/1927
4	–11.4	04/06/1920
5	–11.1	29/05/1927
6	–11.0	05/07/1942
7	–10.9	02/08/1938
8	–10.9	06/07/1943
9	–10.4	06/07/1945
10	–10.4	21/08/1962

The shorter record commencing 1918 is shown in the time series shown in Figure 66. This data shows the 5th and 95th percentiles of DMT have respectively increased at 0.15 and 0.13 °C in the period 1950 to 2010, whilst in the decades preceding 1915 there was no trend. In the decade following the relocation of this site daily temperature percentile warmed by approximately 0.5 °C, corresponding to the mean temperature shift.

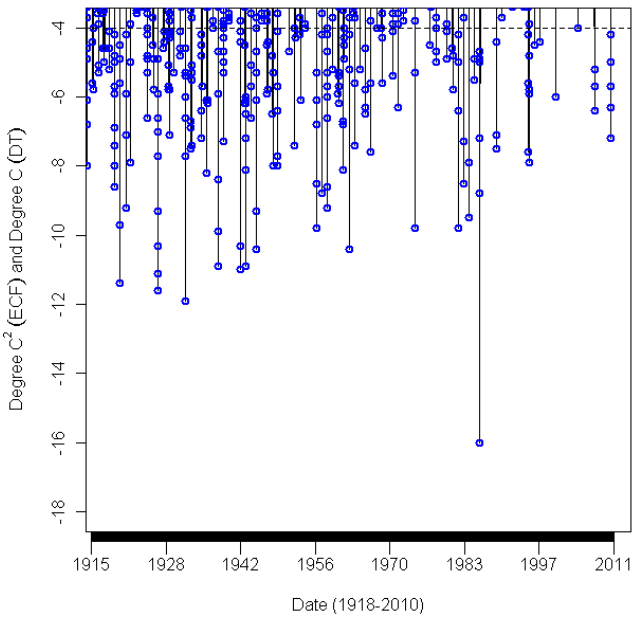

Figure 66: Time series for Sydney (Observatory Hill), NSW for all negative *ECF* values below –4 °C^2 in the period 1918-2010.

The steady fall in *ECF* intensity is attributable to a warming trend in the temperature record. This warming may be due to a combination of increasing urban heat island effect and greenhouse warming.

The severe *ECF* threshold is recalculated for the 1918 to 2010 period, producing a threshold value of –3.5 °C^2 (Figure 67). This is 0.5 °C^2 warmer than that for the 1859 to 2010 period, a consequence of the warmer exposure following relocation.

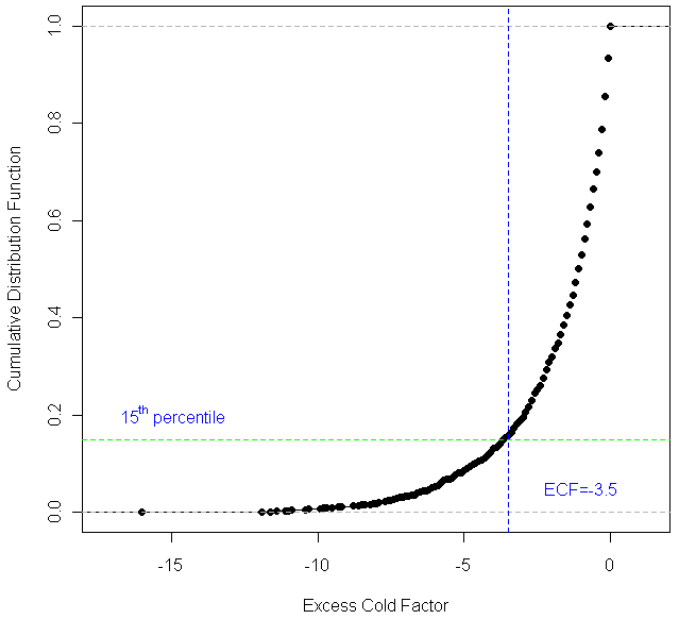

Figure 67: Cumulative distribution function for *ECF* time series for Observatory Hill, 1918 to 2010. Severe *ECF* threshold of –3.5 °C^2.

The severe excess cold event of 1986 shown in Figure 68 was a relatively brief event, reaching a peak intensity of five times the severe *ECF* threshold. The corresponding spatial pattern is shown in Figure 69, and can be seen to have been remarkably widespread across the country. Peak values stretched across inland Queensland, extending into adjacent parts of the Northern Territory and northeast New South Wales.

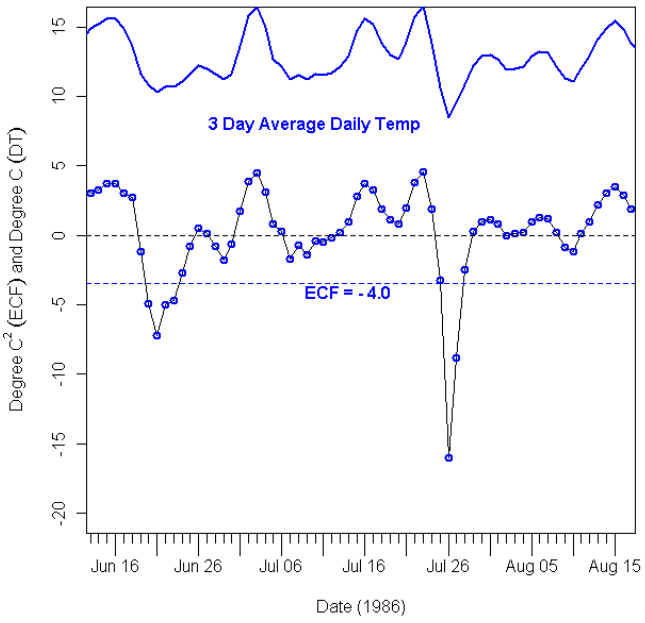

Figure 68: *ECF* time series (black line, blue circles) and three-day-averaged DMT (blue line) for Sydney (Observatory Hill) in mid-1986.

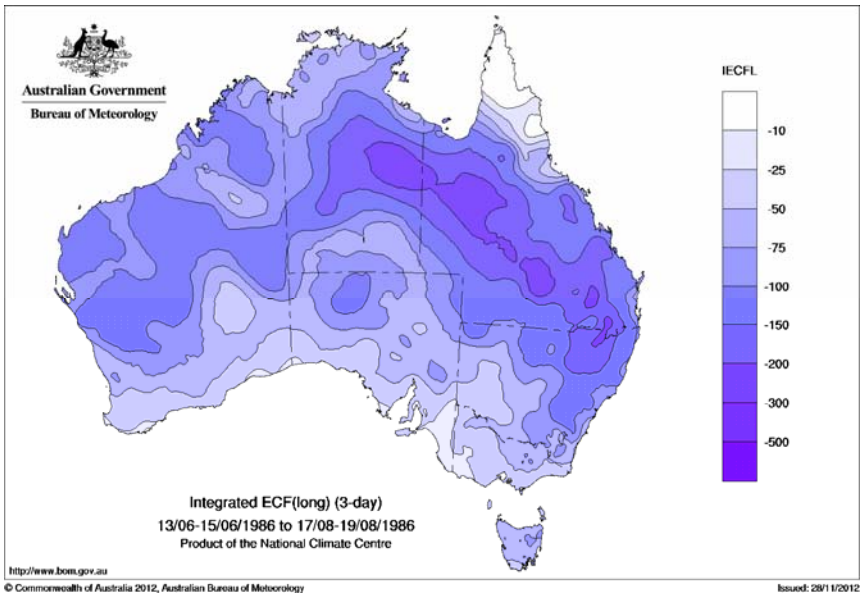

Figure 69: Integrated negative *ECF* across the period 13 June to 17 August 1986.

On 25 July 1986, many Tasmanian locations had their heaviest snow on record. Most principal roads in Hobart were closed (see Figure 71), effectively isolating the city until almost noon. Schools were shut for the day, and mail deliveries suspended. On the same day, snow fell in Melbourne and many suburbs, causing air traffic delays of up to four hours. Melting snow was observed in metropolitan Sydney, and further north at Gosford. *ECF* values for Hobart are shown in Figure 70. The severity threshold is exceed on 23 July (i.e., the three-day period 23-25 July).

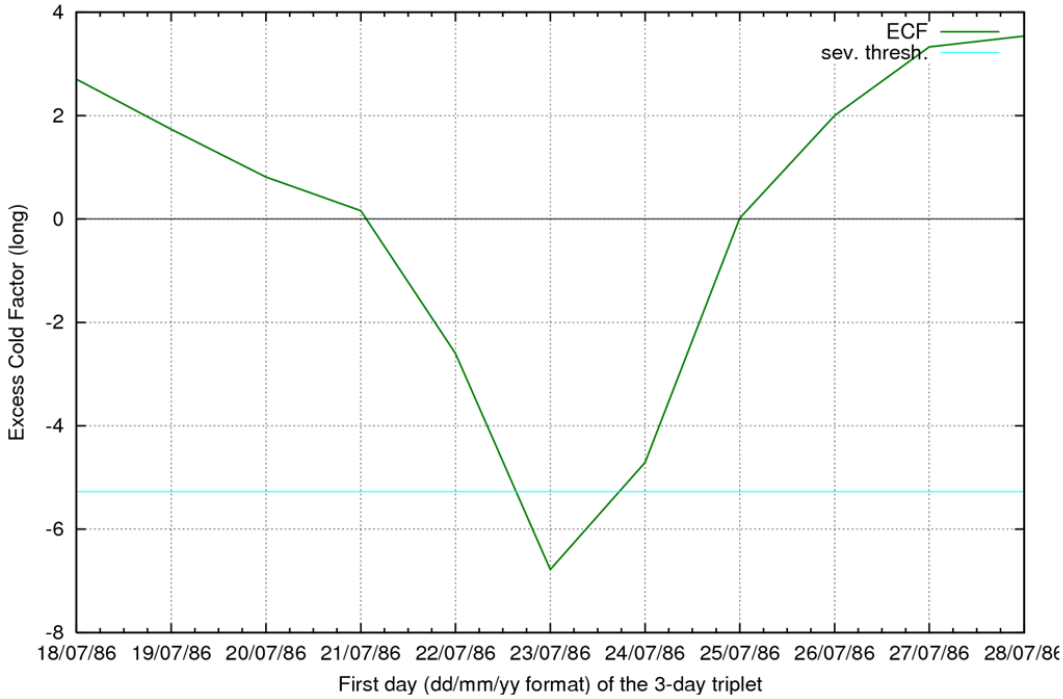

Figure 70: *ECF* time series (green line) from 18 July to 28 July 1986 for Hobart (Ellerslie Road). The *ECF* severity threshold is shown as a light blue line. Data based on gridded daily temperature analyses.

Figure 71: Hobart under a blanket of snow, 26 July 1986. Snow in the Hobart area was 8 cm deep at 9am. (Photograph reproduced with permission: © Newspix / Eddie Safarik.)

Synoptic charts in Figure 72 show the surface pattern is dominated by a large slow-moving anticyclone centred over the southwest corner of the continent, whilst at mid levels a persistent cold trough extends out of the Tasman Sea across southern Australia. South eastern Australia is exposed to the steady intrusion of a cold and relatively dry Southern Ocean air mass. Large areas of snow fall under diurnal convective process would clear overnight providing optimum conditions for radiative cooling and very low minimum temperatures.

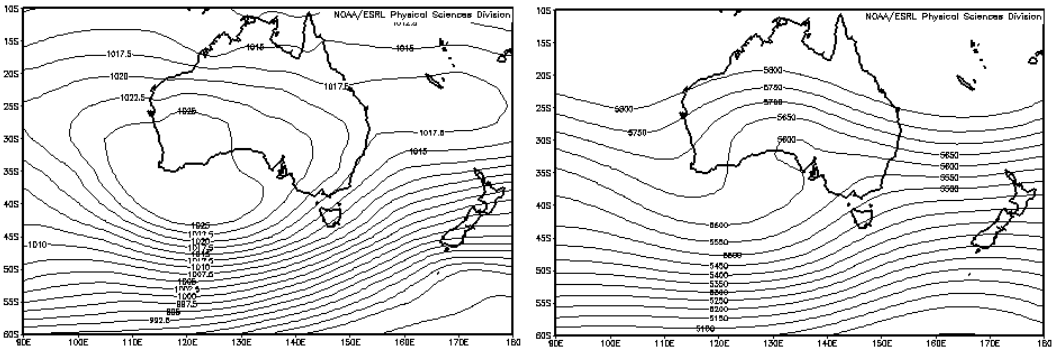

Figure 72: 5-day composite MSLP (hPa, left) and 500 hPa Geopotential Height (m, right) from 00UTC 24 to 00UTC 28 July 1986. NCEP/NCAR reanalysis

A two-wave Rossby Wave (RW) pattern is evident in Figure 73, providing a stationary or retrogressive wave movement. The dominance of the two-wave RW is clearly shown in the anomaly chart where very low anomaly spans the South Pole, from the southwest Indian Ocean to the Southern Ocean in the vicinity of New Zealand. The presence of this pattern set up large amplitude advection of cold, dry polar air into lower latitudes, sustaining the coldwave over eastern Australia.

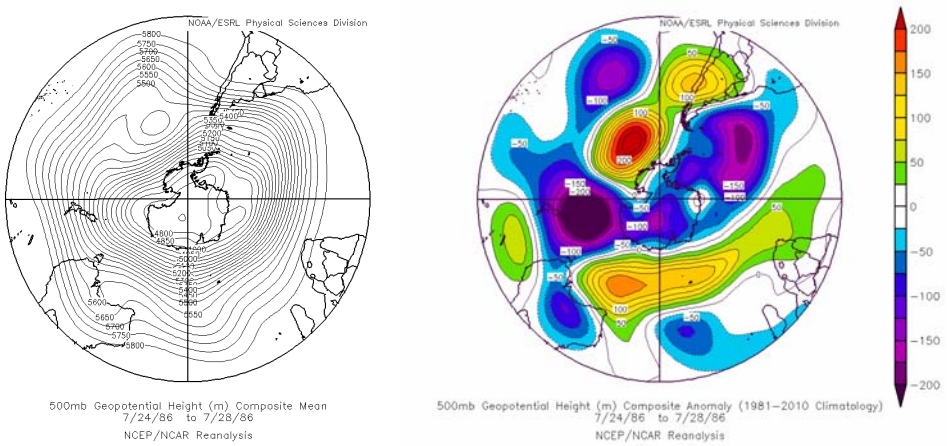

Figure 73: Composite 500 hPa geopotential height (m, left) and anomaly (1981-2010 base period, m, right) from 00UTC 24 to 00UTC 28 July 1986. NCEP/NCAR reanalysis.

6.4 International Coldwaves

6.4.1 Newark, USA Coldwaves

A similar analysis is presented for an overseas example using Newark Airport's (New Jersey USA) record, from 1948 to 2010. Figure 74 provides *EHF* and *ECF* interpretations of Newark's heatwave and coldwave climatology.

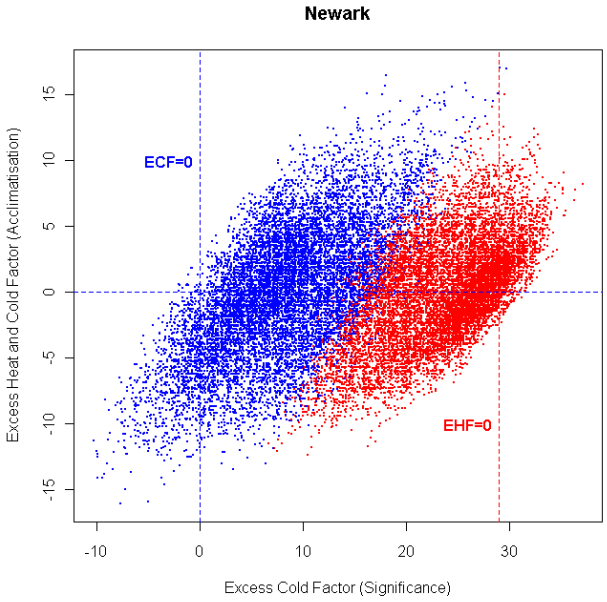

Figure 74: Significance (horizontal axis) and Acclimatisation (vertical axis) Excess Cold (Heat superimposed) Indices over the period 1948-2010 for Newark, USA. Warm season months (April to September) in red, cool season (October to March) in blue. Points in the top-right quadrant, having positive *EHI*s of both types, have positive *EHF*. Points in the bottom-left quadrant, having negative *ECI*s of both types have negative *ECF*.

Newark's severe *ECF* threshold of −38 °C^2 is derived in Figure 75.

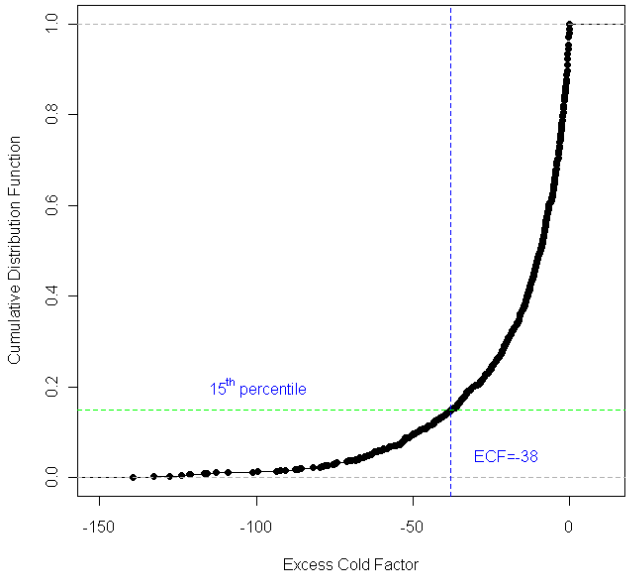

Figure 75: Cumulative distribution function for negative *ECF* at Newark, New Jersey USA. The severe *ECF* threshold is −38 °C^2.

Newark's top *ECF* event in this record occurred in the winter of 1981/1982, with peak intensity approximately three times the severity threshold. This coldwave lasted most of January 1982 and reached extreme intensities for eight *ECF* days (Figure 76) in two bursts.

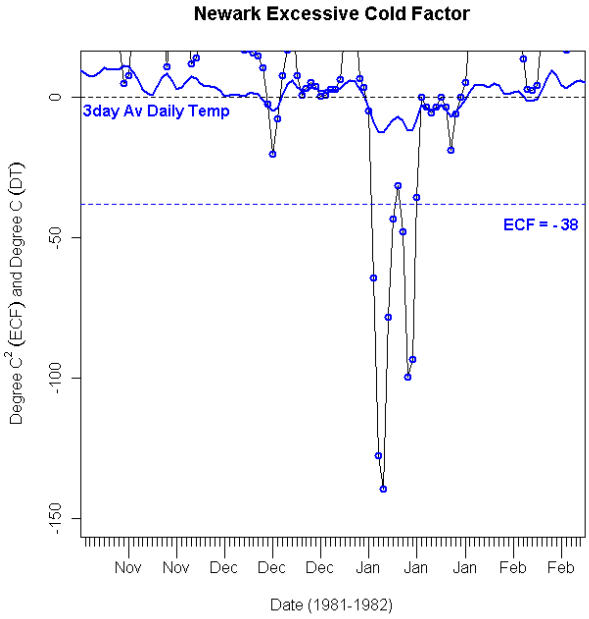

Figure 76: *ECF* time series (black line, blue circles) and three-day-averaged DMT (blue line) for Newark, New Jersey USA, for winter 1981/1982. The severe *ECF* threshold is −38 °C^2.

7. SERVICES

7.1 Heatwave (Coldwave) Definition

It is likely that the community will benefit from access to heatwave products. Apart from the general public, emergency and business sectors across Australia would benefit from a common heatwave measure against which they can build mitigation strategies. Education based around *EHF* will facilitate wider adoption and incorporation of protective strategies within the Australian community.

The heatwave definition used in this paper has recently been incorporated in a report to the Australian Government (PricewaterhouseCoopers 2011). The report found the definition suitable for testing excess mortality sensitivity and found a mortality response to the severe *EHF* threshold in most major cities. Further engagement is necessary with health and research groups with higher quality data to establish the strength and utility of this signal. The provision of a single heatwave (coldwave) definition will allow different jurisdictions to compare regional heatwave (coldwave) challenges and share strategies for mitigating their impact.

The ability to conduct international comparisons of past and projected heatwave (coldwave) challenges can facilitate better information exchange on best practices for mitigating impacts.

7.2 Heatwave (Coldwave) Services

Severe *EHF* (*ECF*) thresholds can be used to create a public service, as illustrated in Figure 77. The severity threshold data shown in Figure 17 has been applied to the data in Figure 78 to establish areas affected by heatwave and severe heatwave. Specialist response agencies would require access to the actual *EHF* data in Figure 78 to characterize each event, recognising that severity can vary across the spectrum from marginal to extreme. Figure 79 shows an experimental *EHF* forecast for 5 January 2013, prepared on 4 January (NWP model base time 12UTC 3 January) using the Gridded Operational Consensus Forecasts (GOCF) system (see Fawcett and Hume 2010 for details).

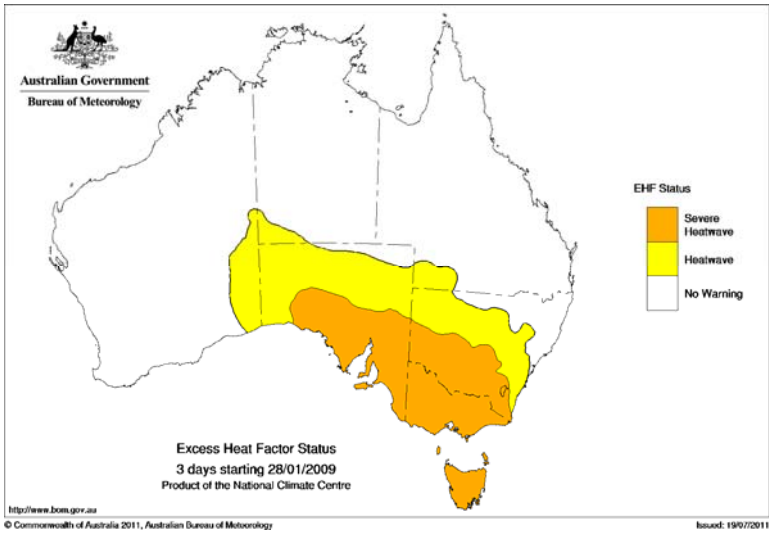

Figure 77: Areas with positive *EHF* for the period 28-30 January 2009, mapped for incidence of heatwave and severe heatwave. Actual *EHF* data are shown in Figure 78..

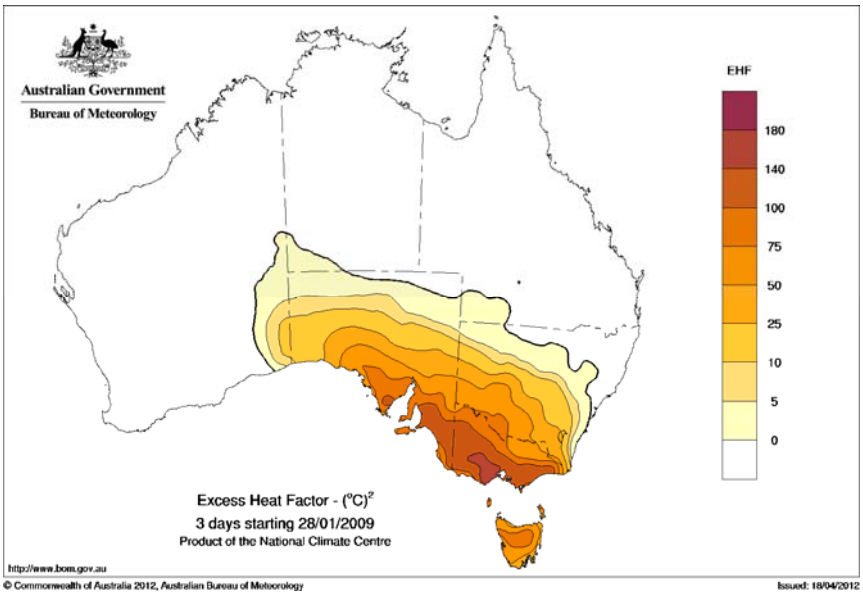

Figure 78: Severity of the January 2009 heatwave shown by magnitude of the *EHF* for the period 28-30 January 2009.

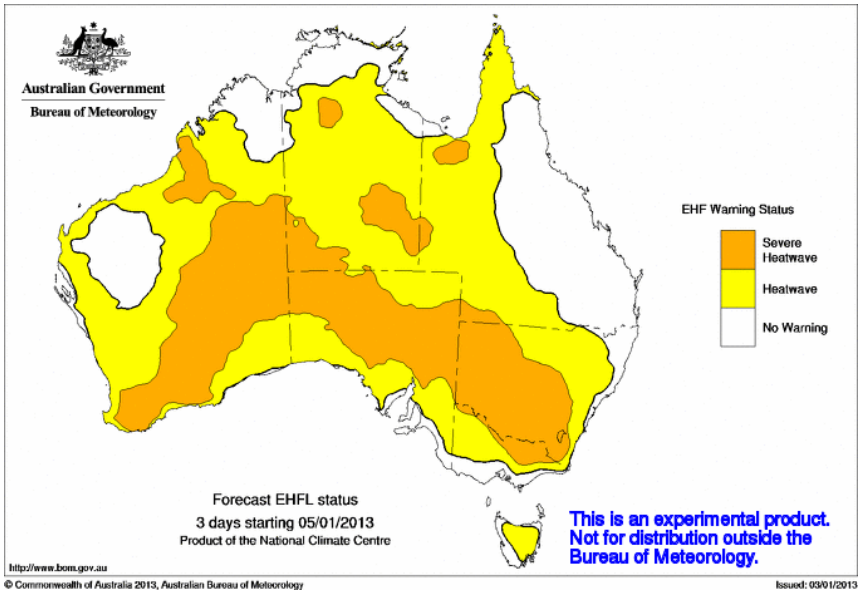

Figure 79: Experimental *EHF* forecast for 5-7 January 2013, prepared on 4 January 2013 (model base time 12Z 3 January 2013).

The potential for deriving an extreme heatwave forecast product is illustrated in Figure 80. Levels of severity have been derived by mapping *EHF* in terms of multiples of the severity threshold EHF_{85}. As concluded in Section 4, events where *EHF* has risen two-fold or more above the severity threshold have resulted in extreme impact. During the heatwave event shown in Figure 80, southeast parts of Tasmania (notably the Tasman Peninsula) experienced a bushfire emergency beginning on 4 January 2013, as strong winds developed in the hot dry conditions ahead of a cold front.

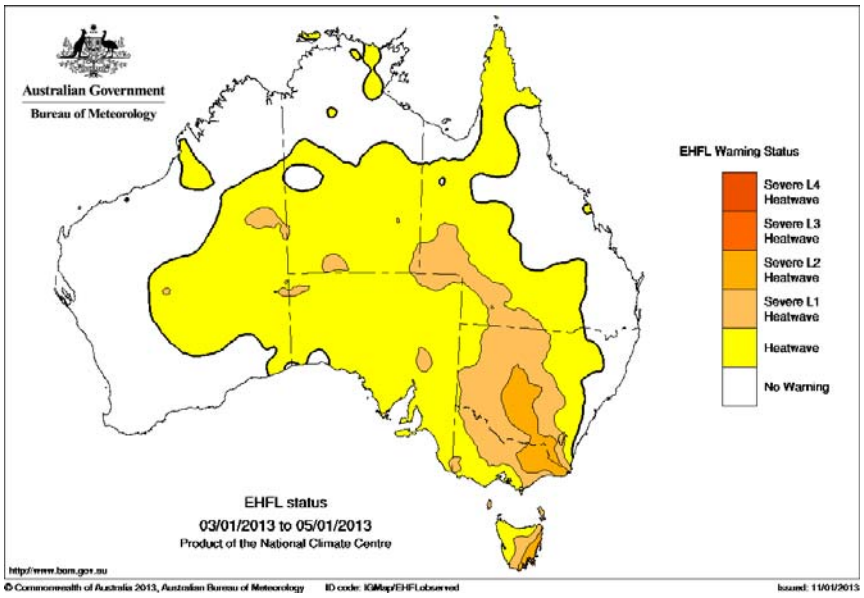

Figure 80: Areas with positive *EHF* for the period 03-05 January 2013, mapped for incidence of heatwave and level of severity. The contour band "Severe L1 Heatwave" indicates *EHF* values between one and two times the *EHF* severity threshold, while the contour band "Severe L2 Heatwave" indicates *EHF* values between two and three times the *EHF* severity threshold, and so on.

7.3 Service Demand

The breadth of impact from severe and extreme heatwaves across several business sectors is reflected in the rising interest in focussed heatwave forecast services.

The Essential Services Commission of South Australia (ESCOSA) conducted an inquiry into ETSA Utilities ability to service client demand during the 2006 severe heatwave (ESCOSA, 2007). ESCOSA found a need for ETSA Utilities to integrate weather forecast data into its response processes. Enquiries are being fielded from national electricity generators and distributors, mining, and agricultural sectors.

As recipients of the 2010 Australian and State Award for Safer Communities the SA State Emergency Service, SA Health Department, Department for Families and Communities and the Bureau of Meteorology were recognised for a range of response strategies that reflected cooperation and coordination of information in the development of a heatwave service (EMA, 2010). Meteorological information supporting this service is currently confined to Adelaide alone, with strong demand to expand the service to the rest of the state.

Similarly, Victorian, New South Wales and Western Australian agencies are interested in heatwave services, each independently developing strategies for managing their mitigation and response strategies for heatwaves variously on capital-city and state-wide basis.

Health agencies wish to differentiate forecast heatwave impact regionally. They are clear in stipulating a strategy that will not over-warn communities so that appropriate strategies are employed regionally when required. Common to emergency management of bushfire and other weather-driven hazards, heatwave mitigation and response strategies will be eroded when communities recognise over-warning and a lack of threat.

Ongoing research into the effectiveness of a potential heatwave service is critical. Verification of a heatwave service must take into account the spatial and temporal accuracy of maximum and

minimum temperatures. Modern operational verification systems are needed to deliver this capability.

Improved assessments of impacts through data sharing with industry sectors are required to build a quality assurance system for any new service.

7.4 Service Policy

The PricewaterhouseCoopers (2011) report has demonstrated that there would be significant benefit from implementing a national framework for heat events. This was recognised in the Munro Review (2011) where Priority Action 5 (Focus the Bureau's evolving environmental information role on natural hazards in the first instance) offered an opportunity for government to consider a stronger all hazards approach for the Bureau of Meteorology in developing emergency services. Munro noted a UK Met Office initiative in leading the development of the Natural Hazard Partnership, where a number of government agencies bring together their knowledge and response capabilities for a wide range of environmental responsibilities. This work identified an opportunity for government to consider whether it is appropriate for the Bureau to play a stronger role in flood management and the development of heatwave services.

Overseas development and evolution of national heatwave policy frameworks offer valuable insights and lessons learnt that can benefit the development of an Australian national framework for heat events. It is anticipated that experiences gathered from overseas agencies will inform future Australian heatwave policy[11].

[11] One of the authors (Nairn) will travel to Germany, France, Great Britain and the United States of America on a Churchill Fellowship (2013) on a mission to gather heatwave policy lessons.

8. CONCLUSIONS

An objective heatwave definition, together with an analogous coldwave definition, has been described that can be applied to any location in Australia. The excess heat indices described in this report rely only on time series of daily temperature data (although the inclusion of daily minimum temperature data in the calculation involves an implicit consideration of humidity effects), which make them easily available to all of Australia and most countries around the world, although we note that the results are rather more applicable to the extra-tropics than to the tropics (e.g. Darwin, Cairns) where daily maximum temperatures can show low day-to-day variability. The relative intensity, distribution, duration and heat load of heatwaves (coldwaves) can now be considered as ingredients within any discipline.

The excess heat indices we have described are not complex. Their intuitive construction is suited to the development of simple graphical products and site time series, and unfolding events can be monitored and forecast values verified against observations on a daily basis. The ability to monitor ongoing events will support people in their decision making, irrespective of their discipline. Importantly, emergency managers and responders can readily verify their decisions, enabling appropriate levels of community support or intervention.

The capacity to extend a heatwave service to the Australian community has grown with the development of gridded climate and forecast data within the Bureau of Meteorology. Numerical Weather Prediction (NWP) models now generate Gridded Operational Consensus Forecasts (GOCF) which can be edited by forecasters where value is deemed to be added. Both formats provide a means by which heatwave (coldwave) data can be generated. It will be important to provide forecast verification data to guide the development of this service. Whilst a strong emphasis has been placed on improvements to maximum temperature forecasts, it is unlikely that the minimum temperature forecasts have received similar treatment. Providing performance feedback is essential if these important forecasts are to improve. As is frequently the case in forecasting, impact-oriented weather services have a positive feedback on the quality of forecast elements. The relevance of each weather element on its own is not always obvious. In this case, minimum temperature forecasts would not currently rate as a high-value weather element. Impact measures and their adoption within the community assist both managers and bench forecasters in understanding where improving forecasts have the capacity to improve adaptive responses within the community. An improved understanding of minimum temperature impacts during heatwaves will result in quality process improvements.

Heatwaves are a significant, yet poorly understood hazard within the Australian community. The work presented in this report provides an opportunity for improving understanding in the community and a means by which they can appropriately prepare and respond according to their level of exposure.

ACKNOWLEDGMENTS

Reviewers' comments and feedback have been particularly helpful, including Alex Evans (Climate Services SA, BoM), Kerryn Mason (Forensic Science South Australia) and Lisa Alexander (University of NSW). The support of South Australian government agencies has contributed significantly to the development of this work, noting especially the release of sensitive data by the State Coroner. Continuing support and encouragement from Beth Ebert (CAWCR) and Alasdair Hainsworth (Assistant Director Services, BoM) have also contributed to the development of this work. The implicit support of regional colleagues has been an important driver for a practical heatwave tool. Formative discussions with Darren Ray (Climate Services Manager, SA, BoM) provided the method for deriving the significance heat index as an anomaly. The anomaly innovation paved the way for treatment of acclimatisation which then enabled formulation of the Excess Heat Factor as described in Nairn et al. 2009 (Appendix A). As an important starting point in this work, Darren's contribution is significant.

An important milestone was achieved in 2010 when state and national Safer Communities Awards recognised advances in heatwave mitigation and response developed in partnership with South Australian State agencies (Department of Health, Department of Families and Communities, and the State Emergency Service).

REFERENCES

ACORN-SAT station catalogue, 2012. www.bom.gov.au/climate/change/acorn-sat/documents/ACORN-SAT-Station-Catalogue-2012-WEB.pdf, last accessed 23 April 2012.

Alexander, L., Hope, P., Collins, D., Trewin, B., Lynch, A. and Nicholls, N. 2007. Trends in Australia's climate means and extremes: a global context. *Australian Meteorological Magazine*, 56, 1-18.

Barriopedro, D, Fischer, E.M., Luterbacher, J., Trigo, R.M. and García-Herrera, R. Published online 17 March 2011. The Hot Summer of 2010: Redrawing the Temperature Record Map of Europe. *Science* 8 April 2011: 220-224.

Black, E., Blackburn, M., Harrison, G., Hoskins, B. and Methven, J. 2004. Factors contributing to the summer 2003 European heatwave. *Weather*, 59, 217-223.

Braga, A.L.F., Zanobette, A. and Schwartz, J. 2001. The time course of weather related events. *Epidemiology*, 110, 859-863.

Climate Education. www.bom.gov.au/climate/environ/snow.shtml, Bureau of Meteorology web site, last accessed 26 September 2012.

Coates, L. 1996. An overview of fatalities from some natural hazards in Australia. in *Proceedings of NDR96 Conference on Natural Disaster Reduction*. Gold Coast Australia.

CSIRO and Bureau of Meteorology. Climate Change in Australia. *Technical Report 2007*. www.climatechangeinaustralia.gov.au. Last accessed 13 January, 2012.

Curriero, F.C., Heiner, K.S., Samet, J.M., Zeger, S.L., Strug, L. and Patz, J.A. 2002. Temperature and Mortality in 11 cities of the Eastern United States. *American Journal of Epidemiology*, 155, 80-97.

Deschene, O. and Moretti, E. 2009. Extreme Weather Events, Mortality and Migration. *Review of Economics and Statistics*, 91, 659-681.

Emergency Management Australia. 2010 Australian safer communities awards. www.em.gov.au/News/Awards/Pages/2010Australiansafercommunitiesawards.aspx, last viewed 18 October 2012.

Essential Services Commission Of South Australia. ETSA UTILITIES NETWORK RELIABILITY PERFORMANCE SECEMBER 20006-MARCH 2007 INFORMATION PAPER. archive.escosa.sa.gov.au/webdata/resources/files/070705-R-ETSAUtilitiesNetworkRelPerformance.pdf, last viewed 17 October 2012.

Fawcett, R. and Hume, T. 2010, The GOCF/AWAP System forecasting temperature extremes, 2010 IOP *Conf. Ser.: Earth Environ. Sci.,* 11, 012005.

Francis, J.A. and Vavrus, S.J. 2012. Evidence linking Arctic amplification to extreme weather in mid-latitudes. *Geophysical Research Letters*, 39, L06801. DOI: 10.1029/2012GL051000.

Guyton, A.C. and Hall, J.E. 2000. *Textbook of medical physiology* 10th ed. Philadelphia, PA: W.B. Saunders Company.

Hajat, S., Armstrong, B., Baccini, M., Biggeri, A., Bisanti, L., Russo, A., Paldy, A., Menne, B. and Kosatsky, T. 2006. Impact of high temperatures on mortality: is there an added heat wave effect. *Epidemiology*, 17, 632-638.

Hajat, S., Armstrong, B., Gouveia, N. and Wilkinson, P. 2005. Mortality displacement of heat-related deaths: a comparison of Delhi, Sao Paulo and London. *Epidemiology,* 16, 613-620.

Huang, C., Barnett, A.G, Wang, X. and Tong, S. 2012. Effects of Extreme Temperatures on Years of Life Lost for Cardiovascular Deaths: A Time Series Study in Brisbane, Australia. Circulation: *Cardiovascular Quality and Outcomes*, 5, 609-614. doi: 10.1161/ CIRCOUTCOMES.112.965707.

Field, C.B., Barros, V., Stocker, T.F., Qin, D., Dokken, D.J, Ebi, K.L., Mastrandrea, M.D., Mach, K.J., Plattner, G.-K., Allen, S.K., Tignor, M. and Midgley, P.M. (eds.). IPCC, 2012: Managing the Risks of Extreme Events and Disasters to Advance Climate Change Adaptation. *A Special Report of Working Groups I and II of the Intergovernmental Panel on Climate Change*. Cambridge University Press, Cambridge, UK, and New York, NY, USA, 582 pp.

Jones, D.A., Wang, W. and Fawcett, R. 2009. High-quality spatial climate data sets for Australia. *Australian Meteorological and Oceanographic Journal*, 58, 223-248.

Juran, J.M. Editor, *Quality Control Handbook* Third Edition McGraw-Hill Book Company, 1974.

Kalnay, E. and Coauthors. 1996. The NCEP/NCAR Reanalysis 40-year Project. *Bulletin of the American Meteorological Society*, 77, 437-471.

Katz, R. Statistics of Weather and Climate Extremes.
www.isse.ucar.edu/extremevalues/extreme.html, last accessed 17 January 2012.

Knochel, J.P., Reed, D. editors. *Disorders of heat regulation*. 5th ed. New York, NY: McGraw-HiII; 1994.

Kosaka, Y. and Nakamura, H. 2010. Mechanisms of Meridional Teleconnection Observed between a Summer Monsoon System and a Subtropical Anticyclone. Part II: A Global Survey. *Journal of Climate*, 23, 5085-5108.

Langlois, N., Herbst, J., Mason, K., Nairn, J. and Byard, R.W. 2013. Using the Excess Heat Factor (EHF) to predict the risk of heat related deaths. *Journal of Forensic and Legal Medicine* (to appear).

Lewis, W., Balderstone, S. and Bowan, J. 2006. *Events That Shaped Australia*. New Holland. pp. 154–158.

Mason, K., Nairn, J., Herbst, J. and Felgate, P. 2010. Heatwave – The Adelaide Experience, Presented at the 20th International Symposium on the Forensic Sciences, September 2010.

McBride, J.L., Mills, G.A. and Wain, A.G. 2009. The Meteorology of Australian Heatwaves. Understanding High Impact Weather, CAWCR Modelling Workshop, 30 Nov to 2 Dec 2009.

McMichael, A.J., Woodruff, R., Whetton, P., Hennessy, K., Nicholls, N., Hales, S., Woodward, A. and Kjellstrom, T. 2003. *Human Health and Climate Change in Oceania: A Risk Assessment* 2002. Canberra: Commonwealth of Australia.

The Meteorology Act 1955. Section 6, "Functions of the Bureau". Accessed online: http://www.austlii.edu.au/au/legis/cth/consol_act/ma1955160/ Last accessed 4 April 2011
Munro, C. 2011. Review of the Bureau of Meteorology's capacity to respond to future extreme weather and natural disaster events and to provide seasonal forecasting services, December 2011. Accessed online, www.environment.gov.au/about/bom/pubs/bom-review.docx, last viewed 18 October 2012.

Met Office, Heat-Health Watch. http://www.metoffice.gov.uk/weather/uk/heathealth/, last accessed 17 April 2012.

Nairn, J., Fawcett, R. and Ray, D. 2009. Defining and predicting Excessive Heat events, a National System. 2009. Understanding High Impact Weather, CAWCR Modelling Workshop, 30 Nov to 2 Dec 2009, Melbourne, Australia.

Nairn, J. 2011. Heatwave defined as a heat impact event for all community and business sectors in Australia. Extended abstract, 19th International Biometeorology Congress, 4-8 December 2011, University of Auckland New Zealand.

National Climate Centre. 2009. Special Climate Statement 17. The exceptional January-February 2009 heatwave in south-eastern Australia, Bureau of Meteorology. (www.bom.gov.au/climate/current/statements/scs17d.pdf). Last accessed 13 January 2012.

National Weather Service. 2010. HEAT: A Major Killer, www.nws.noaa.gov/om/heat/index.shtml, last accessed 20 January 2012.

Nicholls, N. and Larsen, S. 2011. Impact of drought on temperature extremes in Melbourne, Australia. *Australian Meteorological and Oceanographic Journal*, 61, 113-116.

Nicholls, N., Skinner, C., Loughnan, M.E. and Tapper, N.J. 2008. A simple heat alert system for Melbourne, Australia, *International Journal of Biometeorology*, vol 52, Springer, New York USA, pp. 375-384.

Nitschke, M., Tucker, G. and Bi, P. 2007. Morbidity and mortality during heatwaves in metropolitan Adelaide. *Medical Journal of Australia*, 187, 662-665.

Palecki, M.A., Changnon, S.A. and Kunkel, K.E. 2001. The Nature and Impacts of the July 1999 Heat Wave in the Midwestern United States: Learning from the Lessons of 1995. *Bulletin of the American Meteorological Society*, 82, 1353-1367.

Pattenden, S., Nikiforov, B. and Armstrong, B.G. 2003. Mortality and temperature in Sofia and London. *J Epidemiol* Community Health., 57, 628-633.

Perkins, S.E., Alexander, L.V. and Nairn, J.R. 2012. Increasing Frequency, Intensity and Duration of Observed Heatwaves and Warm Spells. *Geophysical Research Letters*, 39, L20714. doi:10.1029/2012GL053361.

Pezza, A.B, van Rensch, P. and Cai, W. 2012. Severe heat waves in Southern Australia: synoptic climatology and large scale connections. *Climate Dynamics*, 38, 209-224.

PricewaterhouseCoopers. 2011. Protecting human health and safety during severe and extreme heat events. A national framework. Commonwealth Government November 2011 (www.pwc.com.au/industry/government/publications/extreme-heat-events.htm). Last accessed on 20 January 2012.

Queensland University of Technology (QUT). 2010. Impacts and adaptation response of infrastructure and communities to heatwaves: the southern Australian experience of 2009, report for the National Climate Change Adaption Research Facility, Gold Coast, Australia. Last downloaded on 1 August 2012 from
http://new.nccarf-partner-dev.rcs.griffith.edu.au/sites/default/files/attached_files_publications/Southern%20Cities%20Heatwaves%20-%20Complete%20Findings.pdf

Robinson, P.J. 2001. On the Definition of a Heat Wave. *Journal of Applied Meteorology*, 40, 762-775.

Sen, P.K. 1968. Estimates of the regression coefficient based on Kendall's tau, *Journal of the American Statistical Association*, 63, 1379-1389.

Steadman, R.G. 1979a. The assessment of sultriness. Part I: A temperature–humidity index based on human physiology and clothing science. *J. Appl. Meteor*., 18, 861-873.

Steadman, R.G. 1979b. The assessment of sultriness. Part II: Effect of wind, extra radiation, and barometric pressure on apparent temperature. *J. Appl. Meteor*., 18, 874-884.

Steadman, R.G. 1984. A universal scale of apparent temperature. *J. Climate Appl. Meteor*., 23, 1674-1687.

Tertre Le, A., Lefranc, A., Eilstein, S., Declercq, C., Medina, S., Blanchard, M., Chardon, B., Fabre, P., Filleul, L., Juso,t J-F., Pascal, L., Prouvost, H., Cassadou, S. and Ledrans, M. 2006. Impact of the 2003 heatwave on all-cause mortality in 9 French cities. *Epidemiology,* 17, 75-9.

Tong, S., Ren, C. and Becker, N. 2010. Excess deaths during the 2004 heatwave in Brisbane, Australia. *International Journal of Biometeorology,* 54, 393-400.

Toulemon, L. and Berbieri, M. 2006. The Mortality Impact of the August 2003 Heat Wave in France. 2006 Population of America Association Meeting, Los Angeles, March 30-April 1st. (paa2006.princeton.edu/papers/60411) Last accessed 27 September 2012.

Trewin, B. 2012. A daily homogenized temperature data set for Australia. *International Journal of Climatology*. (wileyonlinelibrary.com) DOI: 10.1002/joc.3530.

Trewin, B.C. and Vermont, H. 2010. Changes in the frequency of record temperatures in Australia, 1957-2009, *Australian Meteorological and Oceanographic Journal*, 60, 113-119.

Vandentorren, S., Brettin, P., Zeghnoun, A., Mandereau-Bruno, L., Croisier, A., Cocet, C., Riberon, J., Siberan, I., Declercq, B. and Ledrans, M. 2006. August 2003 Heat Wave in France: Risk Factors for Death of Elderly People Living at Home. *The European Journal of Public Health*, 16, 583-591.

Victorian Department of Health. 2009. January 2009 Heatwave in Victoria: an Assessment of Health Impacts. www.health.vic.gov.au/chiefhealthofficer/downloads/heat_impact_rpt.pdf

Victorian Department of Health. 2012. Heat Health Alert System. http://www.health.vic.gov.au/environment/heatwave/agencies/alert.htm, last accessed 17 April 2012.

Williams, S., Nitschke, M., Sullivan, T., Tucker, G.R., Weinstein, P., Pisaniello, D.L., Parton, K.A. and Bi, P. 2012. Heat and Health in Adelaide, South Australia: Assessment of heat thresholds and temperature relationships. *Science of the Total Environment*, 414, 126-133.

Ziser, C.J., Dong, Z.Y. and Saha, T. 2005. Investigation of Weather Dependency and Load Diversity on Queensland Electricity Demand. Australasian Universities Power Engineering Conference 2005.

APPENDIX A[12]

Defining and predicting Excessive Heat events, a National system

John Nairn[1], Robert Fawcett[2] and Darren Ray[1]

[1]*South Australian Regional Office, Adelaide*
[2]*National Climate Centre, Melbourne,*
Australian Bureau of Meteorology

Introduction

Heatwaves are one form of severe weather expected to become worse in Australia under global warming (Solomon et al. 2007). In Australia, heatwaves are defined by the achievement of a minimum sequence of consecutive days with daily maximum temperatures (T_{max}) reaching a designated threshold. Definitions that only apply to individual locations impede our ability to understand and respond appropriately to heatwaves. Daily maximum temperatures are only part of the story when we consider impacts on human health, agriculture, infrastructure, demand on utilities and other environmental hazards such as fire. Incorporating minimum temperature through the average daily temperature is also important (Nicholls et al. 2008, Pattenden et al. 2003), which is not surprising. The extent to which heat load is dissipated overnight ahead of the following high heat day dictates the accumulating thermal load impacting vulnerable people and systems.

In this presentation, we describe a set of three new excess heat indices (EHIs) which we propose for use in real-time and historical climate monitoring of heat-waves across Australia. A scheme for their operational implementation will be outlined, together with possibilities for extension into real-time weather forecasting.

These indices provide a means by which the community can gauge their historical sensitivity to accumulated excess heat load, peak load and duration. Mitigation and response capabilities will also benefit from access to time series and spatial tools applicable to past and forecast events.

Method

The EHIs we propose here are based on average daily temperature (ADT), defined as the average of the maximum and minimum temperature (T_{min}) within a 24-hour 9 am to 9 am (local time) day, which corresponds to the daily temperature observation cycle in Australia. In practice, this means that the early morning T_{min} typically follows the afternoon T_{max} in time.

The first EHI we propose is an acclimatisation index, defined as EHI(accl.) = $(T_i + T_{i-1} + T_{i-2})/3 - (T_{i-3} + \ldots + T_{i-32})/30$, where T_i is the ADT for day i. In other words, EHI(accl.) is the difference between the mean ADT over a three-day period and the mean ADT over the preceding thirty days. Positive values are associated with relatively hot weather, or excess heat, negative values with relatively cool weather. This index is very much a relative one – excess heat according to this index is possible in summer and winter alike. Also, its values are not expected to become more extreme under a general warming trend.

The second EHI is more an absolute index, and is defined as EHI(sig.) = $(T_i + T_{i-1} + T_{i-2})/3 - T_{95}$, where T_{95} is the 95th percentile of ADT. We use the 30-year period 1971-2000 for the calculation of T_{95}, and the calculation is across all days in the year. With this second index, excess heat is typically only possible in the summer half-year, because hot winter weather isn't hot by annual standards. The comparison against T_{95} gives a measure of the statistical significance of the event. Unlike EHI(accl.), this index is expected to become more extreme under a general warming trend, provided a fixed climatological period for T95 is adopted. Lastly, the excess heat factor (EHF) is defined as EHF = | EHI(accl.) | × EHI(sig.), which obviously implies that sign(EHF) = sign(EHI(sig.)) – EHI(accl.) acts as an amplification term on EHI(sig.).

These three indices obviously require continuous time series of daily maximum and minimum temperature. While these can of course be obtained from station-based data, for climate monitoring purposes we use the new Australian Water Availability Project (AWAP) daily temperature analyses (Jones et al. 2009). Initially

[12] CAWCR Modelling Workshop, 30 Nov to 2 Dec 2009, Melbourne, Australia.

we use the low resolution (0.25°) analyses, although the high resolution (0.05°) might be used in time. Gridded forecast values of three indices could be obtained for the next four of five days using the new experimental OCF/AWAP daily temperature forecast system, OCF from ACCESS NWP or from forecaster generated data (optimally within Graphical Forecast Editor).

Results

Figures 1, 2 and 3 show station-based and grid-interpolated results for Adelaide in January and February 2009. The station-based results are obtained using the Adelaide (Kent Town) site (023090), supplemented by Adelaide (West Terrace) site (023000) data in the early part of the base period 1971-2000 to calculate T_{95}. Figure 1 shows daily maximum and minimum temperature – actual station data (solid lines) from Adelaide (Kent Town), and grid-interpolated data (34.921°S, 138.622°E) from the 0.25° AWAP daily temperature analyses. While there is a clear bias in the daily temperature data, the manner in which the two EHIs are calculated largely removes this bias, although as seen in Figure 2, the peak values of the grid-interpolated results are slightly lower than the station-based results. This slight discrepancy is amplified in the EHF calculation (Figure 3), but these results would not lead to a qualitative difference in the interpretation of their results. The three-day EHIs and EHFs in Figures 2 and 3 are plotted against the *last* day of the three-day calculation period. [A forecast strategy would differ, EHIs and EHFs would be plotted against the *first* day of the three-day calculation period, whilst minimum precedes maximum temperatures in forecast systems.]

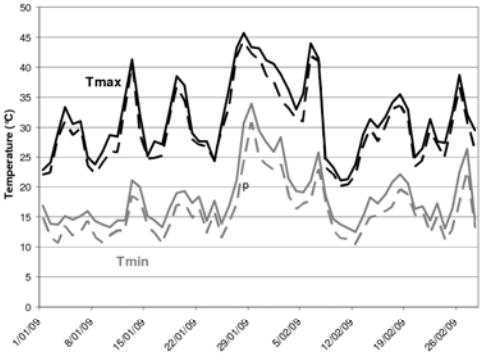

Fig. 1: Station (solid) and grid-interpolated (dashed) daily Tmax (black) and Tmin (grey) at Adelaide for January and February 2009. Following normal Bureau of Meteorology convention, daily maximum (*minimum*) temperatures are recorded for the 24 hours from (*to*) 9 am on the designated day.

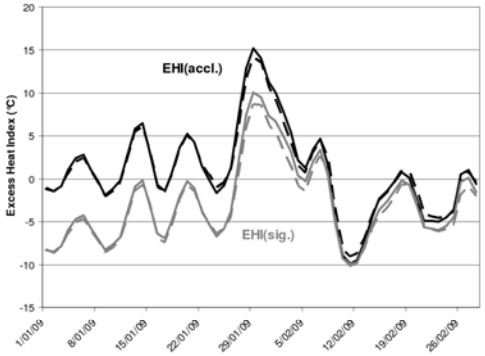

Fig. 2: Station (solid) and grid-interpolated (dashed) daily EHI(accl.) (black) and EHI(sig.) (grey) at Adelaide for January and February 2009. The three-day EHIs are graphed against the last day of the three-day period.

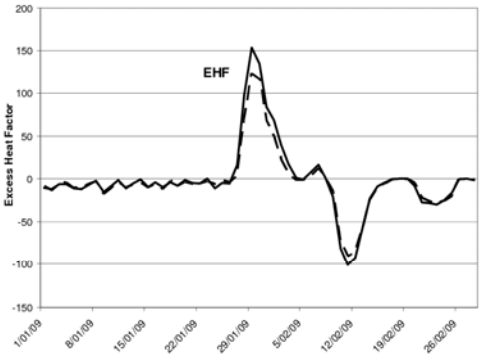

Fig. 3: Station (solid) and grid-interpolated (dashed) EHF at Adelaide for January and February 2009. The three-day EHFs are graphed against the last day of

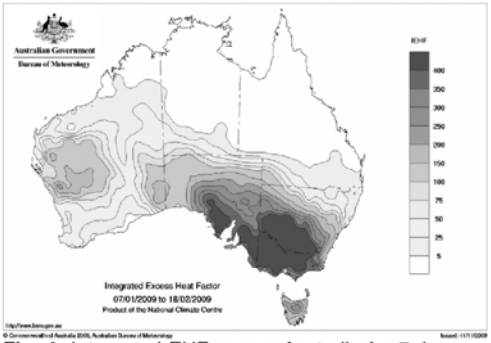

Fig. 4: Integrated EHF across Australia for 7 January to 18 February 2009.

three-day period.

Daily values of the EHIs can of course be mapped, but it is also useful to integrate or sum the daily values across an entire heat wave. Figure 4 shows the integrated EHF from 7 January to 18 February 2009, where only positive daily values of the EHF contribute to the integration – negative values are treated as if they were zero. As with Figures 2 and 3, the range of days represented in Figure 4 refer to the last days of the three-day triplets used in the EHF calculations.

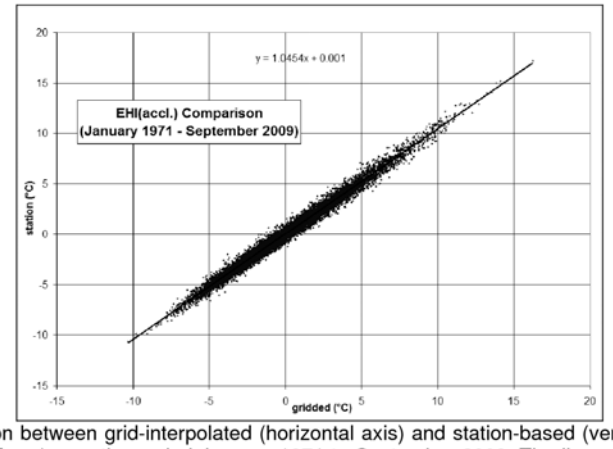

Fig. 5: A comparison between grid-interpolated (horizontal axis) and station-based (vertical axis) EHI(accl.) for Adelaide (Kent Town) over the period January 1971 to September 2009. The linear regression is shown as a solid line, together with the regression equation.

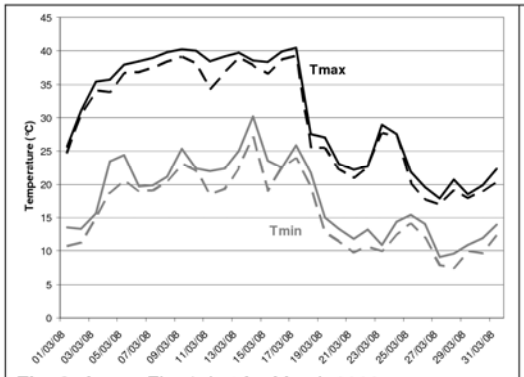

Fig. 6: As per Fig. 1, but for March 2008.

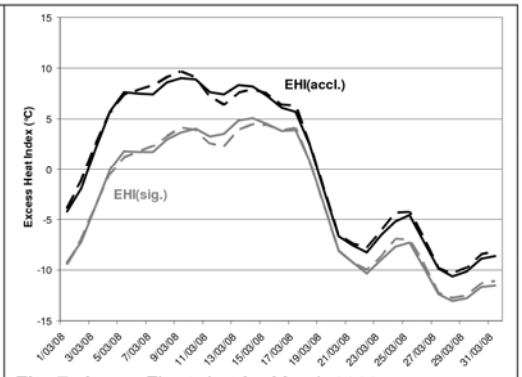

Fig. 7: As per Fig. 2, but for March 2008.

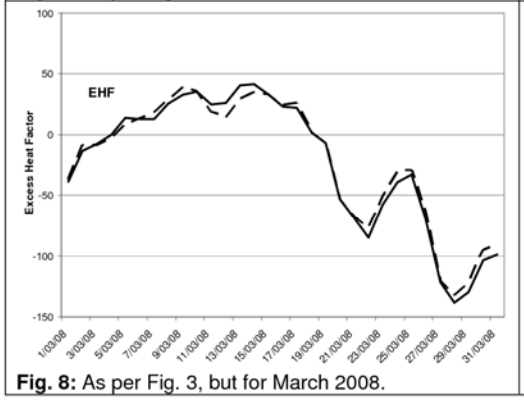

Fig. 8: As per Fig. 3, but for March 2008.

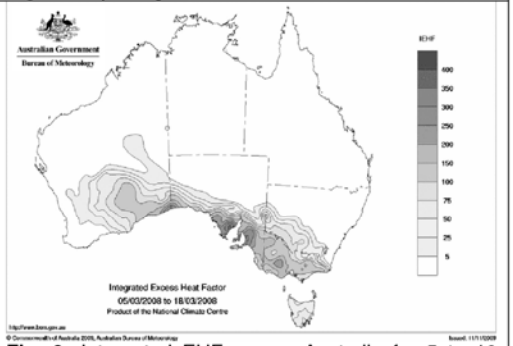

Fig. 9: Integrated EHF across Australia for 5 to 18 March 2008.

Figure 5 shows an extended comparison between the gridded and station-based EHI(accl.) values at Adelaide. Relative to the grid-interpolated values, the station-based values show very little bias but a slight increase (4.5%) in amplitude. This is not altogether surprising, in that the daily temperature analyses represent (to some extent) local areal averages.

Figures 6 to 9 show results (analogous to Figures 1 to 4) for the March 2008 Adelaide heatwave. This Adelaide heatwave was of lesser intensity but longer duration than the subsequent event in 2009 – peak EHI(accl.) values reached +10°C in 2008 compared with +15°C in 2009, while peak EHI(sig.) values reached +5°C in 2008 compared with +10°C in 2009. On the other hand, the EHI(accl.) index remained positive for 16 consecutive daily values in the 2008 event, compared with 14 consecutive daily values in 2009, while 2008 showed greater consistency in the elevation of its temperatures.

Discussion

As seen above the ability to objectively contrast the peaks, ingredients and length of excess heat factor across heat waves provides a new opportunity to test which aspect(s) of an event is impacting heat vulnerable systems. Excess Heat Factor load can also be assessed as demonstrated in Figures 4 and 9, where integrated or summed EHF is presented as an event assessment, once again relevant to any agency, community group or business sector wishing to evaluate their resilience thresholds. This application could also prove highly useful for state and federal government relief arrangements (NDRRA) whereby threshold temperature criteria are currently being developed in order to include heatwaves as a natural disaster.
An interesting challenge is presented to current NWP standards by the longevity of the record breaking Adelaide heatwaves presented. Direct model output and OCF guidance is limited to about 8 days. Experiments are required to establish the utility of 15 and 30 day NWP forecast period objective guidance.

Time series analysis of Adelaide's 120 year temperature record using this technique also produces insights into heatwave climatology. Ranking of events based upon EHF peak and load are not presented.

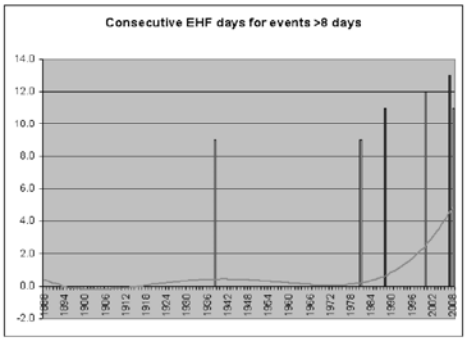

Fig. 10. Length of Adelaide EHF events when greater than 8 days by year.

References

D A Jones, W Wang and R Fawcett, 2009. *High-quality spatial climate data sets for Australia*. Australian Meteorological and Oceanographic Journal (in press).

Natural Disaster Relief and Recovery Arrangements http://www.ema.gov.au/www/emaweb/emaweb.nsf/Page/Emergency_ManagementRecovering_from_Emergencies

N Nicholls, C Skinner, M E Loughnan, N Tapper. *A simple heat alert system for Melbourne, Australia.* Int J Environ Biometeorology (in press, 2008).

M Nitschke, G Tucker, P Bi. *Morbidity and mortality during heatwaves in metropolitan Adelaide.* Med J Aust 2007; 187{11/12}:662-665.

S Pattenden, B Nikiforov and B G Armstrong, *Mortality and temperature in Sofia and London.* J Epidemiol Community Health 2003;57;628-633.

S Solomon, D Qin, M Manning, Z Chem, M Marquis, K B Averyt, M Tignor, H L Miller (Eds.). *IPPC Fourth Assessment Report (AR4). Climate Change 2007: The Physical Science Basis. Contribution of Working Group 1 to the Fourth Assessment Report of the Intergovernmental Panel on Climate Change.* Cambridge University Press, Cambridge, United Kingdom and New York, NY USA, 966 pp.

APPENDIX B[13]

Heatwave defined as a heat impact event for all community and business sectors in Australia

John Nairn,

Bureau of Meteorology, South Australia, Australia.

Abstract

Severe heatwaves impact all natural and human engineered systems in a similar manner. Systems susceptible to failure under thermal duress have natural or engineered design limitations. These limits are an adaptive response to commonly expected rates of heat accumulation found over both the long (climate scale) and short (acclimatisation) term. When these limits are exceeded, systems begin to fail. The larger the thermal load, the deeper is the impact and scale of failure. Definitions are set out as a means of deriving a metric for the measure of excess heat impact. Australia will soon use this objective measure for climate history, forecasts, warnings and assessment of risk arising from climate change.

1. Heatwave Definition

Heatwave: A period of at least three days where the combined effect of excess heat and heat stress are unusual with respect to the local climate. Both maximum and minimum temperatures are used in this assessment.

Excess Heat: Unusually high heat that is not sufficiently discharged overnight due to unusually high overnight temperature. Maximum and subsequent minimum temperatures averaged over a three day period are compared against a climate reference value. This is expressed as a long term (climate scale) temperature anomaly.

Heat Stress: A period of heat which is warmer, on average, than the recent past. Maximum and subsequent minimum temperatures averaged over a three day period and the previous 30 days are compared. This is expressed as a short term (acclimatisation) temperature anomaly.

Excess Heat Factor (EHF): The combined effect of Excess Heat and Heat Stress calculated as an index to provide a comparative measure of intensity, load, duration and spatial distribution of heatwave. Heatwave conditions exist when the EHF is greater than zero.

Severe Heatwave: An event where EHF values exceed a threshold for severity that is specific to the climatology of each location.

2. Introduction

Heatwave literature is predominantly focussed on human health outcomes. Consequently sensible and latent heat are invariably combined together in order to account for effectiveness of thermo-regulation of biological systems. Frequently regression equations (Braga et al., 2001; Curriero et al. 2002; McMichael et al. 2008; Tong et al. 2010; Vandentorren et al. 2006) or synoptic patterns (Kalkstein, 2000) are matched to human health outcomes on city or regional scales. At this level of interplay between multiple variables, units and outcomes it is hard to visualise or compare

[13] Extended abstract, 19th International Biometeorology Congress, 4-8 December 2011, University of Auckland, New Zealand.

heatwaves across time, nor compare local, national or international events. Taking a step back from human impact, it is interesting to consider heatwaves as events where excessive sensible heat accumulates resulting in rising thermal load. This is a simpler heatwave concept than those discussed by Robinson (2001). Heatwaves identified purely by their thermal load can be assessed in terms of peak and accumulated heat load, as well as their evolution in time and space regardless of their location across the globe. Human health considerations under this approach would be taken into account as a second step, if necessary, after establishing the threat and potential magnitude of heatwave.

3. Method

The Excess Heat Factor (EHF) is derived for every location by combining a long-term temperature anomaly by a short term temperature anomaly (Nairn et al., 2009). Average maximum and minimum temperatures) captures the accumulating thermal load. Higher minimum temperatures reflect greater accumulating heat load. Heatwaves are detected where EHF>0.

Rare and relatively common heatwave events are separated by sampling the 85th percentile of each site's positive EHF cumulative distribution function. Local climatology variability results in unique EHF characteristics. Inter-site comparisons of EHF range are best calibrated against the severe threshold.

More traditional measures of human impact heatwaves include humidity. This is not the case for EHF. Strong upward modulation of minimum temperatures in conjunction with humid conditions does however indirectly incorporate humidity into EHF.

4. Results

In January and February 2009 southeast Australia experienced an extreme heatwave sequence culminating in Black Saturday on 7th February (National Climate Centre, 2009a). Figure 1 shows the accumulated heat load from gridded climate data (Jones et al., 2009) across southern Australia encompassing this period.

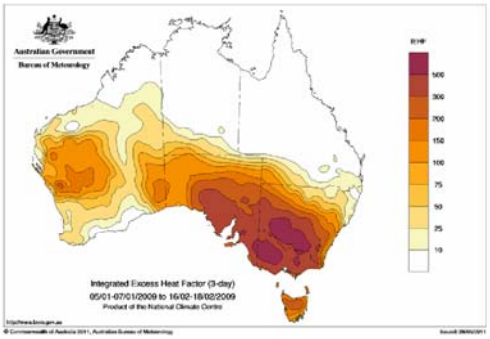

Figure 1: Accumulated Excess Heat Factor (EHF) from 5 January to 16 February 2009.

In January and February 2009 southeast Australia experienced an extreme heatwave sequence culminating in Black Saturday on 7th February (National Climate Centre, 2009a). Figure 1 shows the accumulated heat load from gridded climate data (Jones et al., 2009) across southern Australia encompassing this period. Catastrophic bushfires in the state of Victoria at the end of the heatwave resulted in the death of 173 people (Teague et al., 2010). Prior to this bushfire over 400 excess deaths occurred in the states of South Australia and Victoria (Mason et al., 2010; State of Victoria, 2009). Accumulated EHF over 400°C^2 in these two states is broadly indicative of the area impacted.

The time sequence for EHF and day of death shown in Figure 2 shows a similar power response to this extreme heatwave. Each EHF value on the chart is an expression of the average heat load over a three day period, inclusive of the current and following 2 days. Calculated in this manner EHF shows a predictive capacity for the mortality response.

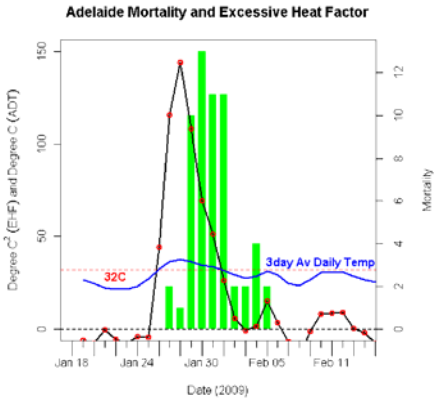

Figure 2: Mortality and EHF for 2009 severe heatwave in Adelaide, South Australia. Heat related mortality (green bars), Excess Heat Factor (black lines with red dots) and three day average daily temperature (blue line). Severe EHF threshold of 32°C^2 (---)

In Adelaide's 120 year climate record the EHF peak amplitude of 144°C^2 is the top ranked event. The accumulated EHF for this event is 586°C^2, also the top ranked event. Adelaide's second ranked heatwave occurred in January 1939. This severe heatwave also coincided with devastating bushfires, with 438 deaths reported in South Australia, Victoria and New South Wales (EMA, 2007).

Examination of the Paris climate record from 1944 to 2010 reveals the top ranked heatwave occurred in 1976. Poumadère et al. (2005) reports 6000 deaths were attributable to this heatwave across France, whilst 14,947 excess deaths were recorded for the 2003 heatwave. Both heatwaves in Figure 3 are similar in magnitude although there was an extended period of low amplitude heatwave prior to the extreme August 2003 event. It would be very informative to analyse the spatial distribution for each of these events. The extended period of heatwaves in 2003 suggests a high amplitude

heatwave over a large area of France, which could account for the larger death toll. In 2003 four heatwaves over eight weeks delivered 290°C^2 accumulated EHF prior to an additional 746°C^2 during the deadly three week August heatwave. In 1976, the solitary significant heatwave for that summer resulted in 920°C^2 accumulated EHF over four weeks.

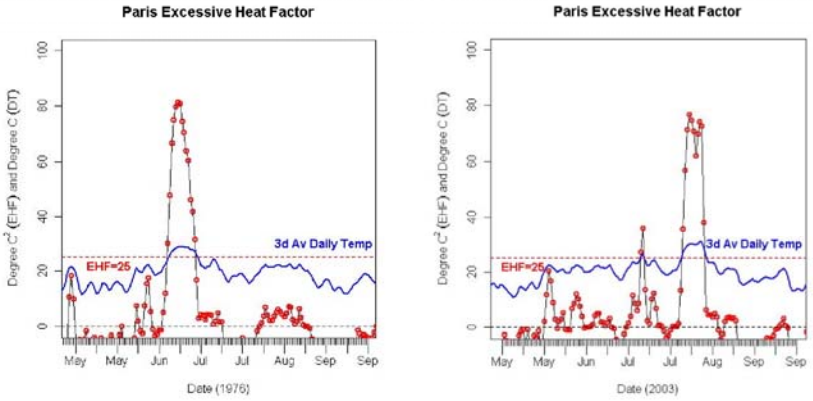

Figure 3: Paris heatwaves of 1976 and 2003. Excess Heat Factor (black lines with red dots) and three day average daily temperature (blue line). Severe EHF threshold of 25°C^2 (---)

Guha-Sapir et al. (2011) reported 55,800 deaths in Russia arising in 2010. Most deaths are attributed to the heatwave during June through to August. In the 1937 to 2010 Moscow climatology the heatwave in 1996 (Figure 4) had a significant peak amplitude of 72°C^2 and heat load of 197°C^2 over about a week. The 2003 heatwave appears as two distinct events for Moscow, and although the peak amplitude was 46°C^2 the heat load was 934°C^2, experienced over an eight week period.

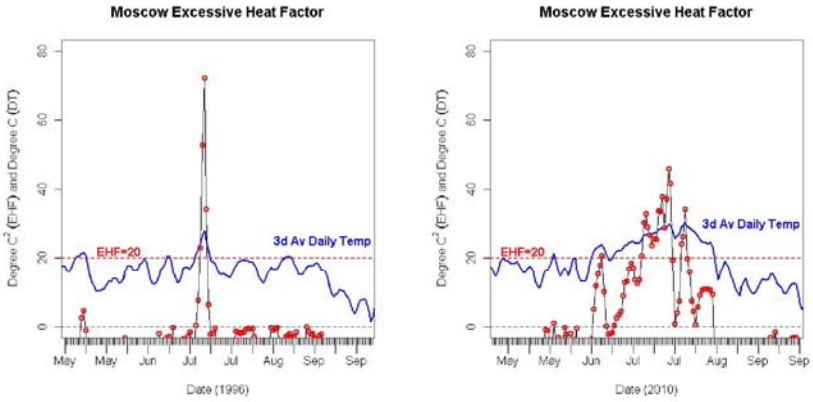

Figure 4: Moscow heatwaves of 1996 and 2010. Excess Heat Factor (black lines with red dots) and three day average daily temperature (blue line). Severe EHF threshold of 20°C^2 (---)

Palecki et al. (2001) notes the Chicago heatwave in 1995 caused approximately 700 deaths, compared to 110 in 1999. This could easily be attributed to the magnitude of the excess heat events shown in Figure 5, with peak EHF values of 57°C^2 and 30°C^2 and accumulated EHF (heat load) of 174°C^2 and 80°C^2 in 1995 and 1999, respectively. Notwithstanding improvements in city planning between events the difference in heatwave power should also be a consideration when evaluating relative impact.

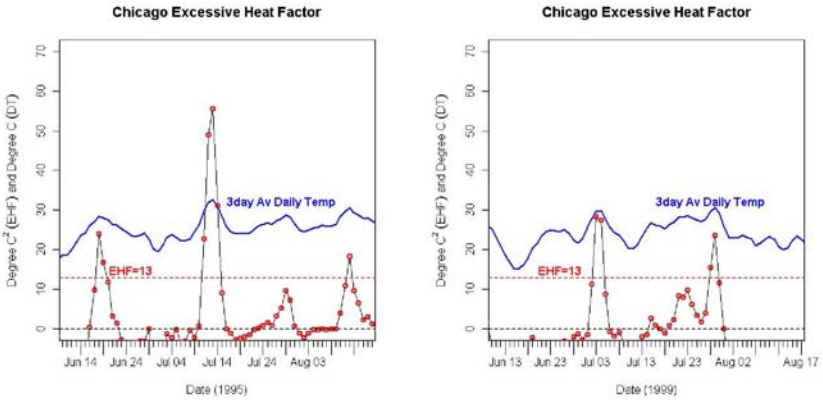

Figure 5: Chicago heatwaves of 1995 and 1999. Excess Heat Factor (black lines with red dots) and three day average daily temperature (blue line). Severe EHF threshold of 13°C^2 (---)

5. Conclusion

Systems susceptible to failure under thermal load will fail where EHF values are sufficiently high and fall outside system design limits.

By considering heatwaves as an excess sensible heat phenomena, a new set of simple physical indices and definitions have been created. These indices have physical units that permit the development of heatwave climatologies similar to other meteorological phenomena. Heatwave can now be compared by peak intensity and event heat load including temporal and spatial distribution. All heatwave impacted sectors are now able to consider excess sensible heat as a significant ingredient before considering other impact variables. Significantly, latent heat (or humidity) can now be treated as a separate but significant physical ingredient for human health outcomes.

Acknowledgements

Robert Fawcett's (National Climate Centre and Centre for Australian Climate and Weather Research, Bureau of Meteorology) statistical advice and manipulation of gridded climate fields has been a tremendous assistance in progressing this work. The support of my colleagues in the Bureau's Weather and Ocean Service Program, CAWCR and the South Australian Coroners Office also gratefully acknowledged.

References

Braga A.L.F., Zanobette A., Schwartz J., 2001: The time course of weather related events. Epidemiology. 110(9):p. 859-863.

Curriero F.C., Heiner K.S., Samet J.M., Zeger S.L., Strug L. and Patz J.A., 2002: Temperature and Mortality in 11 cities of the Eastern United States. American Journal of Epidemiology. 155(1): p. 80-97.

EMA, 2007: Heatwaves – In My Backyard?
www.ema.gov.au/www.ema/schools.nsf/Page/LearnAbout_HeatwavesIn_My_Backyard

Guha-Sapir D., Vos F., Below R., Ponserre S., 2011: Annual Disaster Statistical Review 2010, The numbers and trends. CRED: Brussels. ID 280 www.cred.be/publications

Jones D.A., Wang W. and Fawcett R., 2009: High-quality spatial climate data sets for Australia. Australian Meteorological and Oceanographic Journal. Aust. Met. & Oc. J 58(2009) 233-248.

Kalkstein L.S., 2000: Saving lives during extreme weather in summer. BMJ 2000 September 16; 3321(7262):650-651.

Mason K., Nairn J., Herbst J. and Felgate P., 2010: Heatwave – The Adelaide Experience. 20th International Symposium on the Forensic Sciences, Sydney Australia.

McMichael A.J., Wilkinson P., Kovats R.S., Pattenden S., Hajat S., Armstrong B., Vajanapoom N., Niciu E.M., Mahomed H., Kingkeow C., Kosnik M., O'Neill M.S., Romieu L., Remeriz-Aquilar M., Barreto M.L., Gouveia N., Nikiforov B., 2008: International study of temperature, heat and urban mortality: the 'ISOTHURM' project. Int J Epidemiol. 2008 Oct; 37(5): 1121-32.

Nairn J., Fawcett R., Ray D., 2009: Defining and predicting Excessive Heat events, a National System. Understanding High Impact Weather, CAWCR Modelling Workshop, 30 Nov to 2 Dec 2009.

National Climate Centre, 2009a: The exceptional January-February 2009 heatwave in southeastern Australia. Bureau of Meteorology, Special Climate Statement 17 (http://www.bom.gov.au/climate/current/statements/scs17d.pdf).

Palecki M.A., Changnon S.A., Kunkel K.E., 2001: The Nature and Impacts of the July 1999 Heat Wave in the Midwestern United States: Learning from the Lessons of 1995. Bulletin American Meteorological Socociety, 82, 1353-1367.

Poumadère M., Mays C., Le Mer S. and Blong R., 2005: The 2003 Heat Wave in France: Dangerous Climate Change Here and Now. Risk Analysis, Vol. 25, No. 6.

Robinson P.J., 2001: On the Definition of a Heat Wave. J. Applied Meteorology, 40, 762-75.

State of Victoria, 2009: January 2009 Heatwave in Victoria: an Assessment of Health Impacts. www.health.vic.gov.au/chiefhealthofficer/downloads/heat_impact_rpt.pdf

Teague B. (The Hon. AO), McLeod R. (AM), Pascoe S. (AM) 2010: The 2009 Victorian Bushfires Royal Commission final report. www.royalcommission.vic.gov.au/Commission-Reports/Final-Report.

Tong S., Ren C., Becker N., 2010: Ecess deaths during the 2004 heatwave in Brisbane, Australia. Int. J. Biometeorology (2010) 54: 393-400.

Vandentorren S. et al. 2006: August 2003 Heat Wave in France: Risk Factors for Death of Elderly People Living at Home. Eur J Public Health. 16 583-591.

The Centre for Australian Weather and Climate Research is a partnership between CSIRO and the Bureau of Meteorology.